U.S. ARMY CORPS OF ENGINEERS
Portland District

Evaluation of Smolt Movements Using an Active Fish Tracking Sonar at the Sluiceway Surface Bypass, The Dalles Dam, 2000

FINAL REPORT

Prepared by:

Gary E. Johnson (BioAnalysts, Inc.)

John B. Hedgepeth (Tenera Environmental, L.L.C.)

Albert E. Giorgi (BioAnalysts, Inc.)

John R. Skalski (University of Washington)

September 30, 2001

EXECUTIVE SUMMARY

The Dalles Dam (TDA) sluiceway is an example of a successful surface flow bypass (SFB). It passes 20-50% of total fish passage at the powerhouse in only 1-5% of total powerhouse discharge. Since development of prototype SFB systems is well underway at many Columbia and Snake River dams, it would be useful to have a better understanding of what makes the TDA sluiceway effective. In addition, efforts are underway to decrease turbine passage, and hence improve sluiceway and spillway effectiveness, with turbine intake occlusion plates with "J-sections," which are scheduled to be evaluated at TDA in 2001. The 2001 evaluation would be aided by baseline data on smolt movements at the existing sluiceway without turbine occlusion plates. Thus, the goal of the 2000 study was to improve understanding of why the sluiceway is effective. The objectives in 2000 were to: (a) track smolt movements in the nearfield (<10 m) of the Sluice 1-1; (b) estimate state[1] proportions, fish velocity streamtraces[2], and fate[3] probabilities; and (c) assess specific SFB premises regarding smolt movements in the Sluice 1-1 nearfield.

An active fish tracking sonar (AFTS) was used to sample smolt movements in the nearfield of Sluice 1-1. AFTS is based on the principle of tracking radar. Once a smolt is detected with the digital split-beam hydroacoustic system, two high-speed stepper motors align the axis of the transducer on the target. As the target moves, deviation of the target from the beam axis is calculated and used to re-aim the transducer, thereby tracking the target. For each ping the target is tracked, three-dimensional fish position data are recorded. AFTS provided high resolution (~5 cm), three-dimensional fish position data for the run-at-large. This system is particularly well suited for acquiring data in the nearfield. This population-level study had very high sampling intensity in the region of interest. About 100,000 smolts were tracked and about 5,000,000 positions located during the study from April 17 to July 7, 2000 at The Dalles Dam.

Descriptive data on fish movements revealed that more X, Y, Z fish positions were collected during night than day, although more fish were tracked during day than night (average number of pings per tracked fish was 29 during day and 88 at night). Fish moved in positive and negative directions in each of the three dimensions of the coordinate system, but the trend over the entire sample volume (15 m wide, 10 m out from the dam, and 9 m deep) generally was westward, toward the dam, and downward in the water column. Velocity magnitudes were mostly –0.5 to 0.5 m/s.

State, streamtrace, and fate analyses of fish movements provided data to understand why the TDA sluiceway is effective. From these analyses, we made the following findings: (a)

[1] A *state* is a fish movement pattern in three dimensions (X, Y, Z). States are expressed as proportions, i.e., the proportion of fish exhibiting a particular pattern. There were 27 possible states.

[2] A *streamtrace* depicts the mean direction of fish movement. It is analogous to a flow line in a water velocity plot.

[3] A *fate* refers to the location where smolts exited the sample volume. Fates are expressed as probabilities of passage out a particular side of the sample volume, e.g., the sluiceway side.

Holding[4] was not observed at the sluice entrances, but was seen in front of the top portion of turbine intake entrances (we sampled the upper 4 m of the intake), and was especially prevalent at night off the west pier nose by the Main Unit (MU) 1-1 intake. (b) Smolt movement was complex and multi-directional in the nearfield of the Sluice 1-1 entrance. (c) A zone of entrainment or attraction revealed by the state data appeared to be relatively small (2-3 m from the dam), but this must be substantiated by analyzing water velocity and smolt movement data between the downstream edge of our sampling volume (1.5 m off the plane of the pier noses) and the sluice weir. (d) The zone of influence of the sluice flow net based on the fate data was about 6-8 m from the dam in the surface layer (0-2 m). And, (e) the probability of sluice passage was highest immediately upstream of the east side of the Sluice 1-1 entrance.

The SFB hypothesis tests using fish movement data from AFTS assessed the validity of two SFB premises, attraction and shallow preference. The attraction premise is that smolts are attracted to and actively seek certain hydraulic conditions associated with SFBs. The shallow preference premise is that smolts prefer shallow passage routes at dams, i.e., they prefer not to sound and are reluctant to pass through turbine intakes. The statistical analyses indicated support for the premises.

In summary, the TDA sluiceway is an effective, non-turbine route for passing smolts at The Dalles Dam because, for the most part, the smolt population migrating through the powerhouse is surface-oriented, can be concentrated at the west end of the powerhouse, is possibly attracted to the sluice flow net, and is reluctant to sound, preferring a shallow passage route over a deep one.

We recommend that research at the TDA sluiceway during J-occlusion evaluations address the following points:

- Assess specific hypotheses about smolt movements, such as: (a) the zone of influence associated with the sluiceway will be larger with J-occlusions than without; (b) the proportion of fish moving upward and toward the sluice entrances will be higher with J-occlusions than without; and (c) the overall probability of passage into the sluiceway will be higher with J-occlusions than without.
- Integrate observed smolt movement data with hydraulic data from a computational fluid dynamics model.
- Improve the AFTS tracking algorithm and sample closer to the dam than in 2000.
- Improve computational power to analyze a large Markov-Chain transition matrix for expanded spatial coverage of fate probabilities.
- Test the effects on sluiceway passage of surface illumination using existing lights at Sluice Gates 1-1, 1-2, and 1-3.

[4] Holding was defined as velocity in all dimensions less than 0.175 m/s. Fish were observed moving slowly upstream and downstream and sideways in front of the entrance, but at velocities greater than 0.175 m/s and therefore were not classified as “holding.”

PREFACE

This research was conducted under the auspices of the Corps of Engineers' Anadromous Fish Evaluation Program (study code SBE-P-00-017). The research is related to and complements surface flow bypass research at other dams and fish passage efficiency (FPE) research at TDA. This broader body of research includes Bonneville First Powerhouse prototype surface collector (SBE-P-00-6, 8, and 14), Bonneville Second Powerhouse corner collector (SBE-P-00-15), data integration for Bonneville Dam (SBE-P-0013), Lower Granite prototype surface bypass and collector (SBE-W-00-1, 2, 4, and 5), Rocky Reach prototype corner collector (Mid-Columbia proceedings), and The Dalles FPE (SPE-P-00-8).

This study was contracted by the U.S. Army Corps of Engineers, Engineering Research and Development Center, Waterways Experiment Station (WES), Environmental Laboratory, Fisheries Engineering Team. BioAnalysts, Inc. performed the work under contract to WES (BAA 99-3089, mod. 1) within the Broad Agency Announcement for general area conservation and research area EL-17 fish guidance and bypass systems. Tenera was subcontracted by BioAnalysts through BioSonics, Inc. WES and the University of Washington were funded for this study by the U.S. Army Corps of Engineers, Portland District.

ACKNOWLEDGMENTS

We gratefully acknowledge contributions to this study by:

- BioSonics, Inc. – Tim Acker, Dave Fuhriman, Dale Harkness, Lyle Harkness, Eddie Kudera, Brian McFadden, Colleen Sullivan, and Shui Yang
- Corps of Engineers -- Steve Dingman, John Nestler, Gene Ploskey, Marvin Shutters, and Miro Zyndol
- University of Washington -- Caitlin Burgess

TABLE OF CONTENTS

LIST OF FIGURES

LIST OF TABLES

1.0 INTRODUCTION

1.1 Background

Development of prototype surface flow bypass (SFB) systems is underway or being considered at many Columbia and Snake River dams. These SFB development efforts, however, could benefit from increased knowledge of fundamental smolt behavior at successful SFBs. The sluiceway at The Dalles Dam (TDA) is well known for its relatively high percentage of total project smolt passage (~10-50%) relative to the low percentage of total project flow it discharges (~1-5%) (e.g., Nichols 1979 and 1980; Nichols and Ransom 1980 and 1981; Steig and Johnson 1986; Johnson et al. 1987; BioSonics 1996; BioSonics 1999). In a recent sluiceway study at TDA, Ploskey et al. (2001) reported sluiceway efficiency and effectiveness data relative to the total project and the powerhouse (Table 1). Thus, the sluiceway at TDA is an example of an successful SFB that takes advantage of the surface-orientation of smolts encountering a mainstem Columbia River dam. However, three-dimensional, fine-scale movements of fish at the SFB entrance are not well understood. If we further understanding of why the TDA sluiceway is effective at passing smolts, then we can apply this knowledge to SFB development elsewhere. Furthermore, such information will provide a foundation to assess the effects of the new turbine intake occlusion structures to be evaluated at TDA in 2001.

Table 1. TDA sluiceway efficiency (percentage of fish) and effectiveness (percentage of fish divided by percentage of water) in 1999 from Ploskey et al. (2001). Spill ranged from 30 to 64% of total project discharge.

	SPRING		SUMMER	
	Relative to powerhouse	Relative to total project	Relative to powerhouse	Relative to total project
Efficiency	39%	13%	24%	10%
Effectiveness	13.37	8.57	9.17	6.88

Turbine intake occlusion plates were first tested at TDA in 1995 as a way to increase sluiceway passage and decrease turbine passage. However, no significant differences in sluiceway efficiency with and without occlusion plates were observed (Nagy and Shutters 1995). Occlusion plates were evaluated again in 1996 but the results were inconclusive, mainly because of difficulty estimating turbine passage behind the blockages (BioSonics 1996). In 2001, "J" sections will be added to the occlusion plates to alter hydraulic conditions with the intent to decrease turbine passage and improve biological performance of the sluiceway SFB and the spillway. Accordingly, in 2000 we collected detailed data describing three-dimensional fish movement in front of the sluice entrance and turbine intake at Main Unit 1-1 from April 17 to July 7 to support SFB development at TDA and elsewhere.

1.2 SFB Premises and Hypotheses

Since its inception in 1994, the Corps has attempted to base its surface flow bypass program on fundamental biological premises or assumptions. In 1995, as part of a SFB study conducted at Wells Dam, Johnson (1996) reviewed literature pertaining to two important assumptions associated with SFB development. Those assumptions were (a) smolts are attracted to areas of higher water velocity, i.e., exhibit negative rheotaxis, and (b) smolts prefer not to sound to pass a dam. He reviewed formally published and gray literature from 1950-1995 and concluded that the first premise was only partially acceptable because the information was mixed and collectively inconclusive. The second assumption was accepted, because the available information indicated that smolts were generally surface-oriented and would use a surface outlet when they could effectively locate it. We agree with these conclusions, given the information available at that juncture. Since that report was published, a variety of research efforts have been undertaken to further address surface flow bypass performance and its underlying premises.

A new set of SFB premises that addressed forebay collection using a spatial context was proposed by Johnson et al. (1997), and recently published in Giorgi et al. (2000). These premises were modified by Dauble et al. (1999) to include conveyance and outfall components, and to apply a behavioral context to the forebay component. Using 1995-1999 information from various SFB prototype sites on the Columbia and Snake rivers, both groups tried to establish bioengineering design criteria for SFB development. However, because the design of field studies did not permit isolation of individual treatment conditions, neither effort was able to identify consistent correlations between SFB efficiency and a variety of variables including, relative entrance size in either the vertical or horizontal dimension, flow ratios, entrance velocity, or acceleration indices.

We focused our research at The Dalles Dam sluiceway on smolt movements in the nearfield (within 10 m), also called discovery and decision zones by Dauble et al. (1999) (Figure 1). With the goal of increased understanding of the successful TDA sluiceway surface bypass, the following four SFB premises as applied at the TDA sluiceway were investigated qualitatively in the Discussion section of this report.

- Smolts are surface-oriented as they migrate in dam forebays.
- Horizontal distribution is concentrated in front of the SFB.
- There are certain visual cues at a portal that can facilitate passage of smolts.
- There is an entrainment zone associated with SFB entrances where velocities are sufficiently high to trap smolts and accelerating flows do not result in smolt avoidance.

The following two SFB premises were addressed quantitatively with smolt movement data from the active fish tracking sonar system at TDA in 2000.

- Smolts are attracted to and actively seek certain hydraulic conditions associated with SFBs.
- Smolts prefer shallow passage routes at dams, i.e., they prefer not to sound and are reluctant to pass through turbine intakes.

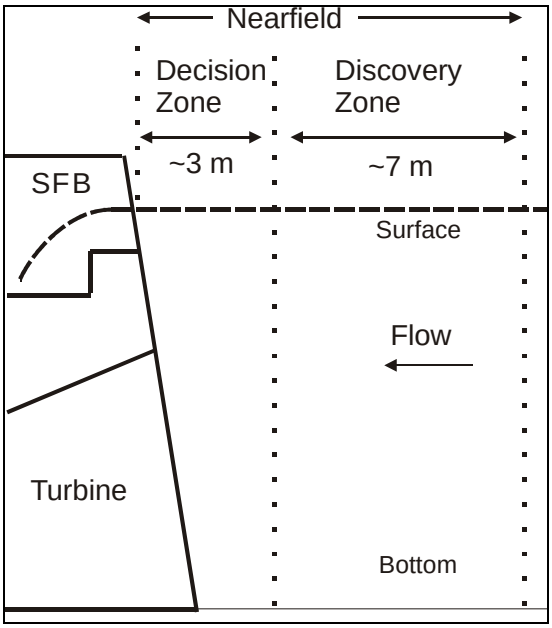

Figure 1. SFB zones, modified from Dauble et al. (1999) and Giorgi et al. (2000).

1.3 Goal, Study Period, and Objectives

The goal of this study was to explain why the sluiceway at TDA is effective at passing smolts. The study period was April 17 to July 7, 2000. In the nearfield (< 10 m) of the entrance at Sluice 1-1, the objectives were to:

1. Track smolt movements.
2. Estimate the proportion smolts displaying a given movement pattern (state[5]).
3. Determine streamtraces[6] of mean fish velocity.
4. Estimate the probability of sluice "passage" (fate[7]) from various locations in the sample volume.
5. Assess the SFB premises as applied to the nearfield sampling volume.

[5] A *state* is a fish movement pattern in three dimensions (X, Y, Z). States are expressed as proportions, i.e., the proportion of fish moving in a particular direction(s).

[6] A *streamtrace* depicts the mean direction of fish movement. It is analogous to a flow line in a water velocity plot.

[7] A *fate* is where smolts exit the sample volume. Fates are expressed as probabilities of passage out a particular side of the sample volume, e.g., the sluiceway side.

1.4 Report Organization

Following the introduction in Section 1, we describe the study site in Section 2. The methods and results are presented in Sections 3 and 4, respectively. The discussion is contained in Section 5. The main body of the report closes with conclusions and recommendations in Section 6 and literature cited in Section 7. Appendix A provides technical data on the active fish tracking sonar. An error analysis for the data acquisition system is presented in Appendix B. Appendix C contains detailed results of the statistical tests of SFB hypotheses.

2.0 STUDY SITE DESCRIPTION

2.1 General

The Dalles Dam (Figures 2, 3, and 4) is located at River Kilometer 308. It has a 637-m long powerhouse with a total generating capacity of 1,814 MW. Total hydraulic capacity of the 22-unit powerhouse is about 10,619 m^3/s (375 kcfs). Full pool elevation is rated at 48.7 m (160 ft) above mean sea level. Minimum operating pool elevation is 47.2 m (155 ft). The sill at each sluiceway entrance is at El. 46.0 m (151 ft). The turbine intake ceiling intersects the trashracks at El. 43.0 m (141 ft). The face of the dam is at an 11.3° angle off vertical (Figure 4). The 421-m long spillway is comprised of 23 bays with Tainter gates. A bathymetric map of the forebay shows the main channel of the river along the south shore, and deep areas in front of the powerhouse (Figure 3). Much of the forebay, however, is relatively shallow (< 20 m deep).

Figure 2. Aerial photograph of The Dalles Dam, Columbia River.

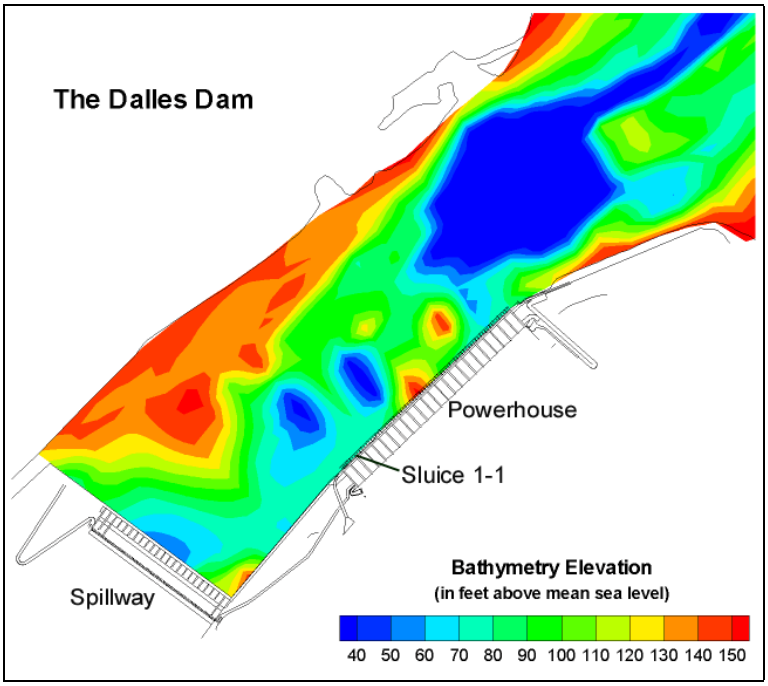

Figure 3. Plan view of The Dalles Dam showing forebay bathymetry.

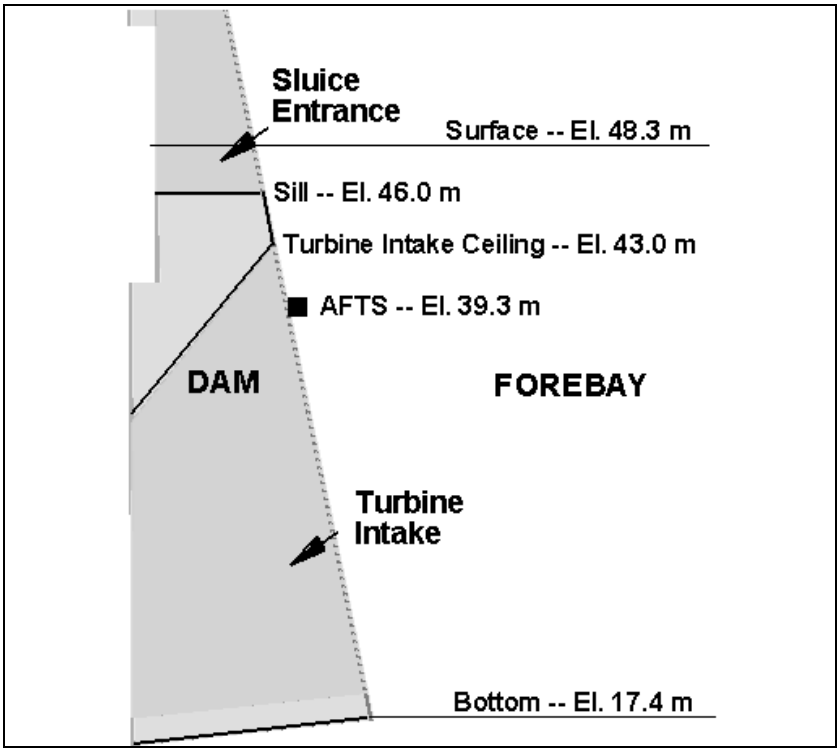

Figure 4. Sectional view of The Dalles Dam powerhouse showing sluiceway channel, sill, turbine intake, and location of the active fish tracking sonar (AFTS).

The TDA ice and trash sluiceway extends the entire length of the powerhouse. During the fish passage season (April through November), the three gates at Main Unit 1 are opened. This operation is based on previous research (e.g., Nichols and Ransom 1980). The capacity of the sluiceway is limited hydraulically to about 135 m^3/s to 142 m^3/s (4,750 to 5,000 cfs) because of a constriction in the downstream end of the channel near where it exits the powerhouse. Water enters the sluiceway from the forebay when automatic hoists move leaf gates off a sill at El. 46 m (151 ft). Sluiceway discharge is a relatively small proportion of total project discharge (~1-5%).

Removable plates resting against the upstream side of the trashracks can form intake occlusions. The occlusions block flow through the trashracks from the top of the intake to El. 30.5 m (100 ft), about one-half of the intake. In 2001, the occlusions are scheduled to be modified and tested with "J-sections" on their lower upstream edge to improve fish passage. In 2000, however, occlusion plates were *not* deployed.

2.2 River Environment and Project Operations

During our study (April 17 to July 7, 2000), river discharge at TDA ranged from 3,483 to 10,619 m^3/s (123 to 375 kcfs) (Figure 5). Mean daily discharge was 6,739 m^3/s (238 kcfs). Discharge peaked in late April and declined throughout the remainder of the study. Overall, discharge in January-July 2000 at TDA was 0.121 km^3 (97.9 kaf), or 92% of normal (50-year average) (Fish Passage Center Weekly Report #00-20). Daily powerhouse discharge during the study averaged 3,993 m^3/s (141 kcfs). The spill level for fish protection in the "juvenile pattern"

was 38% of total discharge, day and night. Daily spill flow during our study varied from 1,388 to 5,890 m^3/s (49 to 208 kcfs), with a mean of 2,747 m^3/s (97 kcfs) (Figure 5).

Forebay elevation during the study ranged from 47.7 to 48.6 m (156.6 to 159.5 ft) (Figure 6). Mean forebay elevation was 48.3 m (158.3 ft). With Gates 1-1, 1-2, and 1-3 fully open and the forebay at El. 158 ft, sluice discharge is 3,800 cfs (rating curve provided by Chris Goodell, Corps of Engineers Portland District, pers. comm.). Thus, sluice discharge was about 1.6% of mean daily discharge for the total project and 2.7% of total powerhouse discharge.

Water temperature during the study generally increased from 10.6 to 18.8° C (Figure 7). Turbidity was generally low at about 5 NTU (Figure 7).

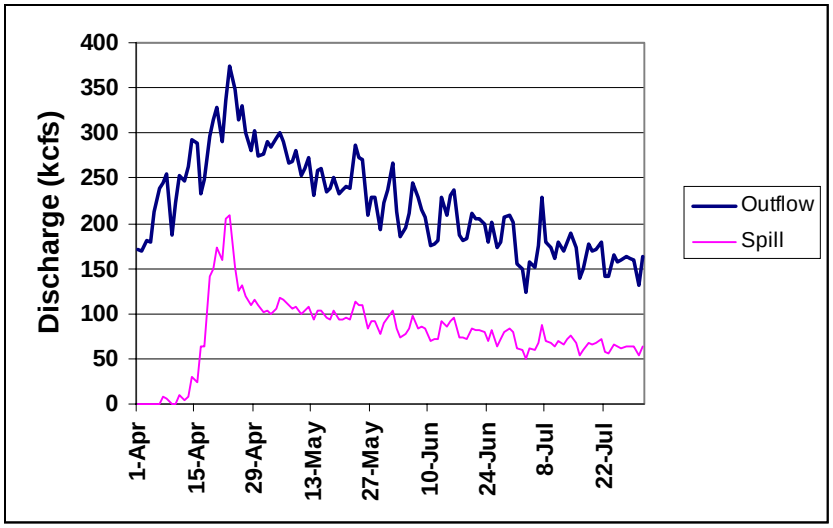

Figure 5. Total outflow and spill (kcfs) in April-July 2000 at TDA. Data were obtained from DART, an Internet website (http://www.cqs.washington.edu/DART/).

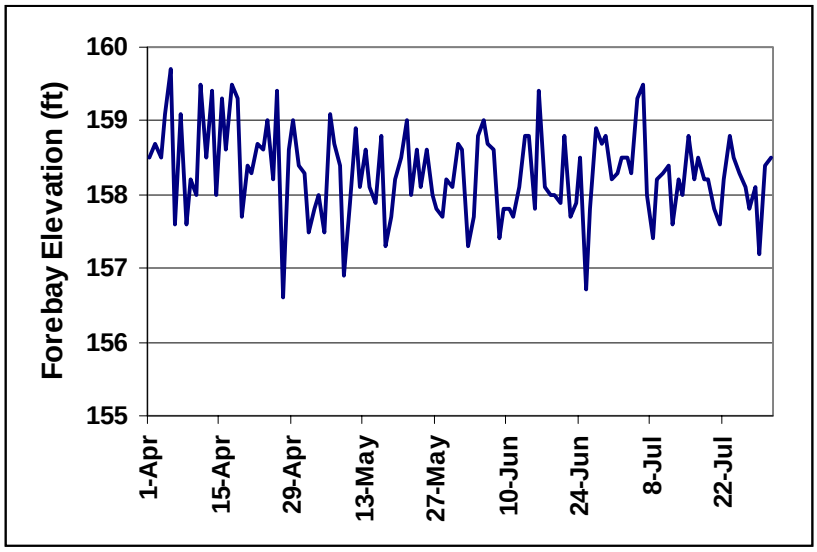

Figure 6. Forebay elevation in April-July 2000 at TDA. Data were obtained from DART, an Internet website (http://www.cqs.washington.edu/DART/).

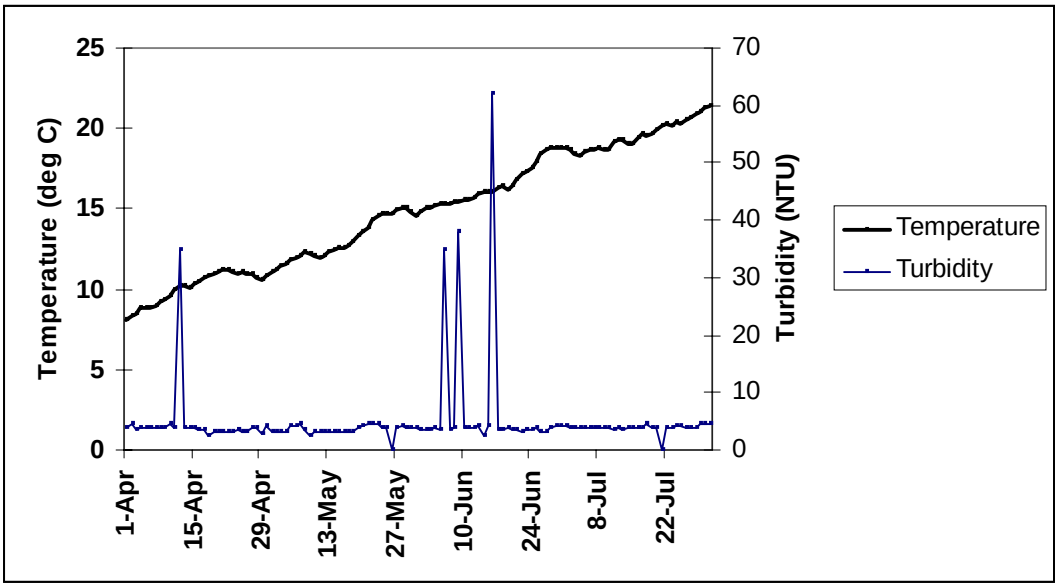

Figure 7. Temperature and turbidity in April-July 2000 at TDA. Data were obtained from DART, an Internet website (http://www.cqs.washington.edu/DART/).

2.3 Smolt Migration Characteristics

Data on smolt migration characteristics at TDA were based on the Smolt Monitoring Program's (SMP) sampling at John Day Dam. This is the closest SMP facility upstream of TDA; SMP sampling is not conducted at TDA. The data were not lagged because travel times between John Day and TDA are relatively fast (generally < 1 d, based on radio telemetry data, John Beeman, U.S.G.S. Biological Resources Division, pers. comm.).

Our study encompassed most of the migrations of yearling steelhead and yearling (stream-type) and subyearling (ocean-type) salmon (Figure 8). Passage of yearling fish peaked on May 2 and by mid-June yearling fish passage was essentially complete. Passage of subyearling fish peaked on June 29, and was relatively high throughout June and part of July (Figure 8). During our study (April 17 to July 7), subyearling chinook (42%) were the most abundant juvenile salmonid, followed by yearling chinook (29%), steelhead (17%), coho (10%), and sockeye (2%) salmon.

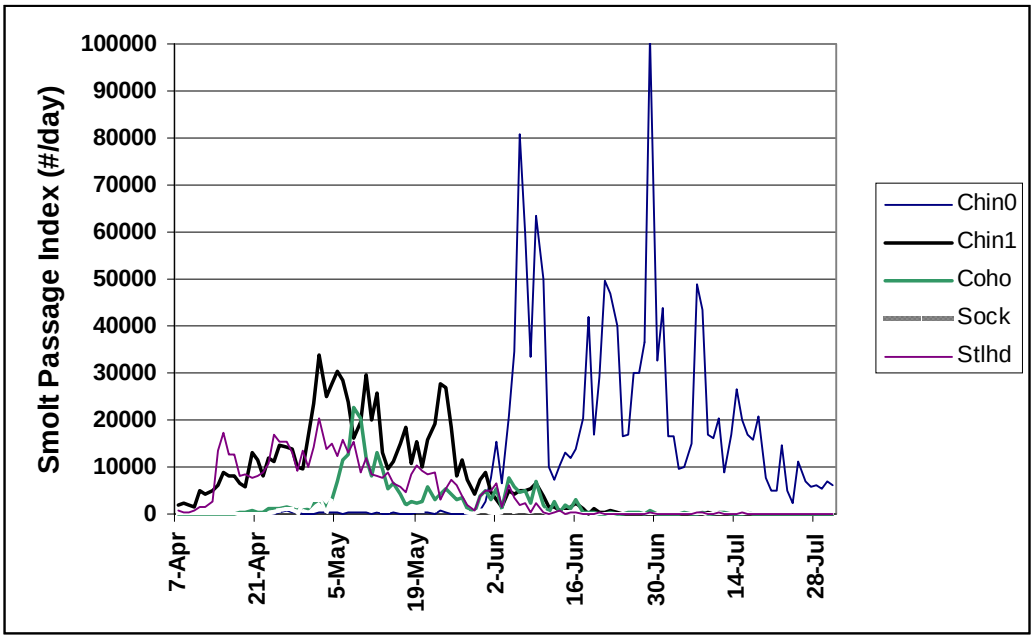

Figure 8. SMP index from John Day Dam for April-July 2000. Designations in the legend are for subyearling chinook salmon (Chin0), yearling chinook salmon (Chin1), coho salmon (Coho), sockeye salmon (Sock) and steelhead (Stlhd). Data were obtained from DART, an Internet website (http://www.cqs.washington.edu/DART/).

(Page intentionally blank.)

3.0 METHODS

3.1 General Approach

Our general approach was to intensively sample fish movements in the region immediately upstream of a sluiceway entrance and part of the turbine intake below it at TDA. We used an active fish tracking sonar (AFTS) to obtain fish movement data. AFTS as applied at a dam (described in Section 3.2.1 below) was first published by Hedgepeth et al. (1999). AFTS was also a key element in the Behavioral Acoustic Tracking System used to track acoustic-tagged fish (Johnson et al. 1998). MacLennan and Simmonds (1992) explain split-beam hydroacoustics, a main component of AFTS. The fieldwork with AFTS was complemented by a re-assessment of the SFB premises based on the review of pertinent literature.

3.2 Data Collection

3.2.1 AFTS System

The components of the AFTS system (BioSonics 1998) (Figures 9 and 10) included a 208 kHz BioSonics DT4000 digital split-beam echo sounder, a 7° split-beam transducer, two high-speed stepper motors for dual axis rotation, a controller unit, a laptop computer, a desktop computer, and cables. AFTS calibration and other technical data are presented in Appendix A.

The underwater portion of AFTS was located on the pier nose between Fish Unit (FU) 2-2 and Main Unit (MU) 1-1 at Elev. 39.3 m (128.8 ft). We measured the position of the transducer relative to Corps of Engineers survey point TDP-1 on the pier nose at FU 2-2/MU 1-1. (TDP-1 is at Northing 711330.7 ft, Easting 1839844 ft, and Elev. 185.2 ft.) The location of the AFTS transducer in Oregon State Plane NAD 27 horizontal datum and NGVD 29/47 vertical datum was Northing 711345.5 ft, Easting 1839853.8 ft, and Elev. 128.8 ft.

AFTS, which is based on the principle of tracking radar, operated as follows. The transducer was randomly aimed into the sample volume. Once a fish was detected, two high-speed stepper motors aligned the axis of the digital split-beam transducer on the target. As the fish moved, deviation of the target from the beam axis was calculated and used to re-aim the transducer, thereby tracking the target. A predictive tracking algorithm was used. It was a discounted least-squares fit (Brookner 1998), where the most recent velocity estimate (magnitude and direction) is weighted by unity, the next most recent by one-half, the next by one-fourth, the next by one-eighth, and so on. If no target was detected after 30 sec of pinging at a given position, the aiming angles were changed to another random position. The ping rate was approximately 10 pps. The echo sounder threshold was set at –60 dB on-axis. For each ping the target was tracked, data on fish X, Y, Z position relative to the transducer and target strength were recorded to disk. Fish position resolution can be inferred from the angular resolution (± 0.35°). At 10 m from the transducer, this would amount to ± 6 cm, and at 1 m the error would be ± 0.6 cm. See Appendix A for details on echo sounding and tracking. See Appendix B for an error analysis of AFTS.

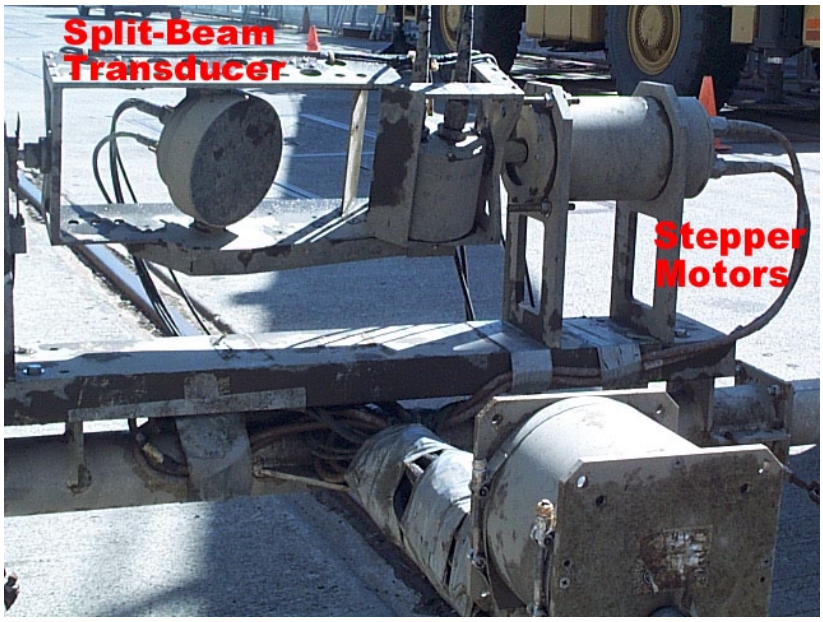

Figure 9. Underwater portion of AFTS.

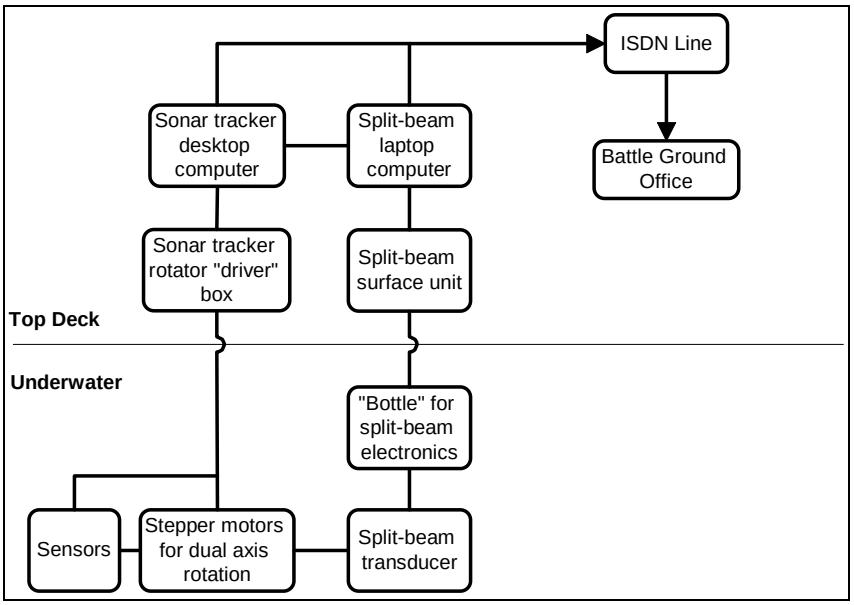

Figure 10. Schematic showing AFTS, with tracker and split-beam components, and data flow from TDA to Battle Ground, WA via ISDN line.

To summarize, we collected data from April 17 to July 7, 2000. Data are missing during June 23-26 and June 30-July 4 because of equipment malfunction. In the 73 days of data collection, we sampled ~5,000,000 fish positions corresponding to ~100,000 tracked fish.

3.2.2 Sample Volume

The sample volume was designed to cover the nearfield (< 10 m) at Sluice 1-1. AFTS was aimed to random positions within a 10 m cube in front of Sluice 1-1 (Figures 11 and 12). Once a target was acquired, AFTS was allowed to track fish that moved outside the initial random sampling zone. Thus, the zone for random positioning was a subset of the larger sample volume for data collection (Figures 11 and 12). In summary, the sample volume relative to origin on the FU 2-2/MU 1-1 pier nose at Elev. 158 ft was: X-dimension 15 m across (5 m west of the origin to 10 m east), Y-dimension from 1.5 m to 10 m away from the dam, and Z-dimension 9 m deep from the surface (Figures 11 and 12). Actual volume was about 1,350 m^3. The surface 0.5-m was excluded because of extraneous noise from wind-induced turbulence.

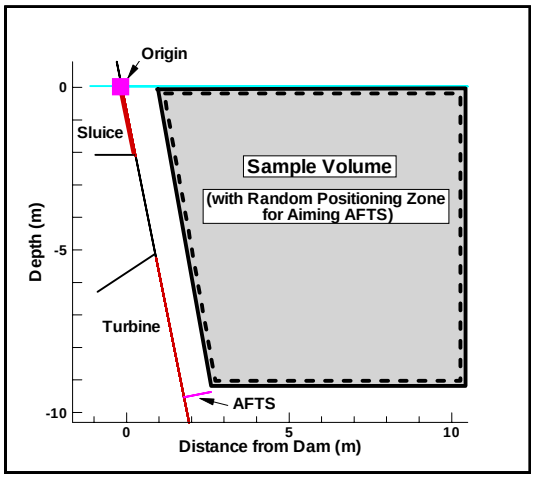

Figure 11. Side view of sample volume and the subset for AFTS random positioning sample zone.

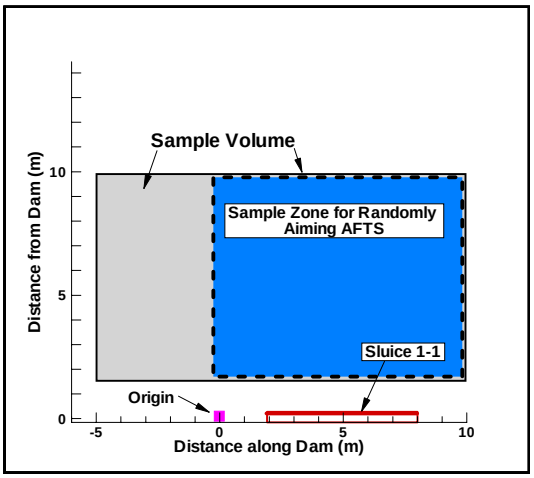

Figure 12. Plan view of sample volume and the subset for AFTS random positioning sample zone.

We established specific terminology to describe the three dimensions of the sample volume for this study (Figure 13). The origin for the "dam" coordinate system was the center of the MU1-1/FU2-2 pier nose at Elev. 48.2 m (158 ft). The sample volume was divided into thirds in each dimension. We designated regions of the three dimensions as follows: X "sections", Y "ranges", and Z "layers" (Figure 13). In the X dimension (parallel to the dam), the sections were "west", "sluice-west", and "sluice-east." In the Y dimension (perpendicular to the dam), the ranges were "near", "intermediate", and "far." And, in the Z dimension (vertically in the water column), the layers were "surface", "mid-depth", and "intake depth."

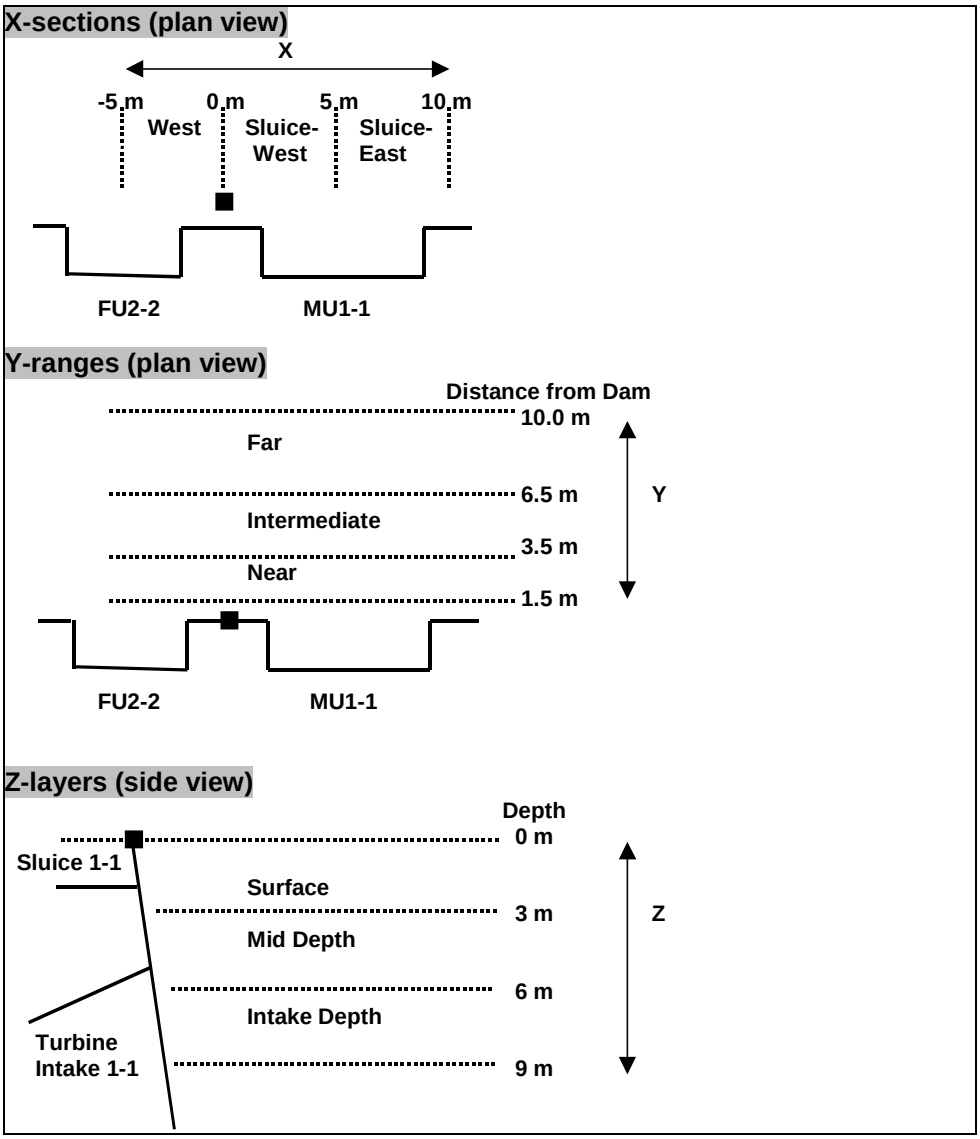

Figure 13. X "sections"(west, sluice-west, sluice-east), Y "ranges" (near, middle, far), and Z "layers" (surface, mid depth, intake depth). The solid black square designates the origin of the coordinate system.

3.4 Data Reduction and Analysis

Data reduction and analysis steps are shown in Figure 14. Hydraulic data were not available; thus, the analysis included only *observed* fish movement data. Typically, day and night periods (see definitions in Section 3.4.2) were analyzed separately because of known day/night differences in sluice passage (Ploskey et al. 2001).

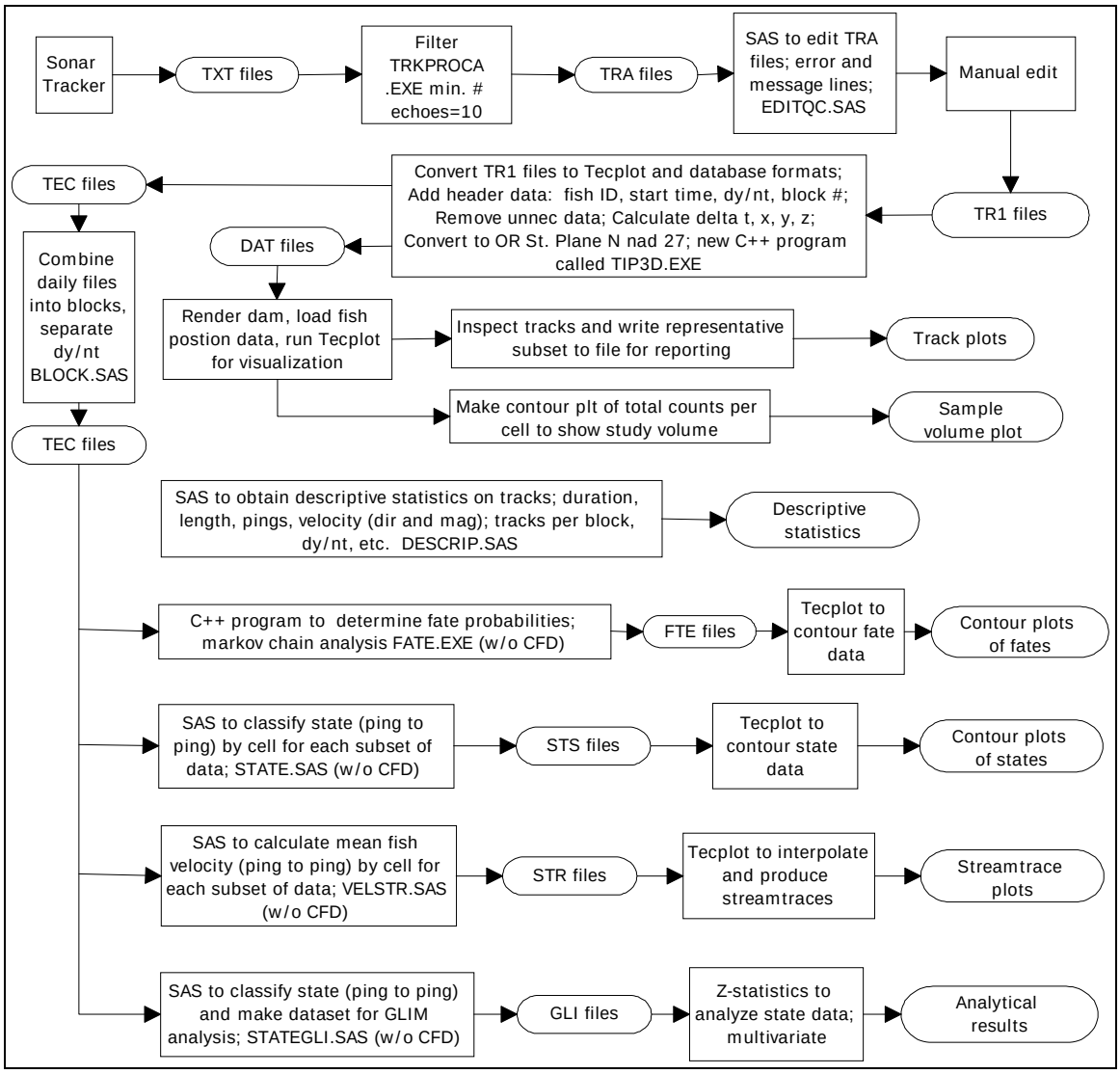

Figure 14. Data flow chart.

3.4.1 Editing

The tracking data from AFTS (TXT files) were filtered for minimum number of echoes per track (10) using a C-compiled program called TRKPROCA.EXE. The TRA output files from this program were reduced in a SAS-program called EDITQC.SAS, which removed unnecessary auxiliary information. The TRA files were also manually edited to delete fish track data for the 30-min period before any system crashes because as follows. During data collection, AFTS performed a positioning self-check every 30 min to check for slippage in rotator position. If there was slippage, AFTS stopped collecting data and waited to be re-started. This occurred seven times during the 73 days data were collected. Thus, data 30 min before these seven events could be erroneous and were deleted. The daily output files from the editing process were called TR1 files.

3.4.2 Database Formation

The daily TR1 files were processed using a C-compiled program called TIP3D.EXE. Two daily output files were produced: DAT files formatted to be loaded into Tecplot software (Amtec Engineering, Inc. Bellevue, Washington) and TEC files for further data and statistical analysis. Data processing by TIP3D included:

- *Reassemble tracks* – Separate tracks adjacent in time and space were reassembled. This usually occurred when AFTS automatically broke-off tracking when the maximum number of echoes per track was reached (800), or when maximum number of missing pings was reached (20).
- *Fish track identification number* – The purpose here was to give each track a unique identification number for subsequent data analysis. A fish track identification number was made from the date and an integer starting at 1 and proceeding consecutively.
- *Day/night determination* – Sunrise and sunset times for each date during the study period were obtained from the U.S. Naval Observatory website (http://aa.uno.navy.mil/AA/data/). The time of the start of a given fish track was then compared to the sunrise/sunset times to determine if the track was in day or night. A day/night designator was then written to the output file: day = 0 and night = 1.
- *Delta X, Y, Z, T calculations* – The difference in three-dimensional fish position (X, Y, Z) and time between consecutive echoes in a track was calculated as follows, using delta X as an example between the i and i+1 echoes of the track:

$$\Delta X = X_{i+1} - X_i$$

- *Conversion to dam coordinates* – The raw position data are in "tracker" coordinates, i.e., relative to the location of AFTS's split-beam transducer and rotators (centered at intersection of axes). This Cartesian coordinate system was converted to "dam" coordinates for the purposes of display and analysis. The origin of the "dam" coordinate system (see Figure 11) was the center of the MU1-1/FU2-2 pier nose at Elev. 48.2 m (158 ft).
- *Conversion to Oregon State plane coordinates* – Similarly, the raw position data were also converted to Oregon State Plane NAD 27 coordinates. This is the same coordinate system that other researchers and CFD modelers will use.

3.4.3 Blocking

For the purpose of SFB hypothesis testing only, we blocked the data into 2-week periods to examine any effects of time of season. The intent of blocking was to represent composite effects from seasonal changes in species composition, river discharge, temperature, and other environmental conditions. A block size of 2-weeks[8] was chosen because this was a reasonable

[8] Block 5 is 3 weeks long because there were nine missing study-days. Thus, the number of days in the block was comparable with the others.

amount of time for these changes to manifest themselves. A larger block size would possibly mask any changes; a smaller block size would run the risk of too few fish tracks. Because of the later point, 1-day blocks certainly would not be acceptable. Hansen et al. (1953, p. 229) stated, "The determination of the strata is a matter in which effective use can be made of prior knowledge, personal intuition, and judgment, as well as of objective statistical information that may be available. Whether objective information is available or not, the final determination of the strata is a subjective matter, in which the decisions must be judgments. Statistical theory does not provide a general series of procedures or steps for determining the one best set of strata."

The SAS-program BLOCK.SAS was used to complete the database. It concatenated the daily TEC files into approximately two-week blocks. In addition, separate day and night files for each block were created. The blocks were:

- Block 1 = 4/17 to 4/30;
- Block 2 = 5/1 to 5/15;
- Block 3 = 5/16 to 5/30;
- Block 4 = 5/31 to 6/14;
- Block 5 = 6/15 to 7/7.

3.4.4 Track Visualization

We used Tecplot software to visualize the fish tracks obtained from AFTS. To do this, we first rendered the dam in Tecplot. Then the specific tracks contained in the DAT files from TIP3D were turned into "zones" in Tecplot. The tracks were superimposed on the dam rendering, both of which were in "dam" coordinates. Tecplot visualization allowed us to manipulate and explore the three-dimensional nature of the tracks relative to the dam.

3.4.5 Descriptive Analysis

Descriptive data on the data set were obtained using the SAS-program DESCRIP.SAS. Using the TEC files as input, DESCRIP.SAS produced the following data for each day/night period in each block:

- number of observations (distinct fish positions);
- mean, minimum, and maximum number of echoes per track;
- mean, minimum, and maximum positions in the X, Y, and Z dimensions;
- mean, minimum, and maximum velocities in the X, Y, and Z dimensions;
- frequency distribution of velocities in the X, Y, and Z dimensions.

3.4.6 Analysis of States

For our purposes, states are fish movement patterns in the three dimensions (X, Y, Z). (These are not the same as Markovian states.) For example, movement west and toward the dam with little change vertically is a state (individual states are formally defined below). The basic

data for the descriptive analysis of states are the ping-to-ping movements (position changes) within AFTS fish tracks. Using successive position changes, velocity (XVEL) was calculated for each dimension as follows, using X as an example:

$$XVEL_{i+1} = \frac{\Delta x}{\Delta t} = \frac{x_{i+1} - x_i}{t_{i+1} - t_i}$$

where,

x_i = *X coordinate of the ith ping;*

t_i = time of the *i*th ping.

A key step in the analysis of states was to distinguish between movement and no movement. (Holding is the term we use for "no" movement.) Thus, we posed a question, "How much movement does it take to be defined as moving?" To make this distinction, we examined the sensitivity of the percentage of holding to the movement velocity threshold (Table 2). We expected some holding and we expected more during night than day based on the echograms. The percentage ping-to-ping velocities classified as holding increased dramatically between movement velocity thresholds of 0.175 and 0.2 m/s. Thus, we set the movement velocity threshold at 0.175 m/s. This corresponded to approximately one body length per second. By definition, less than or equal to 0.175 m/s was holding, greater than 0.175 m/s was moving. In summary, with the permutations of moving and not moving in either of two directions (+ or -) in the three dimensions, there were 27 mutually exclusive and exhaustive states of fish movement (Table 3).

Table 2. Sensitivity analysis of the percentage of ping-to-ping movements classified as holding related to various movement velocity thresholds. By definition, holding was when ping-to-ping movement in all three dimensions was less than or equal to the velocity threshold. Total number of observations (fish positions) was 332,660 in Block 1 Day and 1,079,227 in Block 1 Night. Data for night with velocity at 0.2 and 0.25 were unnecessary because of the dramatic increase from 0.175 in number holding at these levels during day. The chosen threshold is in bold.

	BLOCK 1 DAY		BLOCK 1 NIGHT	
VELOCITY THRESHOLD (m/s)	NUMBER HOLDING	PERCENTAGE HOLDING	NUMBER HOLDING	PERCENTAGE HOLDING
0.1	23,526	7%	79,991	7%
0.15	25,059	8%	84,446	8%
0.175	31,782	10%	122,537	11%
0.2	68,995	21%	----	----
0.25	79,015	24%	----	----

Table 3. Velocity criteria to define states of ping-to-ping fish movement.

NO.	STATE	CODE	X VELOCITY	Y VELOCITY	Z VELOCITY
1	Holding	hold	abs(X)<0.175	abs(Y)<0.175	abs(Z)<0.175
2	East, away, and up	eau	>0.175	>0.175	>0.175
3	East, away, and down	ead	>0.175	>0.175	<-0.175
4	East, toward, and up	etu	>0.175	<-0.175	>0.175
5	East, toward, and down	etd	>0.175	<-0.175	<-0.175
6	West. Toward, and down	wtd	<-0.175	<-0.175	<-0.175
7	West, toward, and up	wtu	<-0.175	<-0.175	>0.175
8	West, away, and down	wad	<-0.175	>0.175	<-0.175
9	West, away, and up	wau	<-0.175	>0.175	>0.175
10	East and away	eaaw	>0.175	>0.175	abs(Z)<0.175
11	East and toward	eato	>0.175	<-0.175	abs(Z)<0.175
12	West and away	weaw	<-0.175	>0.175	abs(Z)<0.175
13	West and toward	weto	<-0.175	<-0.175	abs(Z)<0.175
14	East and up	eaup	>0.175	abs(Y)<0.175	>0.175
15	East and down	eadn	>0.175	abs(Y)<0.175	<-0.175
16	West and up	weup	<-0.175	abs(Y)<0.175	>0.175
17	West and down	wedn	<-0.175	abs(Y)<0.175	<-0.175
18	Away and up	awup	abs(X)<0.175	>0.175	>0.175
19	Away and down	awdn	abs(X)<0.175	>0.175	<-0.175
20	Toward and up	toup	abs(X)<0.175	<-0.175	>0.175
21	Toward and down	todn	abs(X)<0.175	<-0.175	<-0.175
22	East	east	>0.175	abs(Y)<0.175	abs(Z)<0.175
23	West	west	<-0.175	abs(Y)<0.175	abs(Z)<0.175
24	Away	away	abs(X)<0.175	>0.175	abs(Z)<0.175
25	Toward	towd	abs(X)<0.175	<-0.175	abs(Z)<0.175
26	Up	upwd	abs(X)<0.175	abs(Y)<0.175	>0.175
27	Down	down	abs(X)<0.175	abs(Y)<0.175	<-0.175

To perform the state analysis, each ping-to-ping movement was classified into a state. Next, each of these data points was positioned in a $(0.5\ m)^3$ cell in the sample volume. For a given cell, the number of observations for each state and a total were tallied. The binomial (moving in a particular direction of a given dimension or not) unconditional proportion of seeing any one state in that individual cell ($\hat{s}_i$) was computed as follows:

$$\hat{s}_i = \frac{t_i}{total}$$

where,

t_i = number of observations of state i in a given cell (i=1,…,n);

total = total number of observations in a given cell.

The estimated variance of $\hat{S}_i$ was computed as:

$$Var\left(\hat{s}_i\right) = \frac{\hat{s}_i\left(1-\hat{s}_i\right)}{total}.$$

Next, we combined states based on the two general directions of movement in each dimension: X = east (+) and west (-); Y = away (+) and toward (-); and Z = up (+) and down (-). This allowed us to more effectively convey information about general smolt movements at the TDA sluiceway than would have been the case with 27 individual states. The state data were combined as follows (see Table 3 for state codes):

alleast = eau + ead + etu + etd + eaaw + eato + eaup + eadn + east;

allwest = wtd + wtu + wad + wau + weaw + weto + weup + wedn + west;

alltoward = etu + etd + wtd + wtu + eato + weto + toup + todn + towd;

allaway = eau + ead + wad + wau + eaaw + weaw + awup + awdn + away;

allup = eau + etu + wtu + wau + eaup + weup + awup + toup + upwd;

alldown = ead + etd + wtd + wad + eadn + wedn + awdn + todn + down.

Including all states except holding, the proportions of movement in the six combined states for a given cell were computed two ways, unconditional and conditional proportions. Unconditional proportions are based on the database in its entirety, i.e., no conditions. Conditional proportions are based on subsets of the database that do not including holding movements, i.e., the condition is movement in a particular dimension. Z-statistics (Snedecor and Cochran 1980) were used to analyze specific subsets of the conditional proportions to address some surface bypass hypotheses (see Section 3.5).

Unconditional proportions for each cell in the state analysis were computed as follows:

$$\hat{P}_u\left(east\right) = \frac{alleast}{total};$$
$$\hat{P}_u\left(west\right) = \frac{allwest}{total};$$
$$\hat{P}_u\left(away\right) = \frac{allaway}{total};$$
$$\hat{P}_u\left(toward\right) = \frac{alltoward}{total};$$
$$\hat{P}_u\left(up\right) = \frac{allup}{total};$$
$$\hat{P}_u\left(down\right) = \frac{alldown}{total}.$$

Conditional proportions for each cell the state analysis were computed as follows:

$$\hat{P}_c(east) = \frac{alleast}{alleast + allwest};$$

$$\hat{P}_c(west) = \frac{allwest}{alleast + allwest};$$

$$\hat{P}_c(away) = \frac{allaway}{allaway + alltoward};$$

$$\hat{P}_c(toward) = \frac{alltoward}{allaway + alltoward};$$

$$\hat{P}_c(up) = \frac{allup}{allup + alldown};$$

$$\hat{P}_c(down) = \frac{alldown}{allup + alldown}.$$

3.4.7 Analysis of Streamtraces

Streamtraces of fish velocities were produced in Tecplot. (Recall streamtrace definition on p. 3.) Mean ping-to-ping velocity for each dimension (X, Y, Z) was calculated for each 0.5 m cell in the sampling volume. Velocity estimates for cells missing data were obtained using Tecplot's linear interpolation procedure. Two dimensional plots, plan view (X-Y) and side view (Y-Z), were made separately for day and night for data combined over the entire study period.

3.4.8 Analysis of Fates

For the purpose of this study, a *fate* is specified by where fish tracks exited the sample volume. Fates are expressed as probabilities of passage toward a particular area, e.g., the sluiceway. To determine fate probabilities, we applied a Markov analysis (Taylor and Karlin 1988, pp. 95-266), which described smolt movement as a stochastic process. A couple key ideas from Taylor and Karlin (1998, pp. 95-96) are: (a) a Markov process $\{X_t\}$ is a stochastic process with the property that, given a value X_t, the values of X_s, for $s>t$ are not influenced by the values of X_u for $u<t$, and (b) transition probabilities are functions not only of the initial and final states, but also of the time of transition as well. When the one-step transition probabilities are independent of the time variable, then the Markov chain has stationary probabilities. The Markov-chain analysis for the 2000 TDA sonar tracker study included the following assumptions.

- The movements can be described by a one-step Markov process. In other words, movement decisions are based on the smolt's current position and not upon the prior history getting to that position.
- The transition probabilities are estimated from independent fish observations.
- The transition matrix is stationary.

As with the state analysis, the three-dimensional sample volume in front of Sluice 1-1 was divided into cells (modified for fate analysis as follows: 0.5 x 0.5 x 0.5 m for X, Y, Z, respectively). The sample volume was decreased to reduce the size of the Markov matrices: X =

0.0 to 10.0 m, Y = 1.5 to 10.0 m, and Z = 0.0 to –6.0 m. At the boundaries (sides) of the volume, we defined these passage fates:

- Sluice – cells on side facing the sluiceway, 0.0 to 4.0 m deep;
- Turbine – cells on side facing the sluiceway, 4.0 to 6.0 m deep;
- West – west side cells;
- East – east side cells;
- Bottom – bottom cells of the volume;
- Reservoir – cells of side facing the reservoir upstream;
- Unknown – no movement.

The Markov transition matrix was a square matrix the size of k x k, where k is the number of distinct cells being modeled (k = 4,080). The ijth element in the ith row of the jth column of the transition matrix was the estimated probability (p_{ij}) of moving from cell i to cell j in the next time step. These probabilities were estimated by

$$\hat{p}_{ij} = \frac{x_{ij}}{n_i}$$

where,

n_i = number of observations of smolts in the ith cell;

x_{ij} = number of observations where a smolt in cell i moved to cell j in the next time step.

The cells (0.5 x 0.5 x 0.5 m) that bordered the sides of the volume of interest (sluice, turbine, west, east, bottom, and reservoir) were set to unity to absorb any movement that reached a particular "fate." Otherwise, the C-compiled program FATE.EXE tallied the transition matrix T using a time step of 1 sec, and the average position (i.e., $\sum x_t / n$) during each 1-sec interval a fish was tracked. This program required that a fish be tracked for at least two seconds before the transition matrix was amended to obtain indices i and j (i from the first interval, j from the second). Non-boundary (including surface) cells were checked to ensure non-zero and non-unity values. If zero or unity was present in an i,i cell after building the matrix T from a set of data, then the closest i,i cell in Cartesian space was found that contained data and was used to augment that particular set of i,j's. This process created a situation that guaranteed fish movement to one of the absorbing boundaries if there was movement to begin with.

The transition matrix T for one time step was then used to estimate the transition for two or more time steps as:

T^t

where, t = the number of time steps. For this study, t = 4,096 so that the Markov process reached stability, i.e., the transition matrix did not change with additional time steps. The ultimate fate of smolts would be calculated as:

$$T^{4096}.$$

After 4,096 time steps (corresponding to 68 min), probabilities for each of the seven fates for each of the 2,970 cells, not including border cells, were extracted from the transition matrix and written to file. The fate data were displayed in Tecplot.

The key assumption in this analysis is that the data exhibit the Markov property (see first assumption above). The one-step model we used in the analysis of day and night fish movement assumed movement to a future cell depended entirely on the fish's current position, not its prior history. However, movement could depend on both the current and past histories. A R x C table was used to test whether movement from B to C_i is independent of previous position A_i. As many cells as were practical were tested in this manner. Movement and cells were measured using a time step of 1 s and 0.5 m per side cells with x values from 1 to 6.5 m (i=0…10), y values from 1 to 6.5 m (i=0…10), and z value from –3.5 to –0.5 m (k=0…5). Cell codes were formed as i+j*11+k*121. A Chi-Square test was not valid due to the sparseness of the contingency tables. Therefore, conclusions about appropriateness of the first order assumption of a one-step Markov process were based on Fisher's exact test (Sokal and Rohlf 1981, p. 740).

A total of 270 cells during daytime and 226 during nighttime out of the possible 726 were tested. In general, movement was tested to be independent of prior position. P values less than 0.05 showed significance in 24 (8.9 %) of the cases during daytime and 18 (8.0%) of cases at night. That is, the null hypothesis of lack of association was rejected in fewer than 9% of the cases examined. This is a good indication that our use of the Markov chain was appropriate for characterizing movement through the volume near Sluice 1-1.

3.5 Assessment of SFB Premises

Methods for assessing SFB premises included literature review, contour plotting, and exploratory statistical tests using Z-statistics. The logic for the null and alternative hypotheses of the Z-tests was as follows. The working hypotheses stated earlier (i.e., the SFB premises in the Introduction) were the alternative hypotheses in formal testing (H_a). The choice of working hypotheses was based on anticipated mechanisms important in the passage of smolts at a surface bypass collector. This was an important step in the analysis because it attempted to analyze fish movements within a scientific framework for SFB based specific premises. The following specific Z-tests were performed on the conditional proportion data for the movement states, addressing two of the six premises (attraction and shallow preference):

- Attraction -- In the near and intermediate ranges of the surface layer of the sluice sections,

  H_o: $P(\text{toward}) \leq P(\text{away})$, H_a: $P(\text{toward}) > P(\text{away})$.

- Shallow Preference-- In the 1 m layer immediately below the sluice sill (2-3 m deep),

H_o: P(up) ≤ P(down), H_a: P(up) > P(down).

For each statistical analysis, the null hypothesis was tested with a 1-tailed Z-test for each time block and separately for day and night periods (i.e., total of 8 tests). The dependent variable was an observation of movement in one of two directions. Thus, we assumed movement for a particular episode had a binomial distribution. The Z-statistics, p-values and observed proportions estimated along with associated standard error and asymptotic 95% confidence interval are provided. The assumption of independence (randomness) in fish position data was assessed using a runs up/down test (Sokal and Rohlf 1981, pp. 785-787).

In addition, the separate Z-tests were combined in a meta-analysis that examined the null hypotheses for daytime, nighttime, and all times combined. The p-values were determined for the meta-analysis as follows. The observed p-values, which are uniformly distributed (0,1) under H_o, were transformed into chi-square statistics of with 2 degrees of freedom, i.e.,

$$-2\ln P \sim \chi_2^2$$

where *P* is the observed p-value. The overall test was then based on the sum of the independent χ_2^2's such that

$$\sum_{i=1}^{k} \chi_2^2 = \chi_{2k}^{2^*}$$

for k data tests. The overall p-value of the meta-analysis was then found as

$$P\left(\chi_{2k}^2 \geq \chi_{2k}^{2^*}\right) = \text{P-value}\,.$$

Also reported are the proportions estimated separately for day and night time periods. A GLIM analysis was also performed to examine whether the proportions (e.g., up or towards) varied between blocks and day/night periods. An analysis of deviance table (ANODEV) was presented along with F-statistics and p-values. McCullagh and Nelder (1983, pp. 26-28, also pp. 166-167) discuss ANODEV. The asymptotic F-test derived from ANODEV was described by Crawley (1983, pp. 223-225).

4.0 RESULTS

AFTS provided accurate and precise smolt position data (± 0.35°), as demonstrated in the error analysis (Appendix B). Johnson et al. (1998) also substantiated AFTS performance. The 2000 AFTS data set is representative of smolt movements in the nearfield of TDA Sluice 1-1. The 2000 study results are contained in sections on sample volume, descriptive data, smolt movement patterns as analyzed by states, streamtraces, and fates, and statistical analysis of SFB hypotheses. Data were combined over entire study period (April 17 to July 7, 2000), then separated into day and night periods, except for blocking for SFB hypothesis tests.

4.1 Sample Volume Based on Observed Fish

Overall, fish position data were collected over about 19 m in the X dimension (along the dam east/west), 14 m in the Y dimension (toward/away from the dam), and 10 m in the Z dimension (up/down in the water column) (Table 4). Sample coverage was similar between day and night (Table 4). Actual sampling intensity was highest in front of MU 1-1 and the pier nose where AFTS was located (Figure 15) because of a relatively high amount of holding there, especially at night (see results section 4.2). The sampling volume was wedge-shaped, with the widest part near the surface and the thinnest part near the transducer (Figures 16 and 17). Thus, the region of interest in the nearfield immediately in front of Sluice 1-1 was reasonably well sampled. A subset of this volume was taken to smooth the sides for data analysis; the X dimension was 15 m wide, the Y dimension was 10 m out from the dam, and the Z dimension was 9 m deep.

Table 4. Total sampling volume as represented by mean and range of fish positions (in meters) relative to dam coordinate system. The origin is at centerline of MU1-1/FU2-2 pier nose at the water surface (Elev. 158 ft). Positive X is to the east and negative X is to the west. Positive Y is away from the dam and negative Y is toward the dam. Positive Z is upward and negative Z is downward. Data are means of block data for the purpose of this general summary; blocks are defined in Section 3.4.3.

PERIOD	DIMENSION	MEAN	MINIMUM	MAXIMUM
Day	X	2.42	-7.83	11.11
	Y	5.55	1.53	16.16
	Z	-4.25	-10.69	0.06
Night	X	1.67	-7.74	11.13
	Y	5.41	1.64	15.34
	Z	-4.63	-10.29	0.06
Overall	X	2.04	-7.78	11.12
	Y	5.48	1.58	15.75
	Z	-4.44	-10.49	0.06

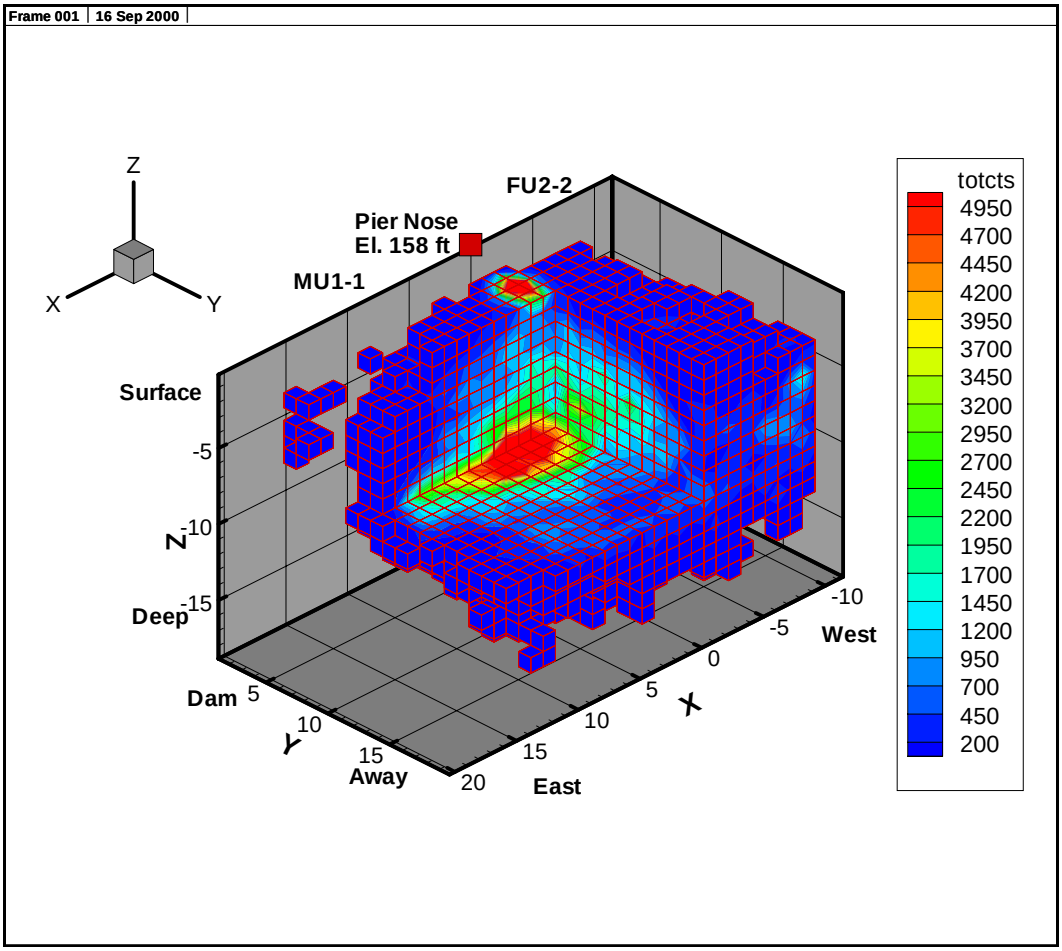

Figure 15. Three-dimensional contour plot[9] of total number of fish position data points per 0.5-m cell. Note the section removed at X = 0, Y = 6, and Z = 9 cells from the origin. The origin of the "dam" coordinate system used in this figure is represented by the square box on the pier nose at Elev. 158 ft. Axis scale is in 0.5 m increments, e.g., X = 10 represents the plane 5 m east of the origin. AFTS was located at X = 0, Y = 0, and Z = -18 cells.

[9] This plot shows that AFTS did not preferentially track fish furthest from the transducer where the acoustic beam was widest, because otherwise highest target concentrations would have been at the edges of the volume in this figure.

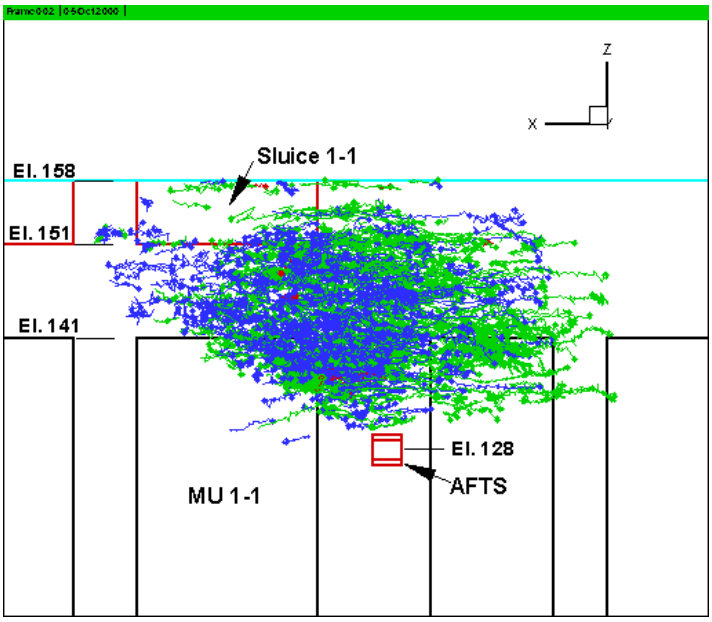

Figure 16. Front view showing the extent of the sample volume as depicted by fish tracks from May 1-10, 2000. Green signifies mean target strength is greater than –45 dB. Blue signifies mean target strength is less than or equal to –45 dB. Note that –45 dB target strength corresponds to a fish length of approximately 100 cm.

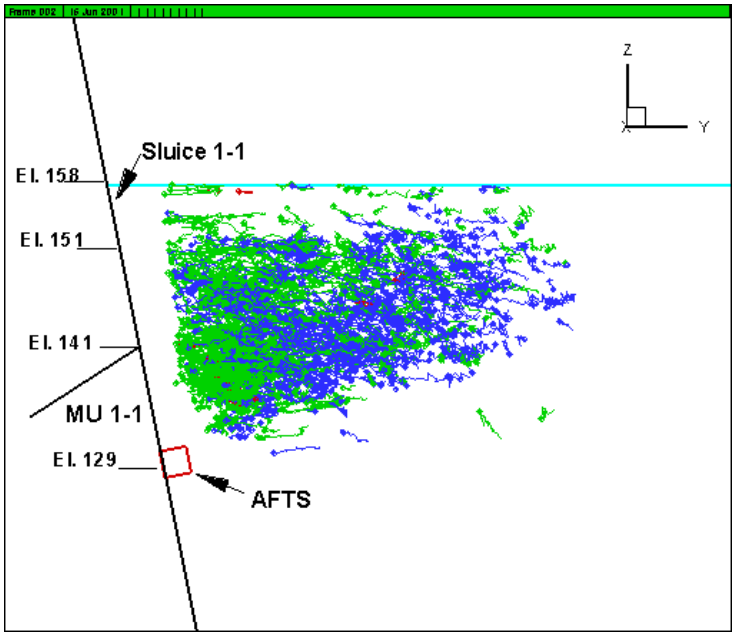

Figure 17. Side view showing the extent of the sample volume as depicted by fish tracks from May 1-10, 2000. Track color codes are defined in Figure 16.

4.2 Descriptive Data

The database for this study consisted of about 5,000,000 three-dimensional fish positions from about 100,000 fish tracks (Table 5). More fish positions were recorded during night than day, but more fish were tracked during day than night. The mean number of positions per track during day was about 1/3 those at night (Table 5). This was due to more "holding" during night than day. Section 4.3 contains further analysis of holding patterns.

Table 5. Summary of fish tracking data from AFTS.

PERIOD	TOTAL X,Y,Z POSITIONS	TOTAL FISH TRACKS	MEAN (POSITIONS/TRACK)
Day	1,791,751	61,050	29
Night	3,155,694	36,040	88
Total	4,947,445	97,090	51

The directions for overall mean velocities for day, night, and combined were negative in each dimension (i.e., X westward, Y toward the dam, and Z downward in the water column), while mean magnitudes were close to 0 m/s (Table 6). Most observed fish velocity measurements (ping-to-ping) were between –0.5 and 0.5 m/s (Figure 18). Numbers of positive and negative values were comparable (Figure 18).

Table 6. Summary of mean fish velocity data (m/s) from ping-to-ping. Data are means of block summary data for the purpose of this general summary. Positive X is to the east and negative X is to the west. Positive Y is away from the dam and negative Y is toward the dam. Positive Z is upward and negative Z is downward.

PERIOD	DIMENSION	OVERALL MEAN
Day	X	-0.09
	Y	-0.06
	Z	-0.02
Night	X	-0.01
	Y	-0.05
	Z	-0.01
Combined	X	-0.05
	Y	-0.05
	Z	-0.01

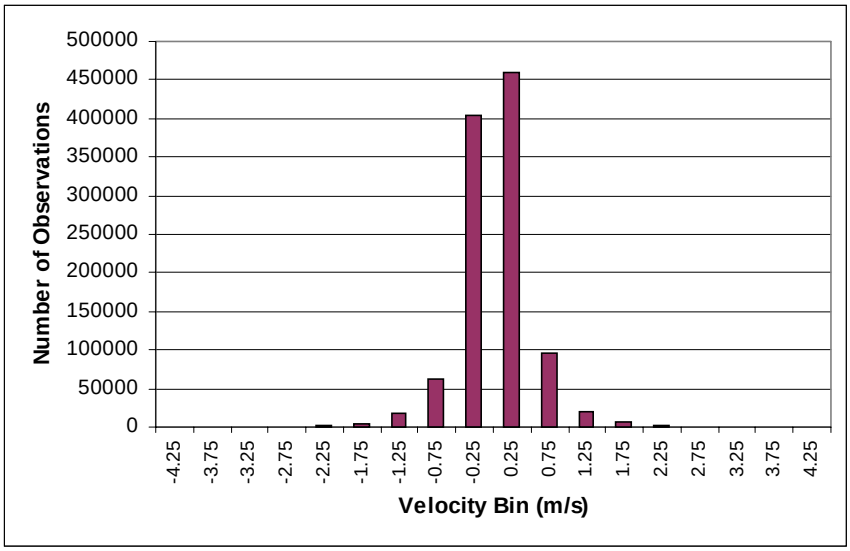

Figure 18. Typical frequency distribution for velocity data; example data for X-dimension from Block 1, night. Velocity bins are 0.5 m/s wide; the label is the velocity for the midpoint of the bin.

Fish tracks in the sample volume were variable in shape and length (Figure 19). Some fish held in front of MU 1-1 or the MU 1-1/FU 2-2 pier nose. Others moved directly up and toward Sluice 1-1. Some fish swam away from the dam, while others moved westward. Fish movements occurred in all directions, revealing active swimming behavior in the nearfield of the dam. Fish apparently were neither passively entrained nor simply following the dominant water currents.

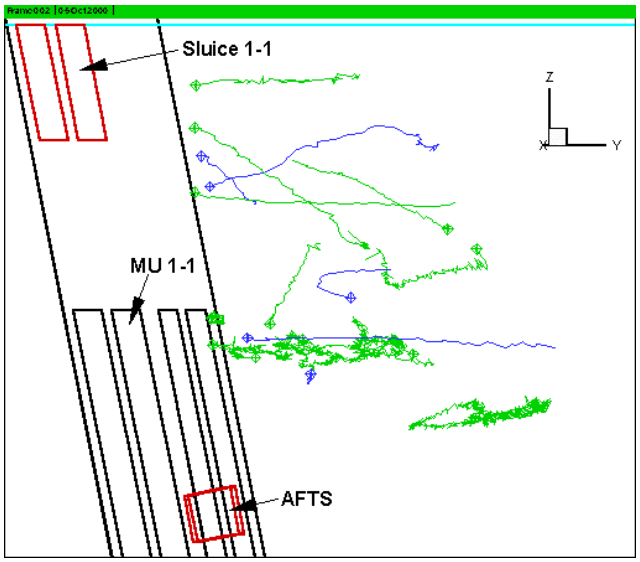

Figure 19. Three-dimensional view of example tracks from AFTS on May 1, 2000. Track color codes are defined in Figure 16. Diamonds depict the end of each track.

Mean target strength of tracked fish was higher during night (-43.0 dB) than day (-48.4 dB) (Table 7 and Figure 20). During night, mean target strength generally decreased as the study progressed (Table 7). During day, block-to-block target strength was relatively consistent (Table 7). Frequency of target strength for both day and night were normally distributed, although day was flatter than night (Figure 20). Since more holding behavior was observed during night than day, higher target strengths at night could have been caused by relatively large fish showing a propensity to hold at night. We suspect that these fish were juvenile steelhead, the largest downstream migrants at TDA, because they started holding at dusk and stopped holding at dawn (see echograms in Figures A.5 and A.6 in Appendix A); predator fish would not be expected to exhibit this behavior.

Table 7. Mean target strength (dB) with standard deviation (s.d.) and sample size (n) by day/night and block.

BLOCK	DAY			NIGHT		
	Mean	s.d.	n	Mean	s.d.	n
1	-47.9	5.3	327,515	-42.4	4.7	1,065,363
2	-48.4	5.4	459,380	-42.7	4.9	1,015,009
3	-47.9	5.5	403,477	-43.5	4.9	763,331
4	-49.3	4.8	428,994	-44.3	5.2	227,588
5	-48.7	5.2	130,434	-47.5	5.6	35,957
Total	-48.4	5.3	1,749,800	-43.0	4.9	3,107,248

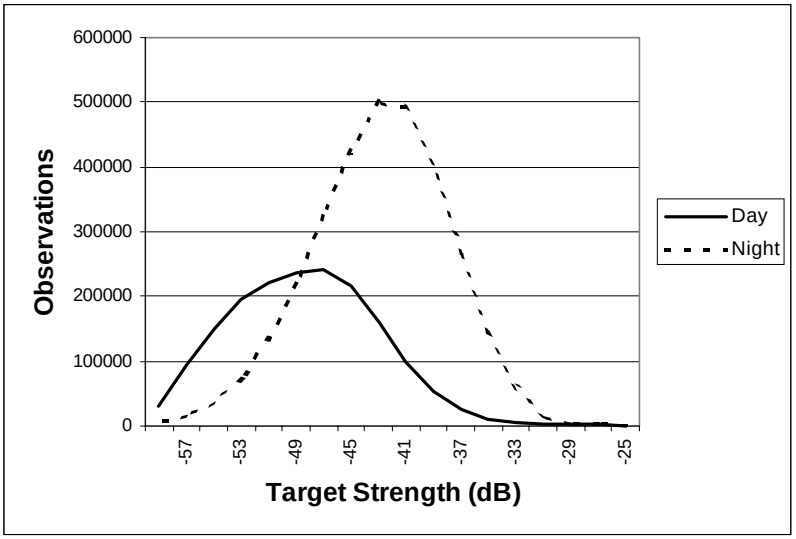

Figure 20. Frequency distribution of target strength for day and night separately.

In summary, the descriptive data showed slow, omnidirectional smolt movement patterns in the nearfield of Sluice 1-1. The database was composed of many relatively short tracks (average 51 pings per track). More X, Y, Z positions were collected during night than day,

although more fish were tracked during day than night. This implies that fish were more active during day than night in front of Sluice 1-1. Fish moved in numerous directions within the three-dimensions of the coordinate system, but the trend was westward, toward the dam, and downward in the water column. Velocities were mostly –0.5 to 0.5 m/s, revealing slow, controlled swimming behavior and not headlong, fast swimming toward the sluice entrance.

4.3 Smolt Movement -- States

The state data provide a general description of smolt movement patterns in the sample volume (Figures 21 and 22). Recall, the states are mutually exclusive and exhaustive combinations of ping-to-ping movement in three dimensions. General results from the state analysis, not including the holding state, follow.

- Of the 26 possible movement states (excluding the holding state), the highest numbers were observed for the state with movement strictly toward the dam (towd), i.e., no appreciable lateral (X) or vertical (Z) movement (Figure 21). Next was west/away/down (wad), followed by west/toward/up (wtu) (Figure 21).
- When moving toward dam, more smolts were also moving up than down. But, when moving away from the dam, they were more likely to be moving down than up (Figure 21).
- When the states are combined, slightly more movement was west than east (X dimension), slightly more movement was toward the dam than away (Y dimension), and slightly more movement was down than up (Z dimension) (Figure 22).
- More movement was horizontal than vertical, as shown by numbers of observations for east/west and away/toward vs. up/down (Figure 22).

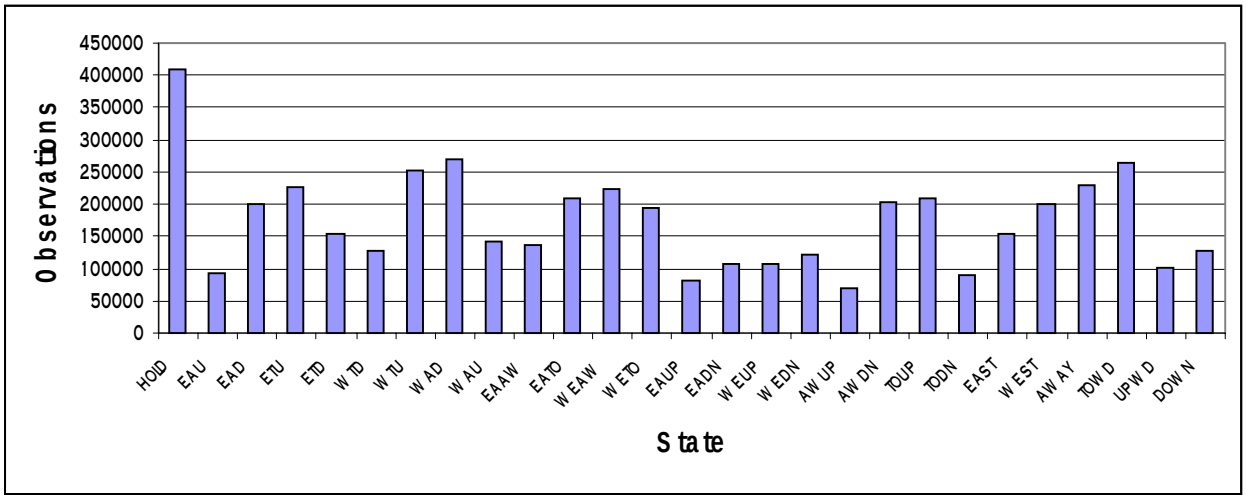

Figure 21. Number of observations for each state. See Table 3 for definitions of state codes. Data are for day and night and all blocks combined.

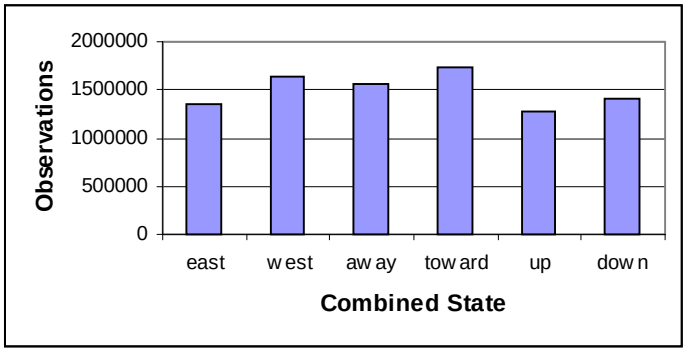

Figure 22. Number of observations for each combined state for the entire database. See Section 3.4.6 for definitions of the combined states.

Contour plots of state data show smolt movement patterns (Figures 23a-r). We selected certain X-sections or Y-ranges or Z-layers (see Figure 13 for definitions) to show spatial trends for specific states. Movement patterns for day and night were different. Results from the states analysis (see plots on next three pages) follow.

- The region in front of the MU 1-1 where holding was observed was more extensive during night than day (Figures 23a-b).
- Holding behavior was observed near the turbine intakes, not the sluiceway (Figure 23a-b). Most holding near the turbine intakes was directly upstream of MU1-1/FU2-2 pier nose.
- Fish movement was up and toward the sluice in the surface ~3 m and within ~3 m of the dam (Figures 23c-f).
- The proportion of fish moving toward the dam generally was greater during day than night (Figures 23e-f, k-l).
- The proportion of fish moving west in region in front of FU2-2 was higher during day than night (Figures 23g-h, m-n).
- The proportion of fish moving toward Sluice 1-1 was greater and more extensive away from the dam during day than night (Figures 23e-f, k-l).
- A high proportion (> 0.8) of fish movement toward Sluice 1-1 was observed within 2-3 m of the dam (Figures 23e-f, k-l).
- The proportion of upward movement was less in front of the MU1-1/FU2-2 pier nose than elsewhere (Figures 23i-j).
- Fish movement into Sluice 1-1 had an easterly component in the west half of the entrance and a westerly component in the east half (Figures 23m-n).
- The holding pattern for big smolts (> -45 dB) was more extensive than that for small smolts (< -45 dB) (Figures 23o-p).
- The proportion of fish moving toward the dam in the surface layer was higher for small smolts than large smolts (Figures 23q-r).

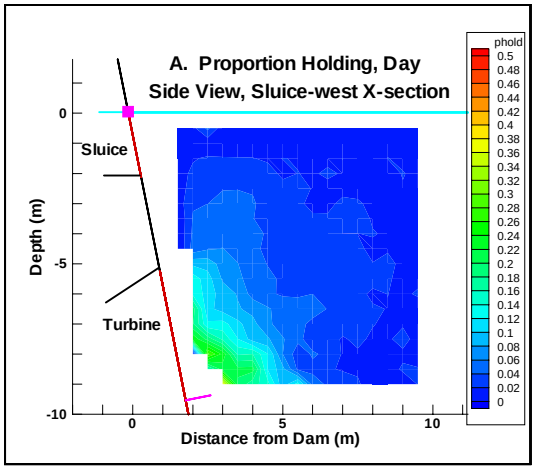

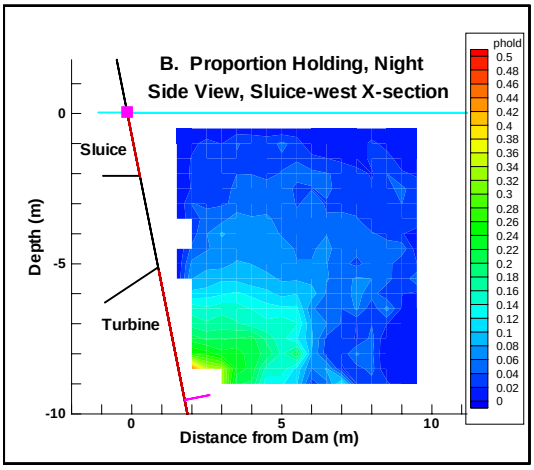

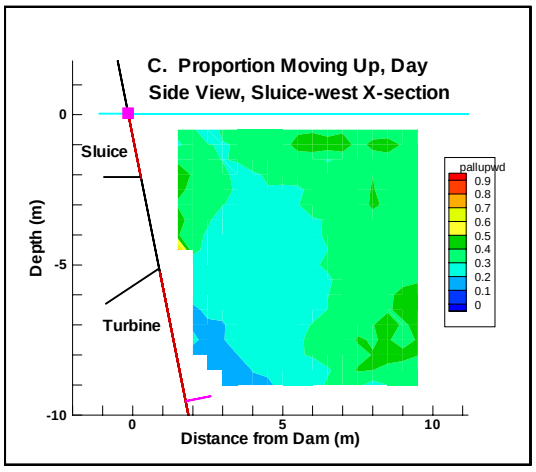

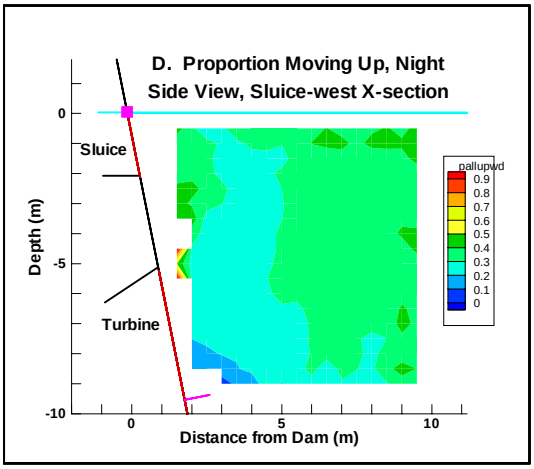

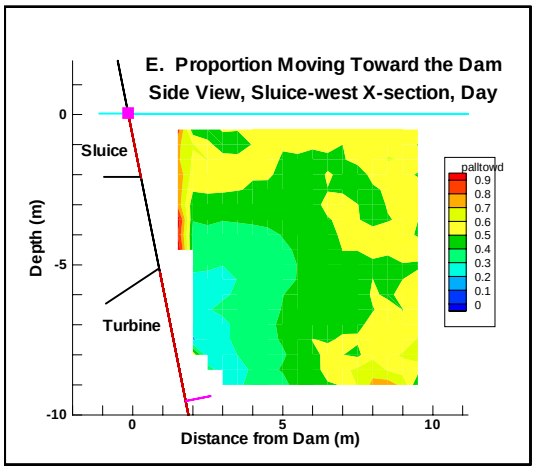

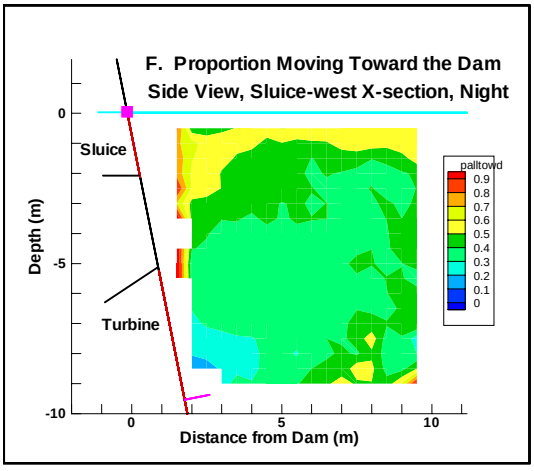

(See caption on p. 35.)

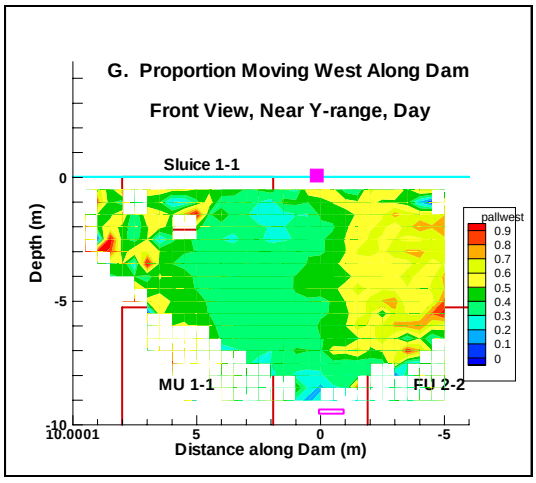

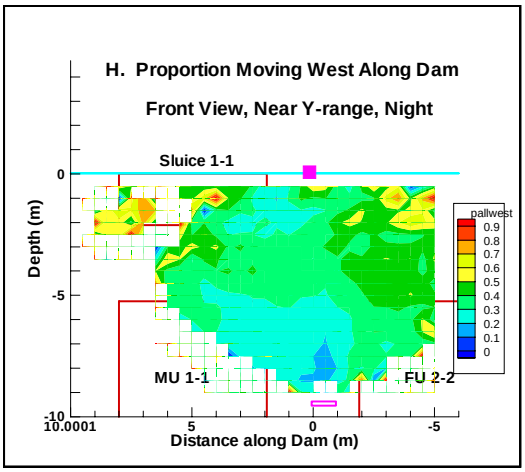

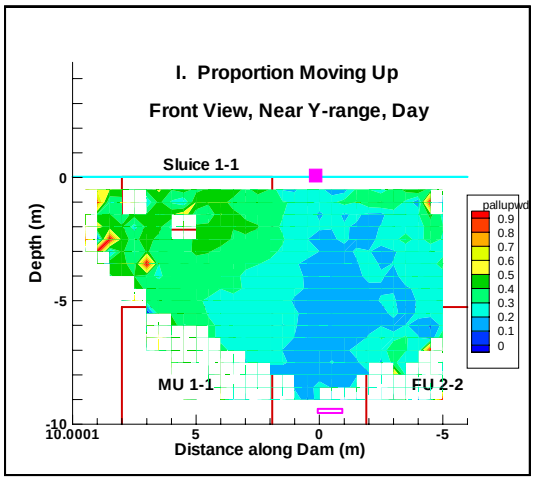

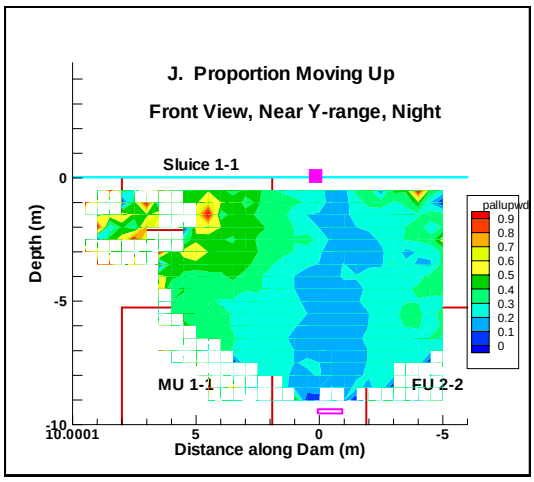

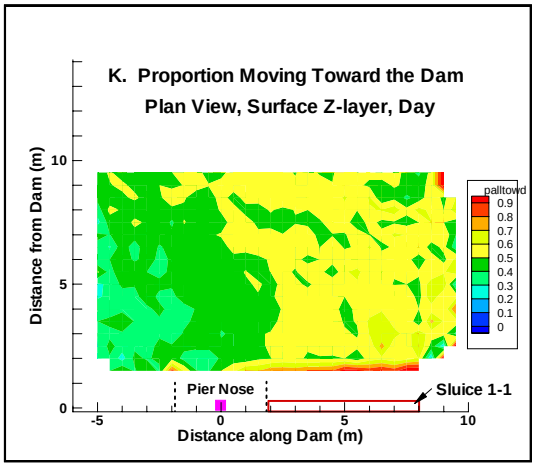

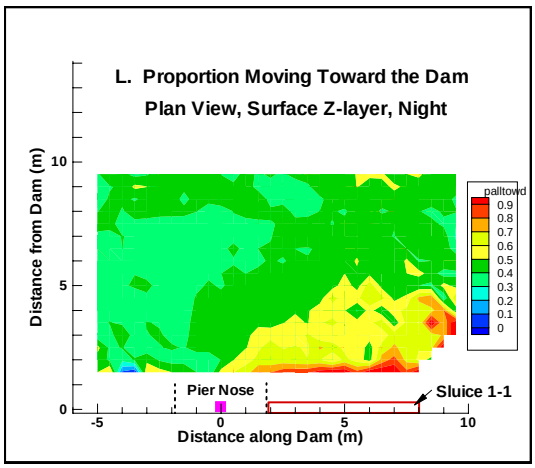

(See caption on p. 35.)

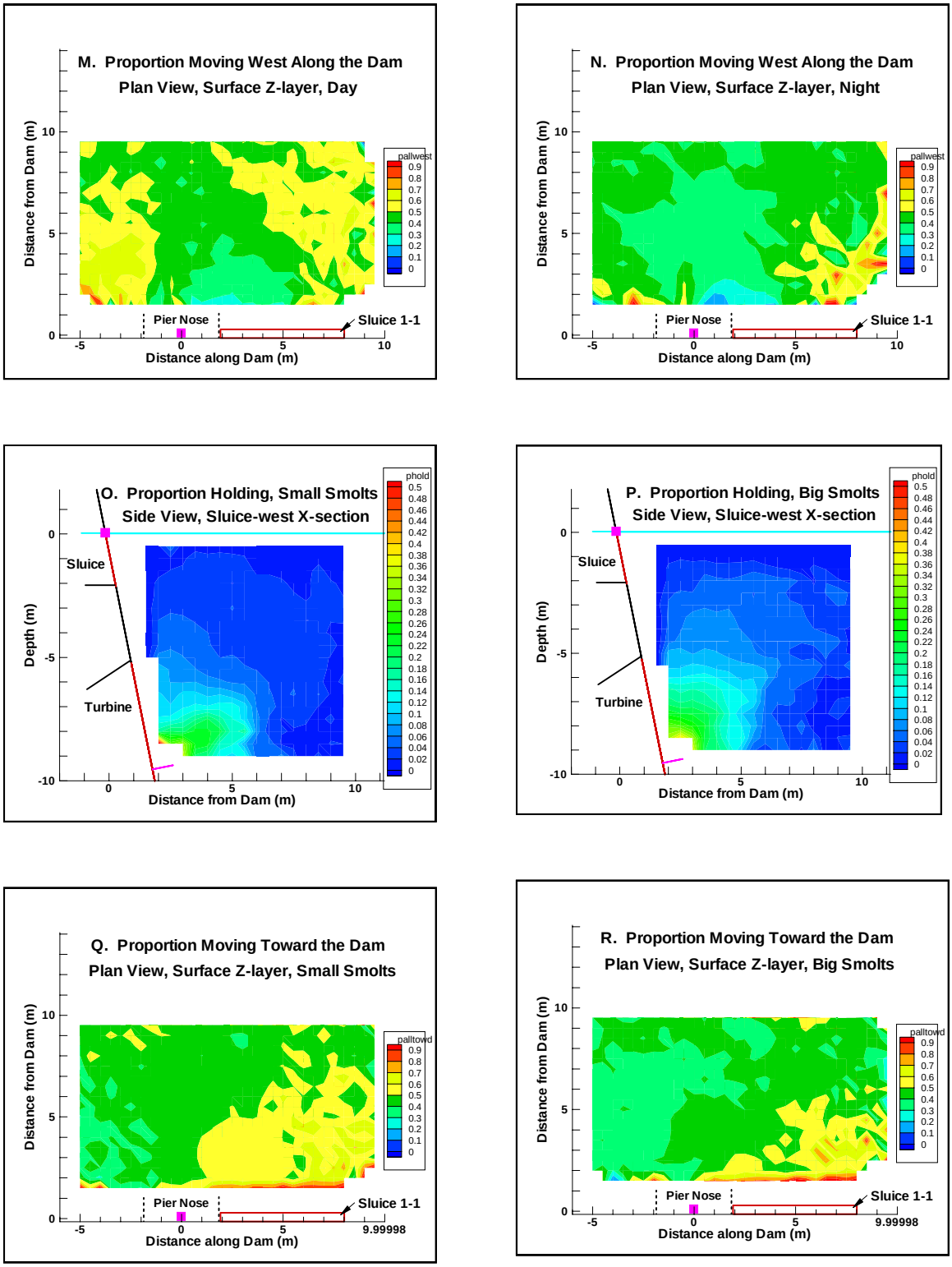

Figures 23a-r. Contour plots of state data, expressed as proportions. Solid purple box represents the origin of the "dam" coordinate system (centerline of MU 1-1/FU 2-2 pier nose at El. 48.2 m). Purple line or unfilled box represents AFTS.

4.4 Smolt Movements -- Streamtraces

Streamtraces provide a description of the direction of fish velocity data. A streamtrace "…is a continuous line drawn in the direction of the velocity vector…" at given points in the sampling volume (John and Haberman 1983, p. 205). The fish velocity data for the streamtrace analysis were based on mean, three-dimensional, ping-to-ping velocities for each 0.5 m cell for the entire study period (April-July). In general, streamtraces were toward the Sluice 1-1 entrance east of the MU 1-1/FU 2-2 pier nose, and westward west of it (Figures 24a and 24b). The streamtraces for our data-set were more disjointed during night than day in the plan view for the layer 0.5-3.0 m deep (Figures 24a and 24b). In cross-section, there was movement toward the dam and upward in the water column in the surface 3 m, but below this depth the vectors had a downward direction (Figures 24c and 24d).

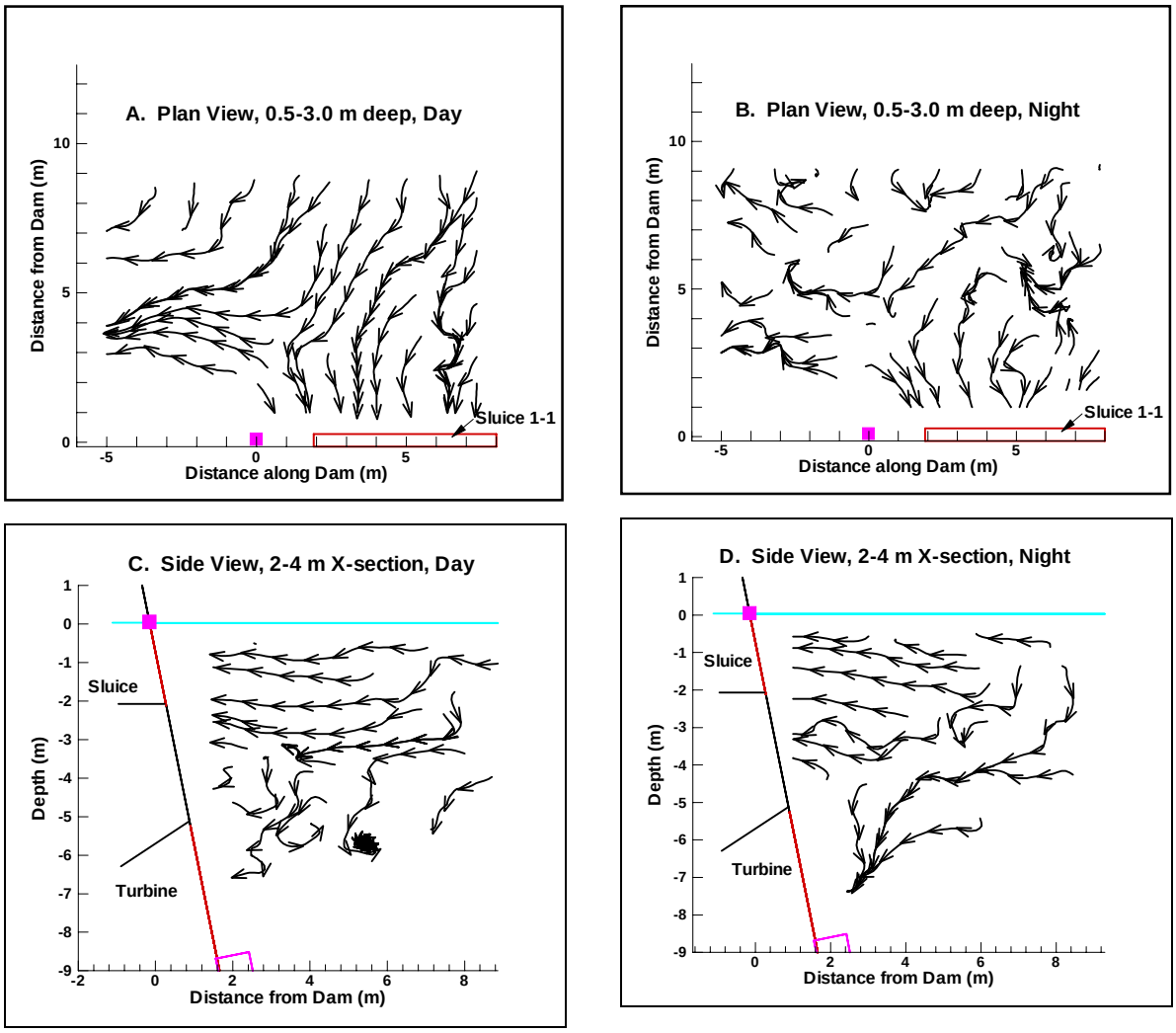

Figures 24a-d. Results of streamtrace analysis of fish velocity for combinations of day/night and plan/side view for the entire study period.

4.5 Smolt Movement -- Fates

The Markov-Chain analysis of movement patterns revealed the *probability* of passage out various sides of the Markov sample volume. That is, it showed "fates" from locations in the nearfield of Sluice 1-1. Recall, possible fates of passage out of the sides of the sample volume were Sluice (dam side, 0-4 m deep), Turbine (dam side, 4-6 m deep), Bottom, West, East, Reservoir, and Unknown. The data are presented in two types of three-dimensional plots: slices and sides. Slice plots show the transition of fates, and inferred movement of fish, for three planes through the interior of the Markov sample volume. The X/Y plane is a slice through the Z dimension 1.5 m deep. The X/Z plane is a slice through the Y dimension 5 m from the dam. And, the Y/Z plane is a slice through the X dimension on the centerline of Sluice 1-1. Side plots show fates for fish in cells nearest the top, east, and reservoir sides of the Markov sample volume. Without assuming how fish at these sides reached the volume boundaries, the side plots show the intensity of fish movement from the Markov sample volume in the nearfield of Sluice 1-1. The slice plots show interior probabilities of fish reaching the boundaries of the sample volume. Adjacent cells with high probabilities indicate possible movement corridors. In all of the fate plots (Figures 25-32), the fate data are superimposed on a scaled rendering of the dam. The entrance to Sluice 1-1 is in the upper left, Main Unit Intake 1-1 is below it, and Fish Unit Intakes 2-1 and 2-2 are on the right side of the plots.

The Sluice fate is especially important because it represents the zone of influence of the sluice flow net. There was a high (> 80%) probability of passage out of the sample volume adjacent to the entrance at Sluice 1-1 ("sluice passage") from cells within 2-3 m deep and about 6-8 m out from the entrance (Figures 25a, 26a, 29a, and 30a). The probability of sluice passage was higher for fish approaching from the east side (> 80%) of the forebay toward Sluice 1-1, than for fish approaching on the westerly (15-65%) half of the entrance (Figures 25a and 26a). The sluice fate decreased dramatically with increasing depth (Figures 25a, 26a, 29a, and 30a). Probability of passage toward the sluiceway from the western part of the nearfield Sluice 1-1 was ~35% greater during night than day (Figures 25a, 26a, 29a, and 30a). In conclusion, the zone of influence of Sluice 1-1 was 5-7 m wide and extended 6-8 m from the dam in the surface layer 2-3 m deep.

The Bottom fate indicates fish movement toward the turbine intakes. The probability of movement out the bottom of the Markov sample volume was about 35% greater during night than day (Figures 25b, 26b, 29b, and 30b). Bottom fate was highest (> 40%) in the layer 5-6.5 m deep. The Turbine fate probability was negligible (< 0.01).

The Reservoir fate suggests movement upstream, away from the dam. Movement out the reservoir side of the volume was generally minimal (usually < 25%) (Figures 25c, 26c, 29c, and 30c). Reservoir fate was somewhat higher during night than day.

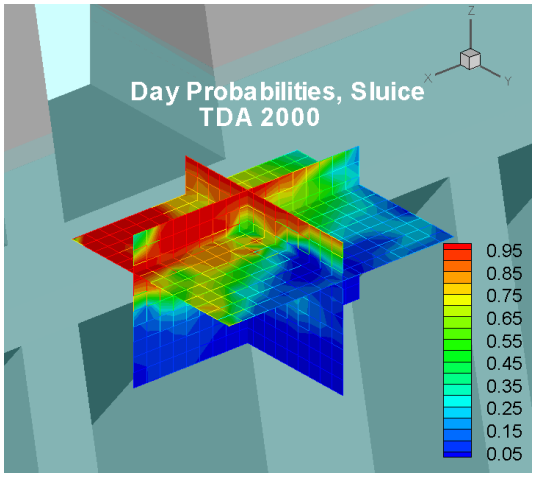

Figure 25a. Slices for sluice, day.

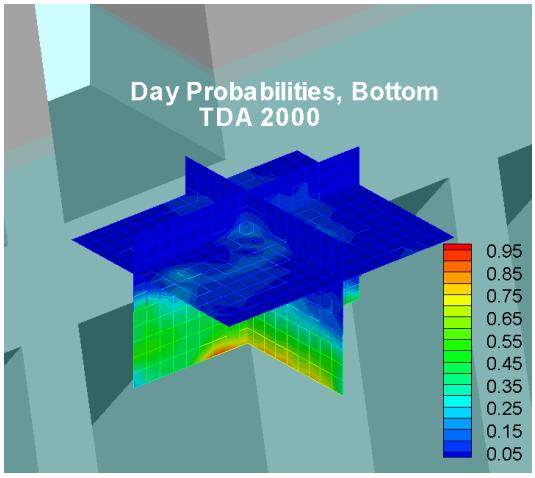

Figure 25b. Slices for bottom, day.

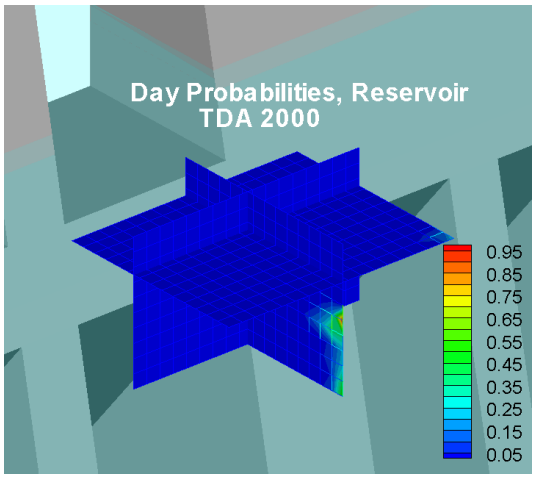

Figure 25c. Slices from Markov-Chain fate analysis --reservoir, day.

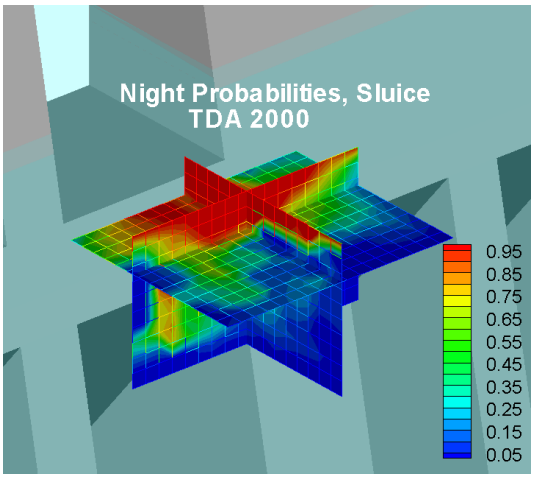

Figure 26a. Slices for sluice, night.

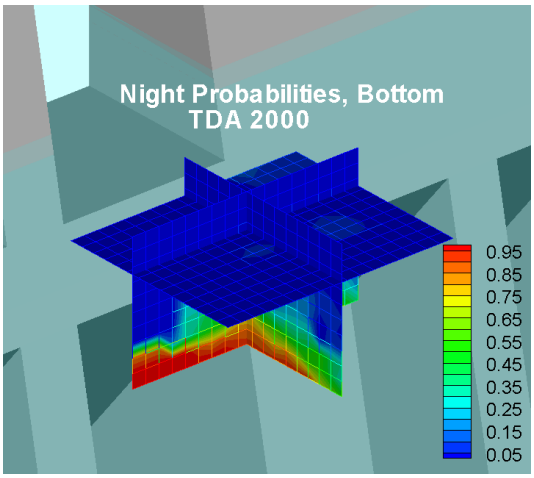

Figure 26b. Slices for bottom, night.

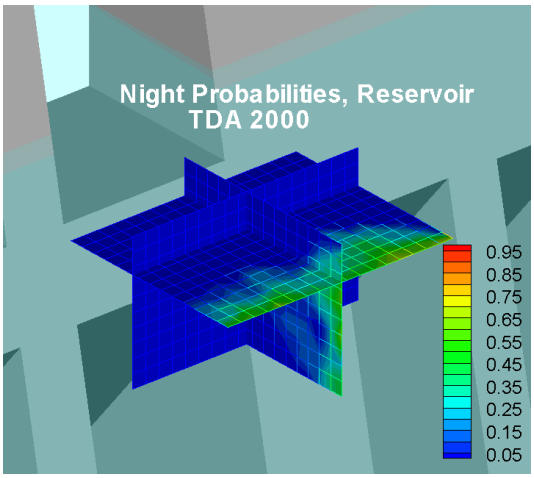

Figure 26c. Slices from Markov-Chain fate analysis – reservoir, night.

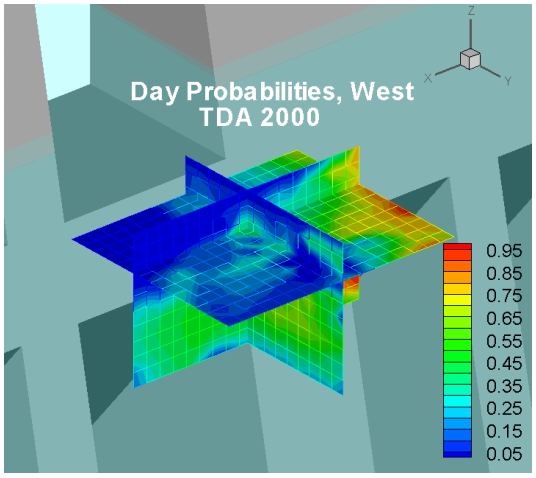

Figure 27a. Slices for west, day.

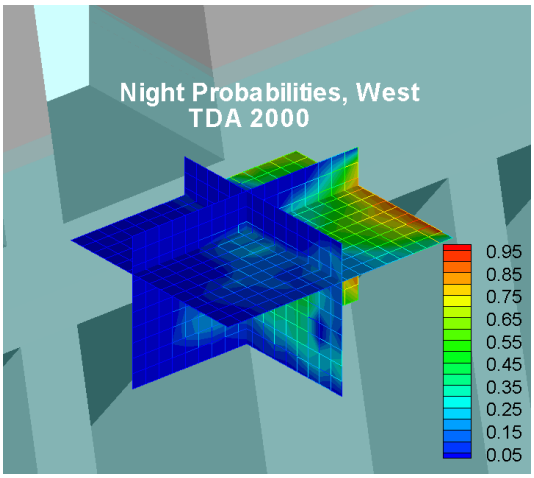

Figure 28a. Slices for west, night.

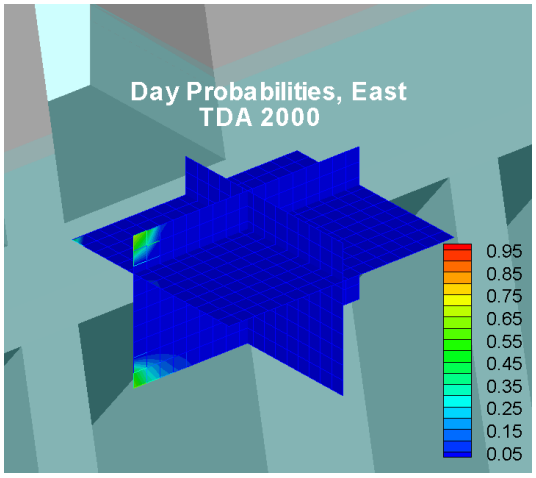

Figure 27b. Slices for east, day.

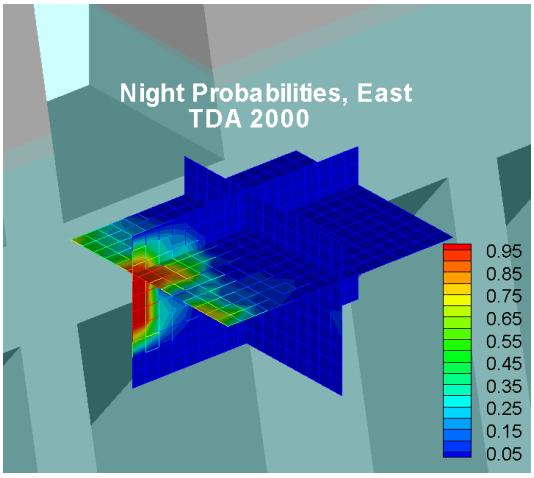

Figure 28b. Slices for east, night.

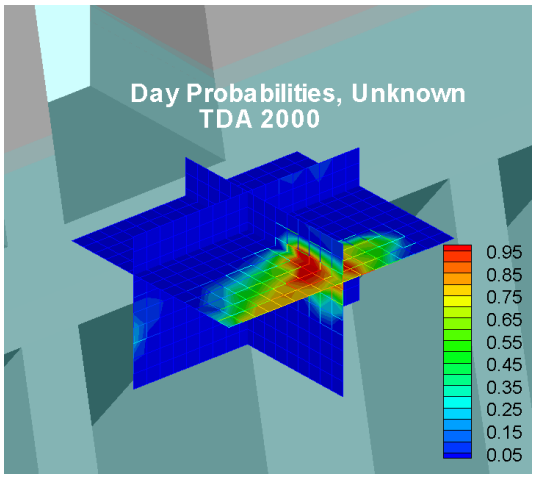

Figure 27c. Slices from Markov-Chain fate analysis – unknown, day.

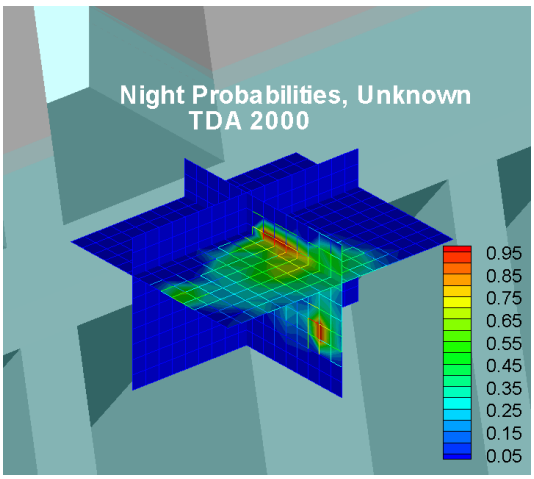

Figure 28c. Slices from Markov-Chain fate analysis – unknown**,** night.

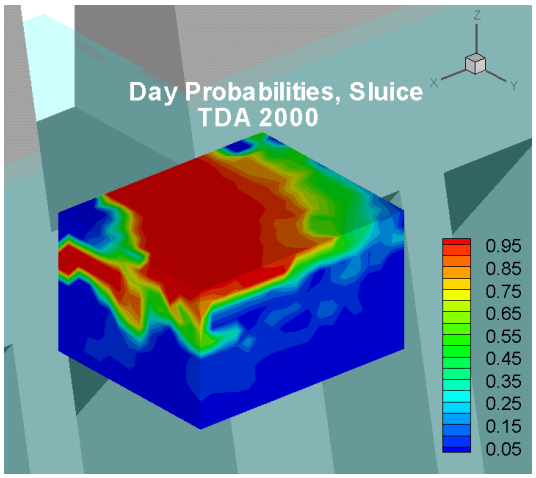

Figure 29a. Sides for sluice, day.

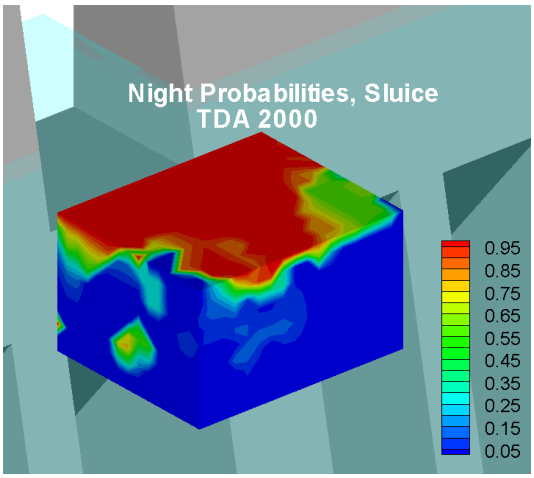

Figure 30a. Sides for sluice, night.

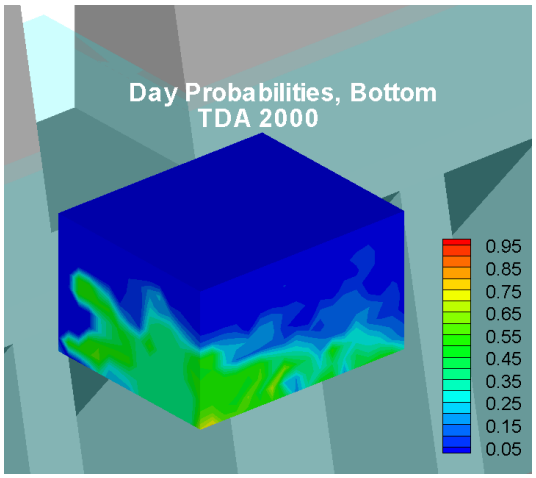

Figure 29b. Sides for bottom, day.

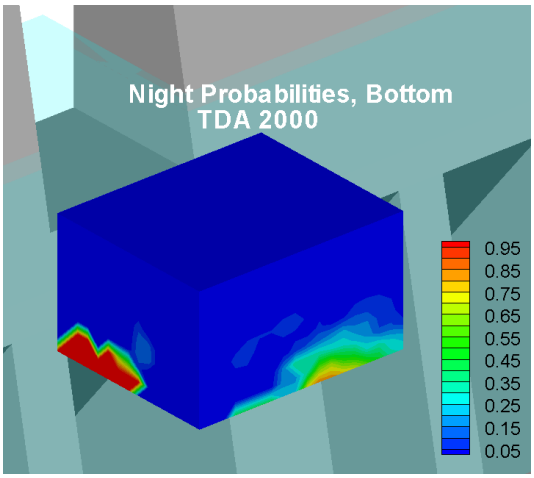

Figure 30b. Sides for bottom, night.

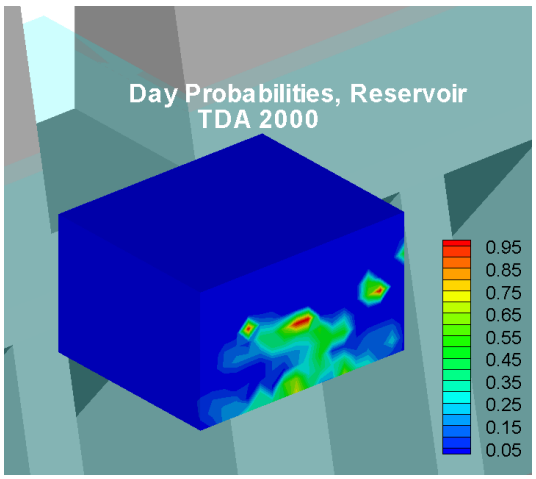

Figure 29c. Sides from Markov-Chain fate analysis -- reservoir, day.

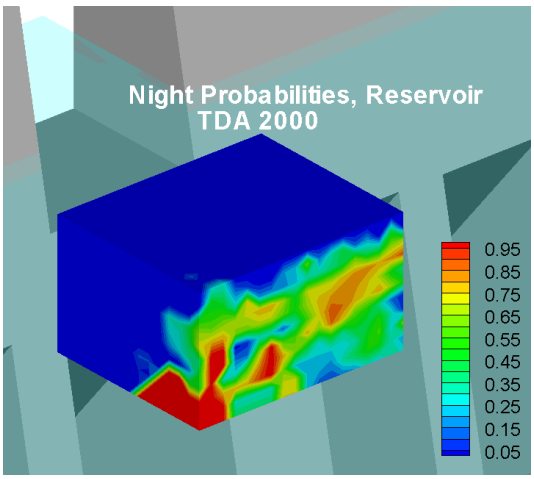

Figure 30c. Sides from Markov-Chain fate analysis -- reservoir, night.

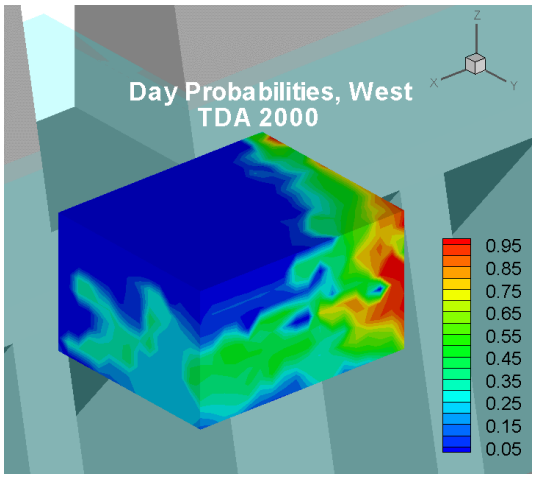

Figure 31a. Sides for west, day.

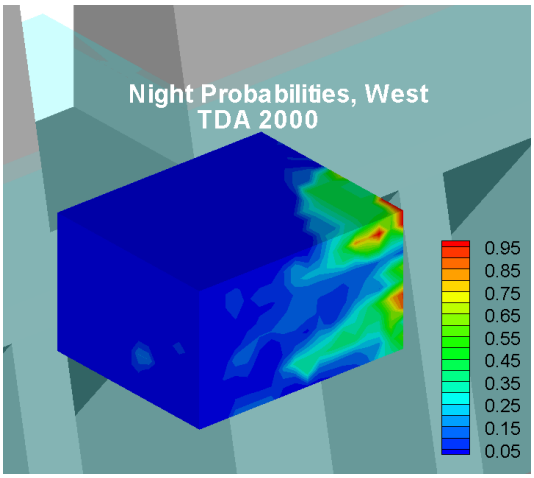

Figure 32a. Sides for west, night.

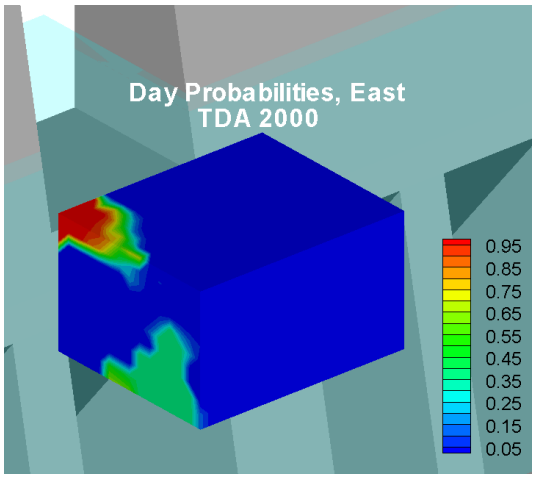

Figure 31b. Sides for east, day.

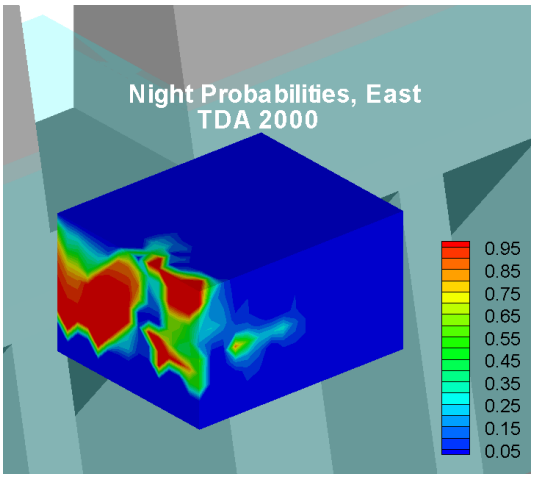

Figure 32b. Sides for east, night.

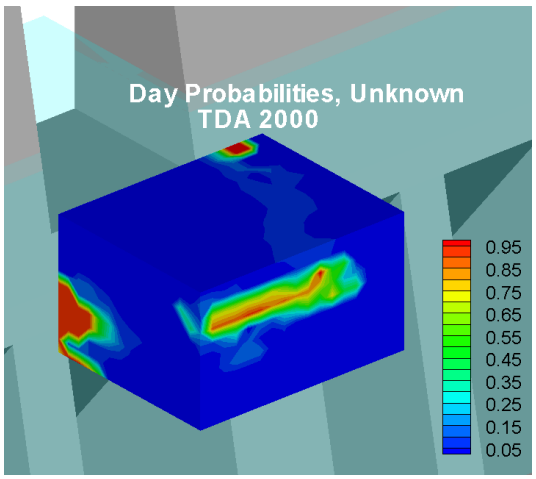

Figure 31c. Sides from Markov-Chain fate analysis -- unknown, day.

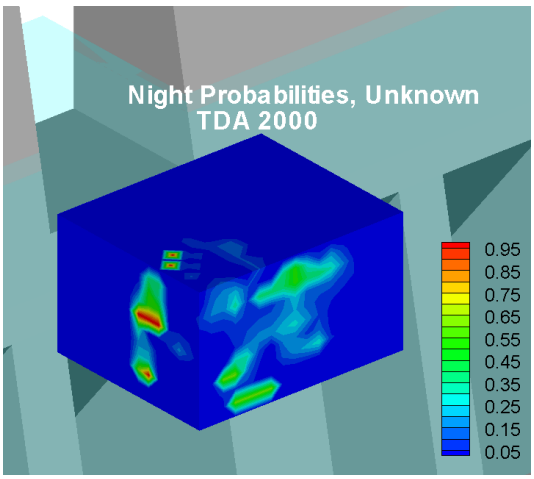

Figure 32c. Sides from Markov-Chain fate analysis -- unknown, night.

The West fate shows movement away from the last sluice entrance on the west end of the powerhouse and toward the spillway. The probability of passage out the west side of the volume was greater during day than night, and was more prevalent on the western half than the eastern half of the nearfield of Sluice 1-1 (Figures 27a, 28a, 31a, and 32a). About 25-35% of the fish entering the lower part of the east side of the sample volume ended up going out the west side (Figures 31a and 32a).

The East fate reveals movement away from Sluice 1-1 and toward the nearfield of Sluice 1-2. Movement out the east side of the volume was negligible (Figures 27b, 28b, 31b, and 32b). Some fish may have entered the east side then presumably reversed direction, especially at night (Figures 31b and 32b).

The Unknown fate is the probability of not passing out of any of the sides of the Markov volume. Some fish located near the reservoir and east sides of the Markov volume exhibited this behavior (Figures 27c, 28c, 31c, and 32c). The Unknown fate is likely a reflection of meandering and holding behavior in the time scale of an hour.

The most common fates for passage out of the Markov sample volume were Sluice, Bottom, and West with average probabilities 21-40% (Table 8). Fate probabilities for Reservoir, East, and Unknown were low at 1-9% (Table 8). About one-third (29-32%) of the fish (assuming a uniform distribution in the volume) moved out of the sample volume toward the sluiceway. Day/night differences were small, except for the West fate which was 17% greater during day than night and the Reservoir fate which was 8% lower during day than night (Table 8).

Table 8. Movement fates expressed as average probabilities calculated from the results of a Markov-Chain analysis. The possible areas of movement out of the sample volume in front of Sluice 1-1 were westward along the dam (West), eastward along the dam (East), away from the dam (Reservoir), out the bottom (Bottom), toward the dam (Sluice), and holding (Unknown). The Turbine fate probability is not included because it was negligible (< 0.01). Probabilities are shown for data collected during day and night separately for the period April 17 to July 7, 2000.

	SLUICE	BOTTOM	RESERVOIR	WEST	EAST	UNKNOWN	SUM
Day	0.29	0.22	0.01	0.40	0.02	0.06	1.00
Night	0.32	0.21	0.09	0.23	0.08	0.07	1.00
Difference	-0.03	0.01	-0.08	0.17	-0.06	-0.01	0.00

In summary, the Markov-Chain analysis of smolt movements showed that the zone of influence of the sluiceway was 2-3 m deep, extended out 6-8 m from the dam, and was stronger on the eastern side of the nearfield of Sluice 1-1 than the western side. The probabilities of passing out the sluice, west, and bottom sides of the sample volume were greater than the probabilities of passing out the east and reservoir sides or not passing out at all. The variability of

the Markov fates is an indication of the dynamic nature of smolt movements in the nearfield of Sluice 1-1.

4.4 Comparison of Fate Probabilities with Vertical Distribution Data

Vertical distribution data were available from the sluiceway passage study in 1999 (Ploskey et al. 2001) to compare to our fate probabilities. Vertical distribution immediately upstream of the face of the dam was concentrated in the upper 4 m of the water column (Figure 33). This pattern corroborates the findings from streamtrace and fate analyses, where we observed that movement in the surface 3 m was toward the sluiceway and the highest probability of passage out of the sample volume was in the surface layer 2-3 m deep (Figures 24, 25a, 26a, 29a, and 30a).

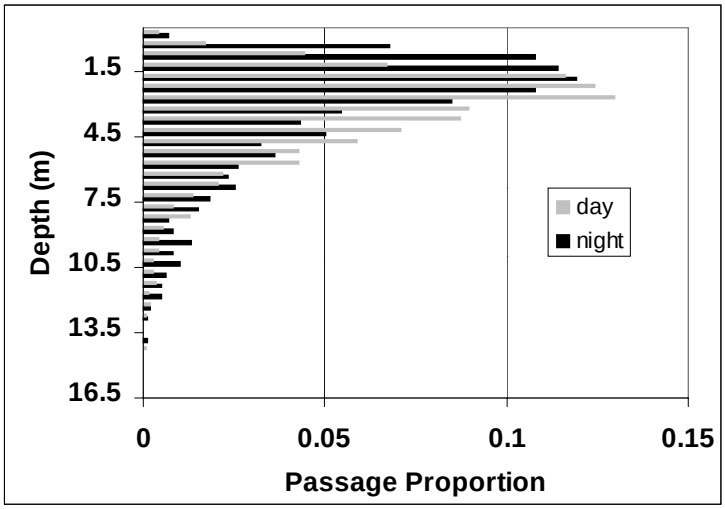

Figure 33. Vertical distribution at Sluice 1-3. Data were obtained from Ploskey et al. (2001).

4.5 Assessment of SFB Premises

For two of the six SFB premises (attraction and shallow preference), we applied exploratory statistical tests using AFTS data on state proportions. The tests were intended to relate observed fish movement data to proposed mechanisms behind successful surface bypasses. The working hypotheses stated in the Introduction section of the report (we called them SFB premises) were the alternative hypotheses in formal testing (H_a). The working hypotheses (SFB premises) were based on anticipated mechanisms important in the passage of smolts at a surface bypass collector. Establishing working hypotheses about SFBs was an important step in the analysis because it allowed us to analyze fish movements at the TDA sluiceway SFB within a scientific framework.

Summary results are presented in Tables 9 and 10. Detailed statistical results are presented in Appendix C. The assumption of independence in ping-to-ping direction of movement was satisfied (Appendix C). The results are presented for each hypothesis separately below the tables that follow.

Table 9. Summary of results of hypothesis tests using the Z-statistic on conditional proportions of smolt movement from the state analysis. Significance level is at 0.10.

TEST	HYPOTHESIS	DY/NT	MOVEMENT PROPORTION	P-VALUE	SIGNIF.
Attraction	$P_{TOWARD} \leq P_{AWAY}$	Day	$P_{TOWARD} = 0.5912$	0	yes
		Night	$P_{TOWARD} = 0.5381$	0.01321	yes
Shallow Preference	$P_{UP} \leq P_{DOWN}$	Day	$P_{UP} = 0.5484$	0	yes
		Night	$P_{UP} = 0.6303$	0.00025	yes

Table 10. Summary of analysis of deviance of differences in conditional proportions of movement between day and night and among blocks. Tests are described in text below. Significance level is at 0.10.

TEST	P-VALUE FOR DAY/NIGHT	SIGNIF.	P-VALUE FOR BLOCKS	SIGNIF.
Attraction	0.0725	yes	0.2626	no
Shallow Preference	0.3179	no	0.0328	yes

4.4.1 Attraction

Premise -- Smolts are attracted to and actively seek hydraulic conditions associated with SFBs.

Movement Data -- The approach to the attraction premise was to use movement data toward/away from the Sluice 1-1 entrance (Figure 34a). Thus, in the near and intermediate ranges (Y = 1 to 6 m) of the surface layer (Z = 0 to –3 m) of the sluice section (X = 0 to 9 m), we tested the following hypothesis using conditional proportion data for toward and away movements:

H_o: *P(toward)* $\leq$ *P(away),* H_a: *P(toward)* $>$ *P(away).*

A descriptive view of the fish movement data for this hypothesis was shown in Figures 23e-f, k-l. The proportion of movement toward the dam increased as distance from the dam decreased and was highest (> 80%) within 3 m of the dam. Streamtraces were toward the dam in this zone (Figure 24). The Markov analysis of fate shows that the probability of sluice passage was high out to 6-8 m from the dam in the east side of Sluice 1-1 (Figures 25-32). The statistical test resulted in rejection of the null hypothesis for both day and night (Table 9). The proportion of movement toward the dam in the zone of interest was 59% at day and 54% at night; this difference was significant (P=0.0725) (Table 10). There was no significant difference between blocks for the proportion of movement toward the dam (P=0.2626) (Table 10).

Conclusion – The fish movement data from this study supports the attraction premise, particularly for surface-oriented fish close to the sluice entrance.

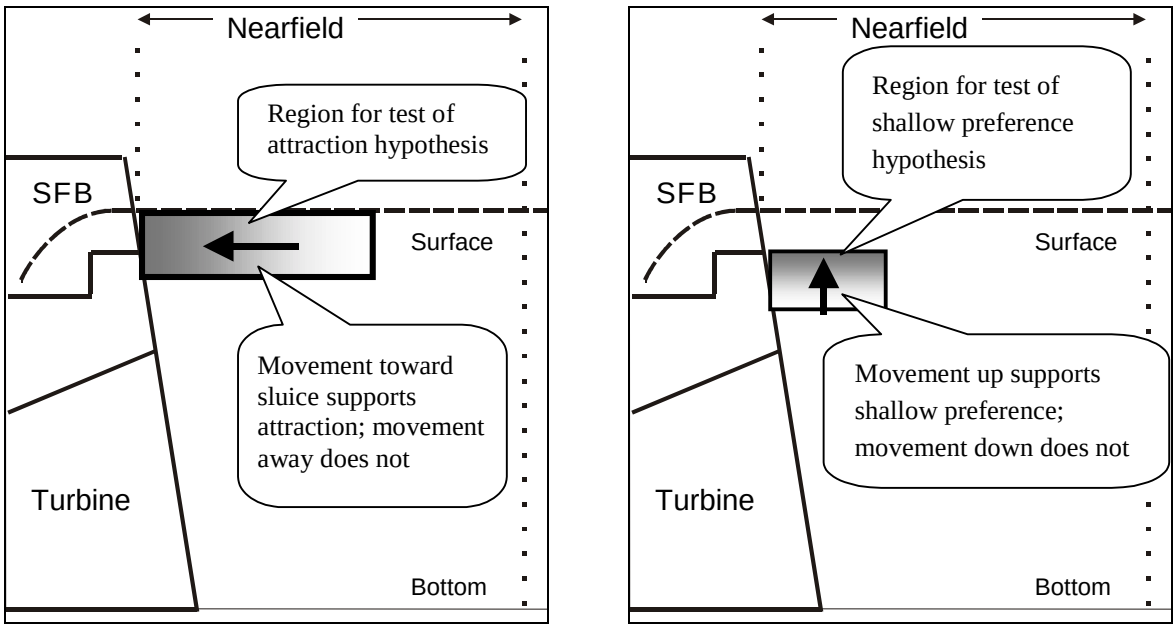

a. Attraction **b. Shallow Preference**

Figure 34. Schematics of the side view of the TDA sluiceway SFB depicting the region of interest and the working hypothesis for the (a) attraction and (b) shallow preference premises.

4.4.2 Shallow Preference

Premise -- Smolts prefer shallow passage routes at dams, i.e., they prefer not to sound and are reluctant to pass through turbine intakes.

Movement Data -- If this premise is true, we would expect smolts below the sill of the entrance at Sluice 1-1 to move up to the sluice flow net (Figure 34b). Thus, in the 2 m layer immediately in front of and below the sluice sill (1.5-3.5 m deep) and within 1-3 m of the dam, we tested the following hypothesis using conditional proportion data for up and down movement:

H_o: $P(up) \leq P(down)$, H_a: $P(up) > P(down)$.

A descriptive view of fish movement data for this hypothesis was shown in Figures 23c-d. The proportion of upward movement increased as distance from the sill decreased. The statistical test resulted in rejection of the null hypothesis for both day and night (Table 9). The proportion of upward movement in the region just upstream and below the sluice sill was 55% at day and 63% at night; this difference was significant (P=0.0655) (Table 10). There was no significant difference between blocks for the proportion of upward movement (P=0.7294) (Table 10).

Conclusion – The results of this statistical analysis of state data support the shallow preference premise.

(Page intentionally blank.)

5.0 DISCUSSION

The discussion section covers existing and future TDA sluiceway configurations. First, we discuss why the existing sluiceway is effective in the context of the SFB premises. After this material, we address Markov-Chain analysis and briefly discuss and compare TDA sluiceway hydraulic control to that at other SFB's. Then we discuss sluice and non-sluice passage and how they might be affected by future (2001 and beyond) trashrack occlusion plates with J-sections.

5.1 SFB Premises

The effectiveness of the sluiceway SFB at TDA can be evaluated in the context of six SFB premises. Two of the SFB premises (attraction and shallow preference) were examined with smolt movement data from the 2000 AFTS study. In addition, literature was reviewed on these premises, as well as the four others (surface orientation, horizontal concentration, visual cues, and entrainment).

1. *Smolts are surface-oriented as they migrate in dam forebays*.

Vertical distribution data from hydroacoustic studies at TDA (Magne et al. 1983; Steig and Johnson 1986; Johnson et al. 1987; Nagy and Shutters 1995; BioSonics 1996) and a netting study in a reservoir (Smith 1974) showed that smolts migrating in dam forebays are surface-oriented. For example, Steig and Johnson (1986) reported that 90% of spring migrants during day were within 7.5 m of surface in front of the TDA powerhouse, and during night fish were distributed deeper (70% above 7.5 m deep). Although they were still surface-oriented, summer migrants were typically distributed somewhat deeper (2-5 m) than spring migrants (e.g., Johnson et al. 1987). In conclusion, this premise is supported by data; smolts are surface-oriented at TDA.

2. *Horizontal distribution is concentrated in front of the SFB.*

TDA powerhouse horizontal distribution has been investigated using radio telemetry, hydroacoustic, and fyke net techniques. Radio telemetry data were reasonably consistent among annual studies in 1995-1997, so we will use 1997 as an example. Hensleigh et al. (1999) reported that there were more first-contacts at east end of the TDA powerhouse than elsewhere in the forebay for radio-tagged spring migrants (56-73% of total first-contacts) and summer migrants (34% of total first-contacts). After encountering the dam, radio-tagged fish moved downstream along the powerhouse in a directed manner, i.e., they did not appear to be milling or holding. Using last contact by the radio receiver as an indicator of horizontal distribution of passage of radio-tagged spring migrants in 1997, Hensleigh et al. (1999) noted that 5 to 10 times as many were last contacted at the west end than the east end of the powerhouse. And, of the radio-tagged fish passing at the west end, 88% used the sluiceway.

Hydroacoustic studies at TDA also provide useful data on horizontal distribution of fish passage at the powerhouse. Johnson et al. (1987) found fish passage (number of fish per unit volume of water flowing into the turbine) was higher at the west end than the east end in spring, but that passage densities were relatively uniform in summer. Ploskey et al. (2001) noted a

similar seasonal trend; highest passage rates (number of fish per hour of turbine operation) were at MU 6 in spring and MU 22 in summer.

Results from fyke net studies were used to establish TDA sluiceway operations. Nichols (1979) found that the sluice entrances at the west end of the powerhouse had higher yearling salmon passage rates than entrance in the middle of the powerhouse. Nichols (1980) recommended west operations (MU 1) for spring migrants. The sluiceway has been mostly operated like this since then.

In conclusion, concentration of smolts horizontally at a dam is site-specific. It depends on forebay bathymetry, project configuration, forebay macro hydraulics, and dam operations, as well as fish behavior. At TDA, the horizontal distribution premise is generally valid.

3. *There are certain visual cues at a portal that can facilitate passage of smolts*.

Perhaps the most obvious visual cue to consider is the presence, absence, or intensity of light at a portal. Feist and Anderson (1991) reviewed information regarding the effect of different variables, or conditions, on fish responses to guidance systems. Light was one of those conditions. They found that responses to light varied with species or stock and prevailing water velocity. Of the information they surveyed, an experiment conducted by Fields (1986) at McNary Dam has the most relevance here. He found that ten times more smolts (mixed species) were caught in surface traps when lights were on, than on dark nights. Attraction lighting has apparently not been tested at TDA. Overhead lights are installed at the TDA sluiceway to aid gate operations at nighttime and, while not presently used to increase sluiceway passage, could be tested. Another aspect of the visual cue premise is that SFB passage is typically higher during day than night (e.g., Ploskey et al. 2001 at TDA). In conclusion, the SFB premise on visual cues is unsubstantiated, but should be the subject of further investigation, perhaps at the TDA sluiceway.

4. *There is an entrainment zone associated with SFB entrances where velocities are sufficiently high to trap smolts and accelerating flows do not result in smolt avoidance*.

This premise asserts that if velocity near the entrance is fast enough, smolts will become entrained or drawn into the bypass system. Obviously velocity increases toward the entrance, if the entrance velocity exceeds ambient forebay velocity. In general, entrance velocity at most prototype and production SFBs ranged from 0.61 to 1.83 m/s (2 to 6 fps) (Dauble et al. 1999). Those sites included Wells, Wanapum, Rocky Reach, and Lower Granite dams and the Bonneville Dam First Powerhouse. Water velocity at the entrance to the Bonneville Second Powerhouse (B2) sluice chute exceeds the others at ~3.66 m/s (~12 fps) under current operating conditions. Entrainment, or trapping, velocity will vary by sluice size and inherent swimming capability of the particular species.

Burst speed is the maximum swimming velocity a fish of a given size can attain (Beamish 1978). Ideally trapping velocity should exceed the burst speed for a given species of given size. In the Columbia River system, the largest smolts are typically steelhead and chinook salmon. There is a further complication in estimating burst speed. Some of the literature

indicates that swimming performance decreases as smolt development progresses. This has been reported for coho (Glova and McInerny 1997) and Atlantic salmon (Thorpe and Morgan 1978). However, Muir et al (1994) studied stream-type chinook and did not detect a depression in swimming performance through smolt development. The discrepancy in the swimming performance tests could reflect species differences or the possibility representative smolts were not used in all experiments. There is information that indicates smolts of some species require active migration for some period before they fully express smolt transformation (Rondorf et al. 1985). Only Muir et al. (1994) monitored changes in swimming performance following active migration. Burst speed has been reported for a variety of fish species including juvenile rainbow/steelhead and Atlantic salmon (Beamish 1978). However, it is not clear if any of these were smolts. Furthermore, the range in burst speed was quite broad. For juvenile rainbow trout (14.3 cm in length) burst speed ranged from 0.3-2.5 m/s, or 2.0 to 17.5 body-lengths per second. Using the maximum burst speed reported, this equates to a trapping velocity near 3.05 m/s (10 fps), for a juvenile steelhead approximately 15.2 cm in length. Again, it is not clear if the smoltification process would reduce swimming performance in this species. If we adopt 3.05 m/s (10 fps) as a general trapping velocity guideline for steelhead smolts (requires experimental verification and refinement), then the velocity at most SFB entrances does not approach this level.

Salmonids are anatomically equipped to detect acceleration or turbulence. Otolith organs respond to changes in body movement in all dimensions. Lateral lines respond to pressure changes such as those created by turbulence. (Turbulence as an attractant or repulsion stimulus is discussed below under Premise 5.) The literature regarding smolt response to acceleration is very limited. Haro et al. (1998) may be the only investigation that directly attempted to measure smolt responses to different acceleration fields. They exposed hatchery juvenile Atlantic salmon (presumably smolts) to two different weir designs in the laboratory. Each configuration created a different acceleration field. The experimental design exposed groups to one then the other configuration; no direct measurement of performance could be documented. Indirectly, they inferred preference by measuring the time required for smolts to pass through the approach field and through the weir. They found that passage time was shorter for the weir that created a gradual acceleration field upstream as opposed to the one that did not. Although they acquired smolts from a hatchery, it is not clear the fish were necessarily fully smolted. As noted previously, there is information that individual smolts of some species require active migration for some period of time before they fully transform. This has been documented for stream type chinook salmon in at least two investigations (Muir et al. 1994 and Rondorf et al. 1985). If the Atlantic salmon were not adequately smolted, their responses may not be indicative of an actual migrant. The other limitation of the study design was that Atlantic salmon had no alternative route to select and to pass from the front to the back of the chute. In field situations a variety of alternative routes may be available in the nearfield zone, e.g., SFB or sluice entrance versus turbine intake. It is not clear that useful information can be derived from these lab tests alone. However, if appropriate lab studies were coupled with field studies, the complement may be insightful.

In conclusion, information acquired to date is inadequate to resolve this hydraulically-based premise. It appears that if complementary field and laboratory studies were conducted

using actively migrating smolts, these issues could be resolved more efficiently. Furthermore, the proper characterization of hydraulic conditions encountered by smolts en route to the SFB entrance is essential.

5. *Smolts are attracted to and actively seek certain hydraulic conditions associated with SFBs.*

This premise is widely held but has yet to be verified, particularly in the nearfield zone. The smolt movement data indicated support for the attraction premise. The underlying mechanisms for attraction, if it exists, remain unknown.

Turbulence is one hydraulic characteristic that has received attention recently. Coutant (1998) posed the theory that turbulence appears to be a feature in natural rivers that serves to guide and assist juvenile salmon migration. Even though he makes a reasonable hypothetical case based on circumstantial information, he acknowledges "Neither the basic biology of salmonid migration in turbulent waters nor the potential value of inducing suitable turbulence and flow at bypass entrances is well enough known for attraction facilities to be designed …" He further stresses the need to conduct biological testing in controlled laboratory settings such as the experimental flume used by Williams et al. (1996). However, researchers have apparently not identified any meaningful units of measurement to quantify turbulent intensity or variability. This deficiency limits any inferences we can distill from information currently available on smolt response to turbulence.

Other commonly referenced hydraulic characteristics include water velocity and acceleration. These parameters are readily measured. Even so, acquiring measurements in conjunction with smolt movements is difficult. One means to approach this problem is to apply a computational fluid dynamics (CFD) model. But, as yet, available research reports or publications to date have not melded and thoroughly analyzed smolt movement data with CFD-generated estimates of hydraulic conditions at specific smolt positions. In conclusion, without adequate descriptions of hydraulic conditions in the nearfield in the vicinity of the fish, we cannot resolve this premise. Field research published to date has not accomplished this, regardless of the tool employed. Evidence from this study of observed smolt movements, however, indicated support for the attraction premise and could be the impetus for further inquiry.

6. *Smolts prefer shallow passage routes at dams, i.e., they prefer not to sound and are reluctant to pass through turbine intakes*.

As noted in discussion of the first premise, conventional wisdom is that smolts in general are surface-oriented, or at least reside in the upper half of the water column as they traverse reservoirs. Upon encountering a dam the surface oriented component of the population is reluctant to sound into the turbine intakes that are situated at some depth (Ruggles and Murray 1983). We have already stated that we accept the tenet of this premise based on Johnson's (1996) review of the information. We have encountered no new information to refute this premise and, in fact, our smolt movement data supported it. Thus, we conclude that the shallow preference premise is generally acceptable.

In conclusion, the formulation and statistical analysis of the SFB hypotheses were exploratory. Our intent was to link observed fish movements at a successful SFB in the field to working hypotheses about phenomena related to SFB performance. Biological mechanisms, however, could not be addressed with these observational, descriptive data. For example, we hypothesized about SFB attraction and examined it using fish movement data, but could not investigate biological mechanisms underlying such a response. Note, too, that season-wide composite data separated into day and night periods were analyzed. Seasonal data may not reflect events on any given smaller time-scale, but they do reveal overall trends, which was a goal of this study. Finally, hydraulic data on the SFB flow net would aid formulation and analysis of SFB hypotheses. Methods to improve the analysis of SFB hypotheses in future studies are presented in Section 6, Conclusions and Recommendations.

5.2 Markov-Chain Analysis of Smolt Movement Fates

The Markov-Chain analysis had some distinct advantages over traditional methods of analyzing smolt movement data. Traditional methods typically use standard univariate analyses to test hypotheses concerning complex three-dimensional movement of the fish. These movement data often are summarized into one or few categories of fish response and restricted to predefined spatial zones that investigators suppose are important to the fish. Alternatively, the data are graphically summarized by discrete zones with little attempt to understand the interrelationships between movements in one zone to that of another. On the other hand, the advantages of the Markov-Chain analyses included: (a) No arbitrary subsets of the spatial zone of inference needed to be specified. The entire zone of inference could be analyzed simultaneously. (b) An inherent property of the Markov analysis was the conductivity between locations. The information analyzed was the probabilities of movement between cells within the zone of inference. (c) A maximum amount of information was extracted from the smolt movement data. Information on non-movement, partial tracking information on smolt movements, and complete information on migration were all combined in establishing a transition matrix. (d) Movement information could be analyzed in the original three dimensions without the need to collapse the data to lower dimensions with an inherent loss of information. Some of the disadvantages, however, were that: volumetric data were needed for every cell; movement was necessary to project the fates, i.e., to absorb the probabilities into a boundary; and, the process must reach stability, which was computationally intense. However, combined with fish distributions, the probabilities generated by the Markov analysis can be used to project numbers of fish in each of the fate categories. In conclusion, because our Markov analysis for fates was specifically developed to analyze movement data and assess the disposition of smolts in three-dimensional space, the methods use more of the original informational content of the data and subsequently convey more information than is usually otherwise the case.

5.3 The TDA Sluiceway as a SFB

The TDA sluiceway SFB is effective[10] at bypassing smolts around turbines. Ploskey et al. (2001) estimated sluiceway effectiveness to be about 13 (Table 1). This is due to several features of the smolt population migrating through the powerhouse. They are (a) surface-oriented; (b) often concentrated at the west end of the powerhouse; (c) possibly attracted to the sluice flow net; and (d) reluctant to sound, preferring a shallow passage route over a deep one.

Smolt response to a SFB is undoubtedly influenced by the effect SFB entrance configuration and hydraulic control have on the SFB flow net in the forebay. Vertical gates aligned with the downstream edge of a sill control flow into the sluiceway at TDA. The configuration is essentially a short, broad-crested weir (Henderson 1966, pp. 211-212). Thus, hydraulic control of sluiceway inflow is achieved at the SFB entrances for the TDA sluiceway. Larinier and Travade (1999) endorsed the broad-crested weir configuration. However, at the entrance to the B2 sluice chute, another "successful" SFB, hydraulic control is achieved with a sharp-crested weir. Other SFBs have vertical slot entrances with flow control at some point downstream of the entrance (e.g., the surface bypass and collector at Lower Granite Dam). These too can be effective, as evidenced by the vertical slot SFB at Wells Dam (Skalski et al. 1996). Whatever the entrance type, it is important to quantify and map SFB flow nets to interpret smolt response, movement, and passage data.

Not all smolts that presumably encountered the sluice flow net at TDA migrated into the sluiceway, as indicated in our study and previous hydroacoustic (Ploskey et al. 2001) and radio telemetry (Hensleigh et al. 1999) studies. Most of the fish that did not enter the sluiceway continued west or went down into the turbines. (Our study was not designed to estimate entrance efficiency or passage proportions for these routes – see fixed hydroacoustic and radio telemetry reports.) Smolts moving west often guided along the non-overflow part of the dam toward the spillway (Hensleigh et al. 1999). Even with the sluiceway SFB, turbine passage occurred because of the relatively large amount of water flowing into the turbine units. Interestingly, Ploskey at al. (2001) noted that passage rates at MU1 (below the sluice entrances) were low compared to adjacent units, presumably because of the effect of the sluiceway. Nonetheless, further decrease of turbine passage and increase of sluiceway and spillway passage is a clear strategy to improve smolt protection at TDA.

5.4 J-Occlusions at TDA

In future studies at TDA, researchers will evaluate turbine intake occlusion plates with J-sections (J-occlusions). The J-occlusions are designed to lower and flatten streamlines of flow into the turbines, i.e., decrease flow into turbines from surface water and increase turbine flow from deep water in the forebay. Biologically, the intent is to increase the availability of surface-oriented smolts to the sluiceway and spillway flow nets. This should result in decreased turbine

[10] Sluiceway effectiveness is defined as the ratio of the proportion sluice passage to the proportion sluice flow relative to the entire powerhouse.

passage and increased sluiceway and spillway passage. For a given nearfield location above the J-section in front of a sluice entrance, hypotheses about the biological effects of the J-occlusions include:

- The zone of influence of the sluiceway will be larger with J-occlusions than without.
- The proportion of fish moving upward and toward the sluice entrances will higher with J-occlusions than without.
- The probability of passage into the sluiceway will higher with J-occlusions than without.

Using the active fish tracking sonar to study of fish movement in front of the sluiceway with and without J-occlusions can contribute to successful bioengineering for smolt bypass development at TDA. AFTS is useful to quantify fish movement patterns in the nearfield of the sluiceway and associated J-occlusions, because AFTS can directly assess the effect the J-occlusions are having on smolt movements in the nearfield. AFTS's detailed, high intensity fish position data can fill the gap between (a) low resolution, broad-scale fish movement data in the forebay obtained from telemetry and (b) passage rate data at or within the dam portals collected with fixed hydroacoustics and radio telemetry. Smolt movement data regarding responses to the J-occlusions will be necessary to interpret and explain the passage data. Passage rate data will be the "bottom-line" on performance of the J-occlusions. However, if the J-occlusions are not successful, it will be essential to know why, i.e., determine what went wrong. And, even if the J-occlusions are a success, it will be useful to know why, i.e., validate the J-occlusion premises. The AFTS study at TDA in 2000 provides a strong foundation for future J-occlusion evaluations.

(Page intentionally blank.)

6.0 CONCLUSIONS AND RECOMMENDATIONS

In conclusion, this baseline study of smolt movements in the nearfield (within 10 m) of Sluice 1-1 at TDA in 2000 substantiated previous data (Hensleigh et al. 1998) that smolts move from east to west through the nearfield and slow down in front of Sluice 1-1. In addition, the study revealed the following new information.

- Holding was not observed at the sluice entrances, but was seen in front of the upper portion of turbine intake entrances (we only sampled the upper 6 m of the intake), and was especially prevalent at night off the west pier nose by the MU1-1 intake.
- Smolt movement in front of Sluice 1-1 was complex and multi-directional into the entrance. This finding was corroborated by preliminary observations using an acoustic camera aimed across the sill at Sluice 1-1 (G. Ploskey, Battelle, pers. comm.).
- A zone of entrainment indicated by the state data appeared to be relatively small (2-3 m from the dam), but this must be substantiated with water velocity and smolt movement data between the downstream edge of our sampling volume (1.5 m off the plane of the pier noses) and the sluice weir.
- The zone of influence of the sluice flow net extended 6-8 m from the dam in the surface layer (0-2 m) based on the Markov-Chain analysis of smolt movements. This seems to correspond well with the sluice flow net, based on a preliminary examination of CFD model output (L. Ebner, Portland District U.S. Army Corps of Engineers, pers. comm.).
- The probability of sluice passage was highest immediately upstream of the east side of the Sluice 1-1 entrance (recall, there was an open sluice entrance to the east of Sluice 1-1, but not the west).
- Attraction to the sluice flow net and preference for a shallow passage route were indicated.

The TDA sluiceway is effective at bypassing smolts around turbines. This is because the smolt population migrating through the powerhouse, for the most part, is surface-oriented, often concentrated at the west end of the powerhouse, possibly attracted to the sluice flow net, and reluctant to sound, preferring a shallow passage route over a deep one.

We recommend that research at the TDA sluiceway during J-occlusion evaluations address the following points:

- Assess specific hypotheses about smolt movements, such as: (a) the zone of influence of the sluiceway will be larger with J-occlusions than without; (b) the proportion of fish moving upward and toward the sluice entrances will be higher with J-occlusions than without; and (c) the overall probability of sluiceway passage will be higher with J-occlusions than without.
- Integrate observed smolt movement data with hydraulic data from a CFD.
- Improve the AFTS tracking algorithm and sample closer to the dam than in 2000 if possible.
- Improve computational power to analyze a large Markov-Chain transition matrix for expanded spatial coverage of fate probabilities.
- Test the effects of surface illumination using existing lights at Sluice Gates 1-1, 1-2, and 1-3 on sluiceway bypass efficiency.

(Page intentionally blank.)

7.0 LITERATURE CITED

Beamish, F. W. H. 1978. Swimming capacity. In: Hoar, W. S. and Randall, D. J. (eds). Fish physiology, Volume 7 - Locomotion. New York, NY. Academic Press. pp. 101-187.

BioSonics, Inc. 1996. Hydroacoustic evaluation and studies at The Dalles Dam, spring/summer 1996. Volume 2 - Smolt behavior. Draft final report submitted to Portland District, U.S. Army Corps of Engineers by BioSonics, Inc. Seattle, WA. November 15, 1996.

BioSonics, Inc. 1999. Hydroacoustic evaluation and studies at The Dalles Dam, spring/summer 1998. Final Report submitted to Portland District, U.S. Army Corps of Engineers by BioSonics, Inc. Seattle, WA. February 28, 1999.

BioSonics, Inc. 1998. DT/DE Series User's Manual Version 4.02. BioSonics, Inc., Seattle WA, 57 pp.

Brookner, E. 1998. Tracking and Kalman Filtering Made Easy. John Wiley and Sons, New York. 477 pp.

Coutant, C. 1998. Turbulent attraction flows for juvenile salmonid passage at dams. Oak Ridge National Laboratory, Publication 4798. Oakridge, TN.

Crawley, M. J. 1983. GLIM for Ecologists. Blackwell Scientific Publications. London, England. pp. 223-225.

Dauble, D. D., S. M. Anglea, and G. E. Johnson. 1999. Surface flow bypass development in the Columbia and Snake Rivers and implications to Lower Granite Dam. Final Report submitted to Walla Walla District, U.S. Army Corps of Engineers by Battelle. Richland, WA. July 21, 1999.

Ehrenberg, J. E. 1981. Analysis of split beam backscattering cross section estimation and single isolation techniques. Applied Physics Laboratory University of Washington. APL-UW 8108. 24 pp.

Feist, B. E. and J. J Anderson. 1991. Review and design criteria of behavioral fish guidance systems. Research report submitted by University of Washington to the U.S. Army Corps of Engineers. January 16, 1991.

Fields, P. E. 1966. Final report on migrant salmon light guiding studies at Columbia River dams. Research report submitted by University of Washington to the U.S. Army Corps of Engineers. Contract DA-45-108, 31 p.

Giorgi, A. E., G. E. Johnson, and M. W. Erho. 2000. Critical assessment of surface flow bypass development in the Lower Columbia and Snake rivers during 1995-1996. Pages 41-56 in Odeh, M. editor. 2000. Advances in Fish Passage Technology, Engineering Design and Biological Evaluation. American Fisheries Society, Bethesda, Maryland.

Glova, G. J. and J. McInerney. 1977. Critical swimming speeds of coho salmon ("Oncorhynchus kisutch") fry to smolt stages in relation to salinity and temperature. Journal of the Fisheries Research Board of Canada 34: 151-154.

Hansen, M. H., W. N. Hurwitz, and W. G. Madow. 1953. Sample Survey Methods and Theory. Volume I. John Wiley & Sons. New York, NY.

Haro, A., M. Odeh, J. Norieka, and T. Castro-Santos. 1998. Effect of water acceleration on downstream migratory behavior and passage of Atlantic salmon smolts and juvenile American shad at surface bypasses. Transactions of the American Fisheries Society 127: 118-127.

Hedgepeth, J., D. Fuhriman, and W. Acker. 1999. Fish behavior measured by a tracking radar-type acoustic transducer near hydroelectric dams. Pages 155-172 in Odeh, M. editor. 2000. Innovations in Fish Passage Technology. American Fisheries Society, Bethesda, Maryland.

Henderson, F. M. 1966. Open Channel Flow. Prentice-Hall, Inc. Upper Saddle River, NJ. 512 pp.

Hensleigh, J. E. and nine co-authors. 1998. Movement, distribution, and behavior of radio-tagged juvenile chinook salmon and steelhead in John Day, The Dalles, and Bonneville Dam forebays, 1997. Final report submitted to Portland District, U.S. Army Corps of Engineers by U.S.G.S. Cook, WA. March 1999.

John, J. E. A. and W. L. Haberman. 1983. Introduction to Fluid Mechanics. Prentice-Hall, Inc. Englewood Cliffs, New Jersey. 587 pp.

Johnson, G. E. 1996. Fisheries research on phenomena in the forebay of Wells Dam in spring 1995 related to the surface flow smolt bypass. Final report submitted to Walla Walla District, U.S. Army Corps of Engineers by Battelle. Richland, WA. March 1996.

Johnson, G. E., A. E. Giorgi, and M. W. Erho. 1997. Critical assessment of surface flow bypass development in the Lower Columbia and Snake rivers. Completion report submitted to Walla Walla District, U.S. Army Corps of Engineers by Battelle. Richland, WA. April 30, 1997.

Johnson, R. L., D. R. Giest, R. P. Mueller, R. A. Moursund, J. Hedgepeth, D. Fuhriman, and A. Wirtz. 1998. Behavioral acoustic tracking system (BATS). Final report submitted to Walla Walla District, U.S. Army Corps of Engineers by Battelle. Richland, WA. January 1998.

Johnson, W. R., L. Johnson, and D. E. Weitkamp. 1987. Hydroacoustic evaluation of the spill program for fish passage at The Dalles Dam in 1986. Final report submitted to Portland District, U.S. Army Corps of Engineers. March 1987.

Larinier, M. and F. Travade. 1999. The development and evaluation of downstream bypasses for juvenile salmonids at small hydroelectric plants in France. Pages 25-42 in M. Odeh,

editor. Innovations in fish passage technology. American Fisheries Society. Bethesda, Maryland.

MacLennan, D. N. and E. J. Simmonds. 1992. Fisheries Acoustics. Chapman and Hall. London, England. 325 pp.

Magne, R. A., W. T. Nagy, and W. C. Maslen. 1983. Hydroacoustic monitoring of downstream migrant juvenile salmonid passage at John Day and The Dalles Dams in 1982. Report by the Fisheries Field Unit. Portland District, U.S. Army Corps of Engineers. Cascade Locks, Oregon.

McCullagh, P. and J. A. Nelder. 1983. Generalized Linear Models. Chapman and Hall. New York, NY. 261 pp.

Muir, W., A. E. Giorgi, and T. C. Coley. 1994. Behavioral and physiological changes in yearling chinook salmon during hatchery residence and downstream migration. National Oceanic and Atmospheric Administration, National Marine Fisheries Service, Northwest Fisheries Science Center, Coastal zone and Estuarine Studies Division. Seattle, WA.

Nagy, W. T. and M. K. Shutters. 1995. Hydroacoustic evaluation of surface collector prototypes at The Dalles Dam, 1995. Draft report by the Report by the Fisheries Field Unit, Portland District, U.S. Army Corps of Engineers. Cascade Locks, Oregon. 3 7 pages.

Nichols, D. W. 1979. Passage efficiency and mortality studies of downstream migrant salmonids using The Dalles ice trash sluiceway during 1978. Report by the Oregon Department of Fish and Wildlife submitted to Portland District, U.S. Army Corps of Engineers. Portland, Oregon.

Nichols, D. W. 1980. Development of criteria for operating the trash sluiceway at The Dalles Dam as a bypass system for juvenile salmonids, 1979. Report by the Oregon Department of Fish and Wildlife submitted to Portland District, U.S. Army Corps of Engineers. Portland, Oregon.

Nichols, D. W. and B. H. Ransom. 1981. Development of The Dalles Dam trash sluiceway as a downstream migrant bypass system, 1980. Report by the Oregon Department of Fish and Wildlife submitted to Portland District, U.S. Army Corps of Engineers. Portland, Oregon. Portland, Oregon.

Nichols, D.W. and Ransom, B.H. 1982. Development of The Dalles Dam trash sluiceway as a downstream migrant bypass system, 1981. Report by the Oregon Department of Fish and Wildlife submitted to Portland District, U.S. Army Corps of Engineers. Portland, Oregon.

Ploskey, G., W. Nagy, L. Lawrence, M. Hanks, C. Schilt, P. Johnson, G. Johnson, D. Patterson, and J. Skalski. 2001. Hydroacoustic evaluation of juvenile salmon passage at The Dalles Dam: 1999. Final report submitted to Portland District, U.S. Army Corps of Engineers by USACE Engineer Research and Development Center. Vicksburg, MS. ERDC/EL TR-01-11. June 2001.

Rondorf, D. W., M. S. Dutchuk, A. S. Kolok, and M. L. Gross. 1985. Bioenergetics of juvenile salmon during the spring outmigration, annual report 1983. Report by the National Fishery Research Center submitted to the Bonneville Power Administration, Project 82-11. Cook, Washington.

Ruggles, C. P. and D. G. Murray. 1983. A review of fish response to spillways. Can. Tech. Rep. Fish. Aq. Sci. No. 1172.

Sherman, S. M. 1984. Monopulse Principles and Techniques. Artech House, Norwood MA. 363 pp.

Skalski, J. R., G. E Johnson, C. M. Sullivan, E. A. Kudera, and M. W. Erho. 1996. Statistical evaluation of turbine bypass efficiency at Wells Dam on the Columbia River, Washington. Canadian Journal of Fisheries and Aquatic Sciences 53(10): 2188-2198.

Smith, J. R. 1974. Distribution of seaward-migrating chinook salmon and steelhead trout in the Snake River above Lower Monumental Dam. Marine Fisheries Review 36(8): 42-45.

Snedecor, G. W. and W. G. Cochran. 1980. Statistical Methods. The Iowa State University Press. Ames, Iowa. 507 pp.

Sokal, R. R. and F. J. Rohlf. 1981. Biometry. W. H. Freeman and Company. San Francisco, California. 859 pp.

Steig, T. W. and W. R. Johnson. 1986. Hydroacoustic assessment of downstream migrating salmonids at The Dalles Dam in spring and summer 1985. Final report. Portland, Oregon: U.S. Department of Energy, Bonneville Power Administration; 1986; DOE/BP-23174-2.

Taylor, H. and S. Karlin. 1984. An Introduction to Stochastic Modeling. 3rd ed. Academic Press. San Diego, CA. 631 pp.

Thorpe, J. E. and R. I. G. Morgan. 1978. Periodicity in Atlantic salmon (*Salmo salar L.*) smolt migration. Journal of Fish Biology 12:541-548.

Williams, J., M. Gessel, B. Sandford, and J. Vella. 1996. Evaluation of factors affecting juvenile salmon fish guidance efficiency. Research report by Coastal Zone and Estuarine Studies Division, Northwest Fisheries Science Center, Seattle, WA.

Appendix A TECHNICAL DATA ON AFTS

In this appendix we present technical data on AFTS. Included are list of equipment, calibration data, echo sounder acquisition file, tracker configuration data, and example echograms.

A.1 AFTS Equipment

The AFTS equipment we used in this study is listed in Table A.1.

Table A.1. List of AFTS equipment.

SERIAL NO.	DESCRIPTION
DT4000-96-036	DT echo sounder surface unit (208 kHz)
DT-Xmit-0165-04	DT underwater unit (“bottle”)
DT6-CH-200-6x15-007	Split-beam transducer, full beam width @ half-power (one-way) 6.6 degrees
141-95-946	Digital cable @ 100 ft
141-98-1239	Tracker cable @ 6 ft (bio p/n: 7000-2032)
#3	Tracker system, underwater unit with stepper motors and misc. cables
CPR-96-190	Tracker cables
N/a	Tracker motor control box, surface unit, with 50pF-50pF bus cable
2496-9103A	Dell Inspiron 7000
17971-98K-A6CH	DELL adapter
9078400043	LINKSYS ethernet adapter
F3X171-10	BELKIN serial cable
Asset#2-300	Komodo monitor
M1055744	Keyboard
LTN60402395	Mouse
24X	24X MAX computer P166

A.2 Calibration Data

The acoustic calibration data for the split-beam system used in this study are presented in Table A.2.

Table A.2. Calibration data for AFTS’s split-beam hydroacoustic system.

PARAMETER	VALUE
Receiver #1 Sensitivity @ 1 m	-123.40 dB_v || uPa
Receiver #2 Sensitivity @ 1 m	-126.75 dB_v || uPa
Source Level (Xmit = -6 dB)	219.39 dB_{uPa} @ 1 m

A.3 Echo Sounder Configuration

The following data are from the VISACQ.INI file that controls data acquisition with the DT4000 split-beam echo sounder system. Software version 4.02 was used.

- The SYSTEM section controls overall operation of the VISACQ program

  System
- Which drive to log data to

  FileDrive=C
- Begin running as soon as the program is started

  AutoRun=N
- Do we want to automatically save files

  AutoLog=N
- How are we limiting auto-named files: P for ping count, T for time (minutes) or S for size (kB)

  LimitType=T
- What value for the limit: pings, minutes, or kB

  LimitValue=10
- Do we save the screen bitmaps (Y=save all bitmaps, 800 pings in each)

  SaveBitmaps=Y
- Which COM port has the GPS connected (-1 = not used)

  GpsPort=-1
- Main window placement - DO NOT CHANGE

  WindowPlacement=ffe9001003110254
- Default TVG for all views: 20 or 40 (default is 40)

  DefaultDisplayTVG=40
- Salinity of the water

  Salinity=0.0
- Temperature of the water

  Temperature=10.0
- Real Time Processing Configuration - how do we send the data?

  RTPUseTcpip=Yes
  RTPTcpipPort=2048
  RTPUsePrinter=Yes
  RTPPrinterPort=2049
  RTPPrinterChannel=1
  RTPUseSerial=No
  RTPSerialMode=BINARY
  RTPSerialPort=
  RTPSerialBaudRate=19200
  RTPTcpipTarget=90.0.0.1
  RTPUseFile=No
  RTPOutputFile=C:\DT4000.DTE
- The CHANNEL sections control the configuration of each transducer channel

[Channel 1]

- Where does this window appear - DO NOT CHANGE

  WindowPlacement=00160046021f01df

- Do we autorun this channel

  Run=Y

- Starting depth, in meters

  Start=1.0

- Stopping depth, in meters

  Stop=14.0 (also used 10.0 m about ½ time)

- Data threshold, in dB

  Threshold=-60.0

- Mode to threshold (0=FLAT, 1 = LINEAR, 2 = SQUARED)

  ThresholdMode=2

- Ping rate, in pings per second

  PingRate=30.0 (effectively only ~10 pps)

- Pulse width, in mSec

  PulseWidth=0.3

- Type of pulse (A=AMBIENT/NONE, C = CHIRP, M = MONOTONE)

  PulseType=M

- Do we want to use the timer functions for this channel (Y/N)

  UseTimer=N

- How long do we run for each burst

  MinutesOn=20

- How long to stay off between bursts

  MinutesOff=10

- How long to "hold off" on start - initial delay time

  StartAfter=1

- Real Time processing configuration for this channel

  RTPOutput=No
  RTPBottomPeakThreshold=-35.0
  RTPBottomPeakWidth=0.10
  RTPBottomBlankingThreshold=-60.0
  RTPBottomBlankingZone=0.25
  RTPBottomBottomWindow=1.50
  RTPBottomUsePreset=YES
  RTPBottomPresetDepth=60.0
  RTPTrackingCorrelation=0.90
  RTPMinTrackingEchoStrength=-70.0
  RTPMaxTrackingEchoStrength=-30.0
  RTPMinTrackingRange=1.00
  RTPMaxTrackingRange=60.00
  RTPMinTrackingEchoWidth=0.80
  RTPMaxTrackingEchoWidth=1.20
  RTPMinTrackingAlongshipAngle=-6.0

RTPMaxTrackingAlongshipAngle=6.0
RTPMinTrackingAthwartshipAngle=-6.0
RTPMaxTrackingAthwartshipAngle=6.0
RTPMinDualBeamTrackingEchoDifference=0.0
RTPMaxDualBeamTrackingEchoDifference=6.0
RTPMaxTrackingEchoes=25

- Tracker

Output=Y
Channel=1
Start=1.0
Stop=20.0
Threshold=-60
ComPort=1
MinTargetRatio=0.5
MaxTargetRatio=3.5
TimerDuration=30
PassiveMode=N

A.4 Tracker Configuration

The tracker configuration was contained in a file called TSS1.CFG. This file is printed below. For the purpose of this appendix, we embedded in the TSS1.CFG descriptions of some of the parameters.

- NOTES

Primary Configuration file for TSSOPER & TSSOPERB software for BioSonics TSS

Note: Comments allowed, mark with "/" on new line or end of datum line.

Comment key: [parameter format] {R/O/W/U, default}; R-required, O-optional, W-optional with warning, D-requirement depends on value of other parameter (some lines are not required if parameters not used).

03-23-00 initial config for The Dalles, 2000 based on Fuhriman's initial config 04-15-00 alpha min 30 deg, alpha and beta offsets 2 deg, start study.

04-15-00 final set-up 1400 h w/ Hedgepeth.

- MAIN MISC.

maximum ping rate [real, pings/sec] = 10 /{R}

This parameter is adjustable during operation. The ping rate will not exceed this value, but might be less than this. The ping rate is as-fast-as-possible, not fixed.

max lines in file [int] = 10000 /{R}

This is the maximum number of echoes (one per line) stored in each data file. A value of 10000 typically allows two data files to fit uncompressed on a single 1.44 MB floppy disk. This value does not affect how much data is lost if there is a power outage, as the file is written frequently, so there is no advantage to having a small file. Each new file is named with a MMDDHHMM.txt format.

display graphs [Y/N] = Y /{W,N}

This turns on or off the line graphs showing target placement on the X, Y, Z and R axes. The graphs display can be turned on and off during operation.

graph scales equal [Y/N] = Y /{DW,Y}

If 'N', the graph scales are each adjusted to fit the screen width. If 'Y', all graph scales are equal (normally preferred if the ranges are similar).

- POSITIONING MISC

key move angle [real, degrees] = 5.0 /{R}

This is the angle in degrees that a key press will move the rotator for manual positioning. This is adjustable during operation.

allow angle error [real, degrees] = 2.0 /{R}

The +/- angle in degrees that the rotator position can slip and not put an error tag in the data file. This is checked during the position check.

install alpha [real, degrees] = 10.0 /{R}

The angle in degrees that the rotator's Y axis points relative to the horizon or desired alpha = 0 reference point.

alpha margin [real, degrees] = 2.0 /{R}

beta margin [real, degrees] = 2.0 /{R}

Used when calibrating the range of movement when starting operation or after a position check. The system sets the operational limits less than the actual limit switch points by these angular amounts.

auto position check [Y/N] = Y /{R}

If 'Y', the system periodically checks for rotator position slippage, and recalibrates position.

minutes between position checks [real, minutes] = 30.0 /{DW,20}

Sets the interval at which rotator position calibration is automatically checked.

max idle time minutes [real, minutes] = 0.10 /{R}

The length of time the system will remain idle (not tracking a target) before resetting the rotator position.

free track time minutes [real, minutes] = 2.0 /{R}

The amount of time the system tracks targets at will. When this time is elapsed, and no target is being tracked, the rotator moves back to its home position or a new random position, as set elsewhere in this configuration file.

reset idle pings/track threshold [integer] = 5 /{W,5}

The number of consecutively tracked pings required to reset the idle timer for max idle time minutes.

- POSITIONING OPTIONS -- RANDOM START POSITION

random start position [Y/N] = Y /{R}

If 'Y', the rotator is moved to a new "start" position at regular intervals defined by free track time minutes. If set to 'Y', this overrides specific start position.

pos radius min [real, meters] = 1.0 /{DR}

pos radius max [real, meters] = 14.0 /{DR}

pos alpha min [real, degrees] = 30.0 /{DR}

pos alpha max [real, degrees] = 95.0 /{DR}

pos beta min [real, degrees] = -5.0 /{DR}

pos beta max [real, degrees] = 52.0 /{DR}

The random start position is determined within the targeting X, Y, Z boundaries defined in this configuration file. The parameters here further limit the direction the transducer can point for random positioning.

- POSITIONING OPTIONS -- SPECIFIC START POSITION

specific start position [Y/N] = N /{W,N}

Enables a fixed rotator start position defined below. If 'N', the start position is set to the installed alpha = 0, and beta = 0.

start alpha angle [real, degrees] = 30 /{DR}

start beta angle [real, degrees] = -6 /{DR}

These angles define the "home" rotator position.

- SPECIAL CONTROL 1

special control 1 [Y/N] = Y /{W,N}

This sets a control mode developed for riverine work, but adapted for application elsewhere. Used in conjunction with a specific start position, the system initially acquires a target within the range gate defined below. When a target is tracked outside of the range gate, it is tracked exclusively until lost. If a target is lost outside of the range gate, it tries to reacquire the target within a small space (max reacquire distance). The system then returns to the specific start position. If used with a random start position, the reacquire feature is enabled, but the range gate is disabled.

range gate width [real, meters] = 20 /{DR}

range gate middle [real, meters] = 10 /{DR}

These parameters set the initial target acquisition boundaries with respect to distance from the transducer. The range boundaries are at range gate middle +/- ½ range gate width. These parameters are only used if specific start position = Y. If random start position is used, these parameters are ignored.

range width change increment [real, meters] = 1.0 /{DW,2.0}

range middle change increment [real, meters] = 1.0 /{DW,2.0}

These values set the increments for adjusting the previous parameters using the keyboard during operation.

max reacquire distance [real, meters] = 3 /{DR}

When the reacquire mode is active after losing a target (using special control 1), the system will look for a target no more than this distance from the currently estimated position within the TARGETING BOUNDARIES.

max reacquire pings [integer] = 20 /{DR}

The reacquire mode will be terminated if no suitable target is found within this number of pings.

range gate angle width (+/-) [real, degrees] = 3 /{DR}

The range gate will be used to limit target selection range when the rotator position is within +/- this value from the specific start position.

- MOTOR CONTROL

  motor settle delay seconds [real, seconds] = 0.02 /{W,0.02}

  The time in seconds which the control software waits to trigger a ping after the rotator has finished moving to its new position. While no specific measurement to determine an appropriate value has been made, the default value seems to work well.

  motor speed number [integer] = 2 /{W,2}

  This is a value loaded in the stepper motor driver hardware that controls the stepping rate. Other values also control the step rate, but this is the only one available to the user. The smaller the value, the faster the motor (range 1 to 255). This value should not be changed for normal operation except on the recommendation of a BioSonics technician.

  range step error [integer] = 3 /{W,3}

  When the rotation range is initially calibrated at start-up, a step range between the limit switches is saved for each axis. When the position is re-calibrated after each position check, the step ranges must be within +/- this value of the original ranges, or the system will halt. This prevents continued operation of the rotator if it is jammed or a limit switch fails. The equivalent in degrees for each step is 0.09 for the outside axis (10:1 gearbox), and 0.1875 for the inside axis (4.8:1 pulleys). The default value is recommended, and should not cause the system to halt unnecessarily, whereas a value of 1 will. The backlash of the drives is around 0.5 degree for both axes.

- TELEGRAM RECEIVING

  com port [1/2] = 1 /{R}

  com rate [integer, bps] = 115200 /{W,115200}

  These are the settings for the com port used to transfer data between the echosounder and the rotator control computer. The com port is set here for the rotator control computer.

- COORDINATE ROTATION

  rotate coordinates [Y/N] = N /{W,N}

  lock coordinates [Y/N] = Y /{DW,Y}

  The (X,Y,Z) coordinates displayed on the screen and written to the data file can be rotated to suit the user's coordinate system and installation orientation. The user may change between "system" coordinates and "user" coordinates during operation unless the coordinates are locked. It is recommended to lock coordinates during actual data acquisition to prevent inadvertent changing of the coordinate mode during operation. It is best to only used the rotation matrix if install alpha cannot set the (X,Y,Z) coordinates to the desired orientation.

  Cxx [real] = 1 /{DR}

  Cxy [real] = 0 /{DR}

  Cxz [real] = 0 /{DR}

  Cyx [real] = 0 /{DR}

  Cyy [real] = 1 /{DR}

  Cyz [real] = 0 /{DR}

  Czx [real] = 0 /{DR}

Czy [real] = 0 /{DR}

Czz [real] = 1 /{DR}

These values define the coordinate rotation matrix. The matrix is displayed in standard mathematical form when the program is started. If the user is not familiar with rotation matrices, references on this subject are readily available, or a BioSonics technician can set the values.

- TRANSDUCER -- STANDARD TS COMPENSATION

The rotator control software performs the beam corrections to add flexibility to deviate from the stored calibration values in the transducer. These values are provided by BioSonics.

beam angle [real, degrees] = 6.6 /{DR}

- TRANSDUCER -- SPLIT-BEAM ANGLES

phase aperture [real, degrees] = 6.8 /{DR}

These values are taken from the transducer calibration. The separate along and athwart values are not typically used.

invert angle sign [Y/N] = Y /{DR}

These parameters should be set according to the transducer used. For frequencies other than those in the comment above, consult BioSonics. The system will not track if the value is incorrect. Most transducers do not need the separate along and athwart values, and they should be removed.

along offset [real, degrees] = 2 /{W,0}

athwart offset [real, degrees] = 2 /{W,0}

These values are for correcting the beam angle values from the transducer, and are derived from test calibration data. They are provided by BioSonics for each individual transducer. They were required due to a computer code problem that has since been corrected.

- TRANSDUCER -- PARALLAX CORRECTION

Tells the software to correct the beam angles at close range.

soft PC [Y/N] = Y /{R}

space along [real, meters] = 0.039 /{DR}

space athwart [real, meters] = 0.039 /{DR}

approx. for 208k: space along = 0.03735, space athwart = 0.03735

approx. for 201k: space along = 0.03839, space athwart = 0.03839

approx. for 430k-6x5: space along = 0.0185, space athwart = 0.0185

These values are needed to calculate correct beam position at close range. They are provided by BioSonics.

- TRACKING

track error beep [Y/N] = N /{W,N}

If there is a tracking error the computer will beep. Should be set to 'N' except if desired during test and observation.

continue track with errors [Y/N] = N /{W,Y}

Do not enable when using special control 1. This tells the program to continue tracking the best match target even if there is a tracking error (e.g. target too fast). The 'C' tag is placed in the line in the data file. During data processing, the user can select whether or not to treat the 'C' as an 'N' or a 'T' tag. See the data file description for more information.

max pings in track [integer] = 799 /{W,799}

The default value prevents errors in the data processing software, which can currently handle a maximum 800 ping single track length. It also allows the system to break free from a fixed target such as structure.

max pings in error track [integer] = 1200 /{W,1200}

If continue track with errors is enabled, this is the longest a track with 'C' tags will be before the system "breaks free".

max speed [real, meters/sec] = 4.0 /{R}

This is the maximum ping to ping speed of the tracked target before a tracking error is set.

min dist mult [real] = 3.0 /{R}

This limits the density of the echoes around the tracked target. If the second best choice for continuing the track is closer than this value times the ping-to-ping movement of the best fit track, a tracking error is set.

max delta time [real, seconds] = 0.5 /{W,1.0}

This is the maximum time between pings before a tracking error is set. This only happens if the program is paused during operation.

- PREDICTIVE TRACKING

predictive tracking [Y/N] = Y /{R}

weight 1 = 1.0

weight 2 = 0.5

weight 3 = 0.25

weight 4 = 0.125

Predictive tracking is normally enabled. The weights are applied to ping-to-ping movement, with weight 1 being applied to the movement of the target from the most recent ping, and weight 4 being the oldest movement. The weights only need to be entered if the user wishes to change the defaults for some reason. The weights are automatically normalized. Predictive tracking allows the beam to be centered most effectively on the tracked target. The rotator tries to center the beam on where the target is expected to be in the next ping, instead of where it was (if predictive tracking is disabled).

- TARGETING BOUNDARIES

The values are entered in the user's coordinate system (rotated, if enabled), and are only used when selecting a new target from a set of echoes in a ping.

compTS low [real, dB] = -60 /{R}

compTS high [real, dB] = -10.0 /{R}

target radius min [real, meters] = 1.00 /{R}

target radius max [real, meters] = 17.0 /{R}

target x min [real, meters] = -5 /{R}

target x max [real, meters] = 20 /{R}

target y min [real, meters] = -2 /{R}

target y max [real, meters] = 20 /{R}

target z min [real, meters] = 0 /{R}

target z max [real, meters] = 9.0 /{R}

- TRACKING BOUNDARIES (no compTS check for tracking)

  These values are used while actively tracking a target. If tracking use target bounds is enabled, these values are replaced by the applicable targeting parameters, and are not necessary, but may be left in the configuration file if desired.

tracking use target bounds [Y/N] = N /{W,Y}

track radius min [real, meters] = 1.0 /{DR}

track radius max [real, meters] = 20.0 /{DR}

track x min [real, meters] = -10 /{DR}

track x max [real, meters] = 25 /{DR}

track y min [real, meters] = -2 /{DR}

track y max [real, meters] = 25 /{DR}

track z min [real, meters] = -10 /{DR}

track z max [real, meters] = 9 /{DR}

- ADDITIONAL TRACKING BOUNDARIES

  These values have no equivalent in the targeting parameters, so must be set here as desired.

track alpha min [real, degrees] = -72 /{R}

track alpha max [real, degrees] = 95 /{R}

track beta min [real, degrees] = -62.0 /{R}

track beta max [real, degrees] = 52.0 /{R}

- SAVED DATA FILTER BOUNDARIES

  The echoes saved to the data file can be filtered based on these parameters. This can reduce “garbage” echoes in the data file, as all echoes in each ping are saved, not just the tracked echo (target). The filter may be turned on or off, and may use the tracking parameters to override or replace parameter entries here.

saved data filter [Y/N] = N /{W,N}

saved use tracking bounds [Y/N] = Y /{DW,Y}

save radius min [real, meters] = 1 /{DR}

save radius max [real, meters] = 50 /{DR}

save x min [real, meters] = -50 /{DR}

save x max [real, meters] = 50 /{DR}

save y min [real, meters] = -50 /{DR}

save y max [real, meters] = 50 /{DR}

save z min [real, meters] = -50 /{DR}

save z max [real, meters] = 50 /{DR}
save alpha min [real, degrees] = -100 /{DR}
save alpha max [real, degrees] = 100 /{DR}
save beta min [real, degrees] = -55 /{DR}
save beta max [real, degrees] = 55 /{DR}

A.5 Example Echograms

Figures A.1-A.6 are examples of echograms from the split-beam system. Note that the transducer is usually moving and we do not know where it is aimed by only examining the echogram.

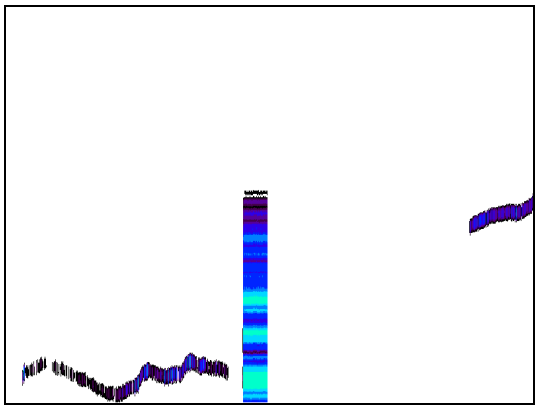

Figure A.1. Tracked fish moving into the dam.

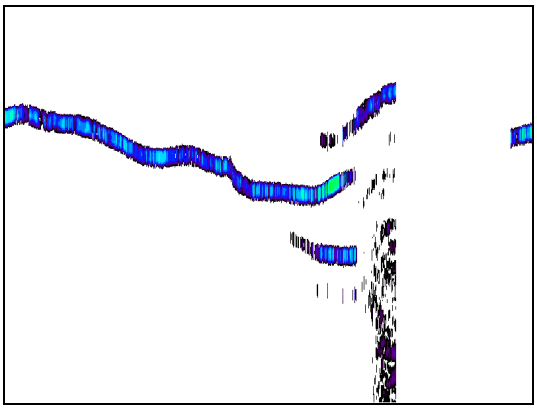

Figure A.3 Example of AFTS tracking one fish then losing track when two more enter the beam.

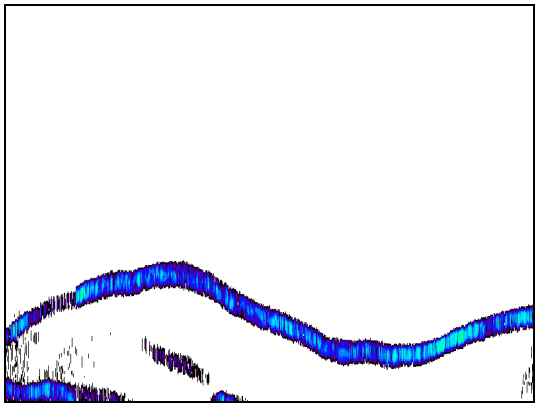

Figure A.2. Example of long track at night, likely holding deep off the MU1-1/FU2-2 pier nose or the MU1-1 turbine intake.

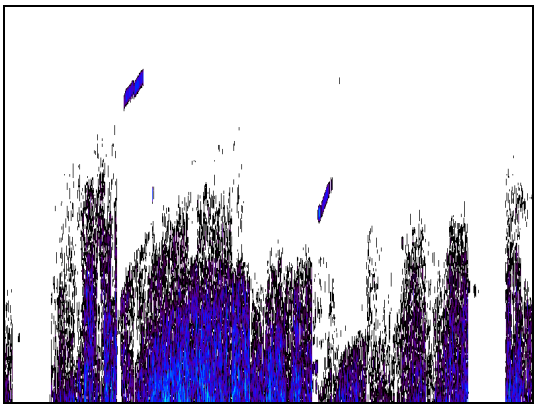

Figure A.4. Echogram showing surface turbulence present on windy days at TDA.

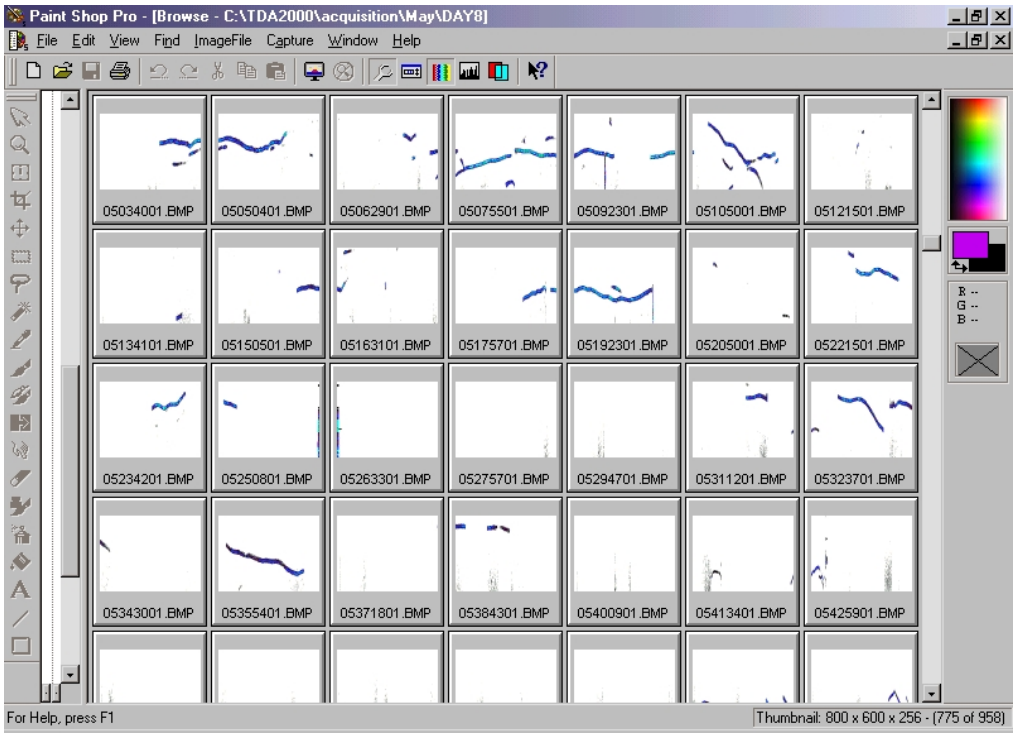

Figure A.5. Example of sequence of echograms from one study-day showing the decrease in fish holding behavior from night to day (dawn; 0507 to 0542 h). Each frame is about 100 sec long.

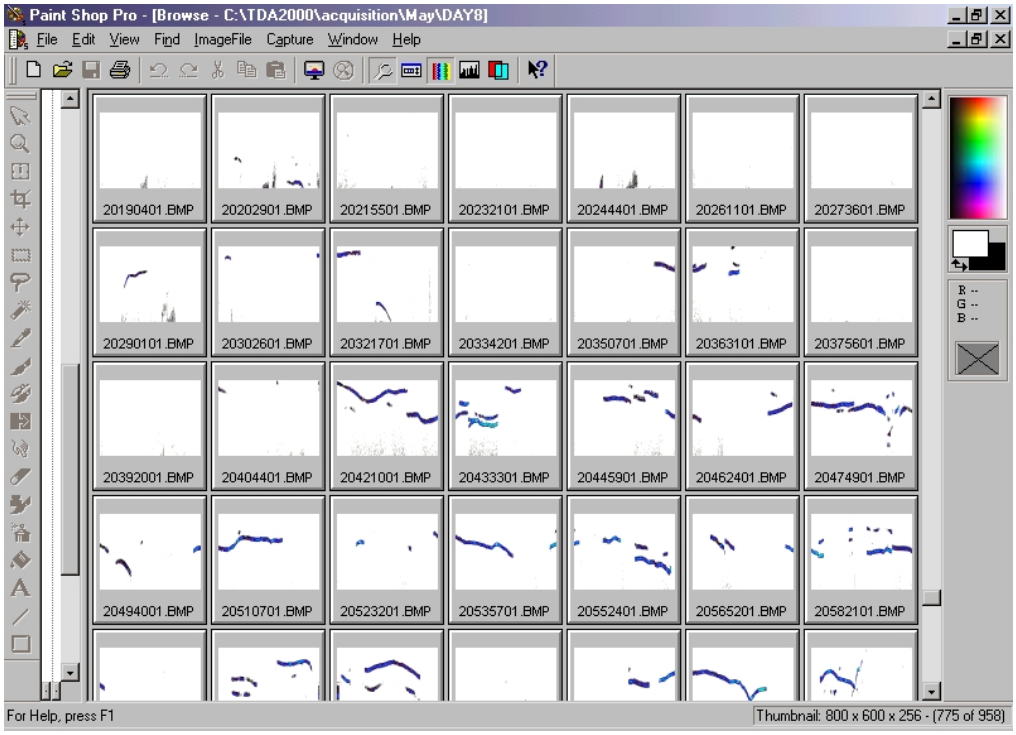

Figure A.6. Example of sequence of echograms from one study-day showing the increase in fish holding behavior from day to night (dusk; 2019 to 2058 h). Each frame is about 100 sec long.

Appendix B ERROR ANALYSIS

B.1 Introduction

The Active Fish Tracking Sonar (AFTS) uses four angles plus range to track a fish target (Figures B.1 and B.2). Two of the angles are planar angles from a split-beam transducer to the fish. The other two angles are from the two rotator motors, which are required to drive the transducer to point directly at the fish target. These four angles and range to the fish target enable a fish position to be estimated in terms of a Cartesian coordinate system: X, Y, and Z.

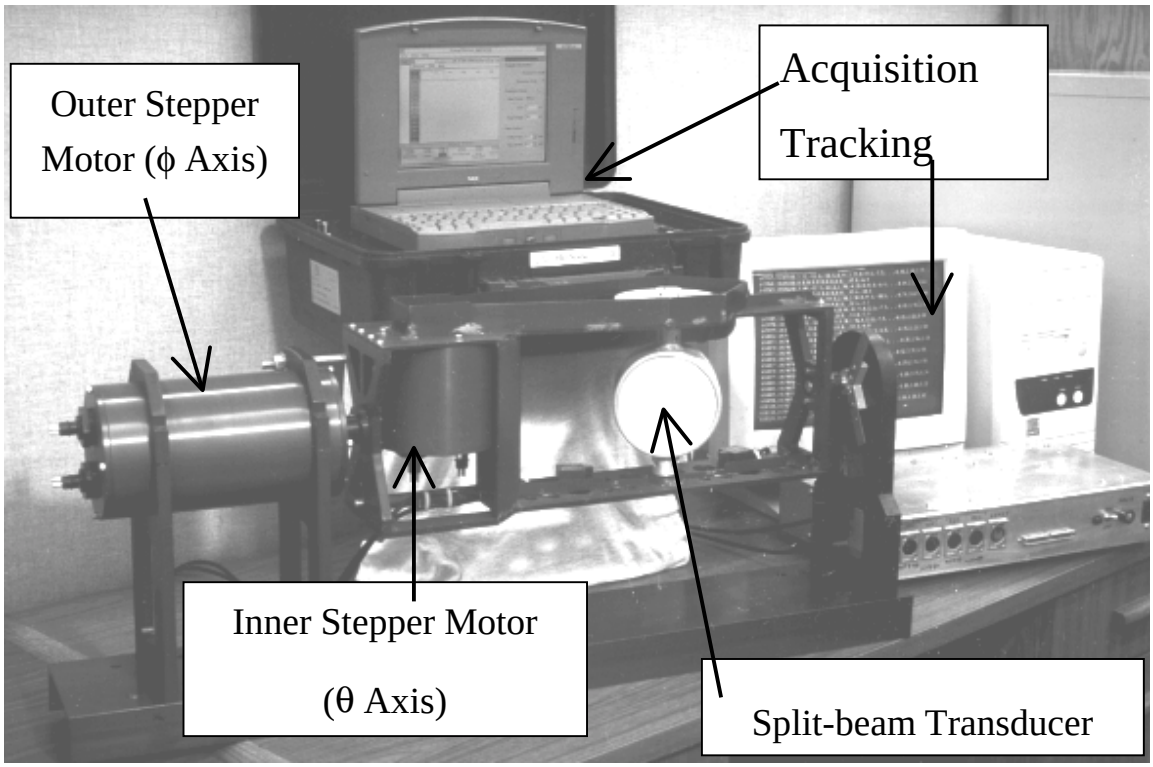

Figure B.1. Photograph of active fish tracking sonar.

The BioSonics DT6000 split-beam echosounder (DT) is unique. The split-beam transducer angles are measured from three circular piezo-electric ceramics in the transducer: center, x and y. A fourth, larger, circular ceramic in the transducer transmits the sound pulses which are reflected from a fish and used by the angle-measuring elements. The reflection into the large ceramic is used to determine the range to the fish target (and also for measuring sound intensity for target acquisition and acoustic size estimation).

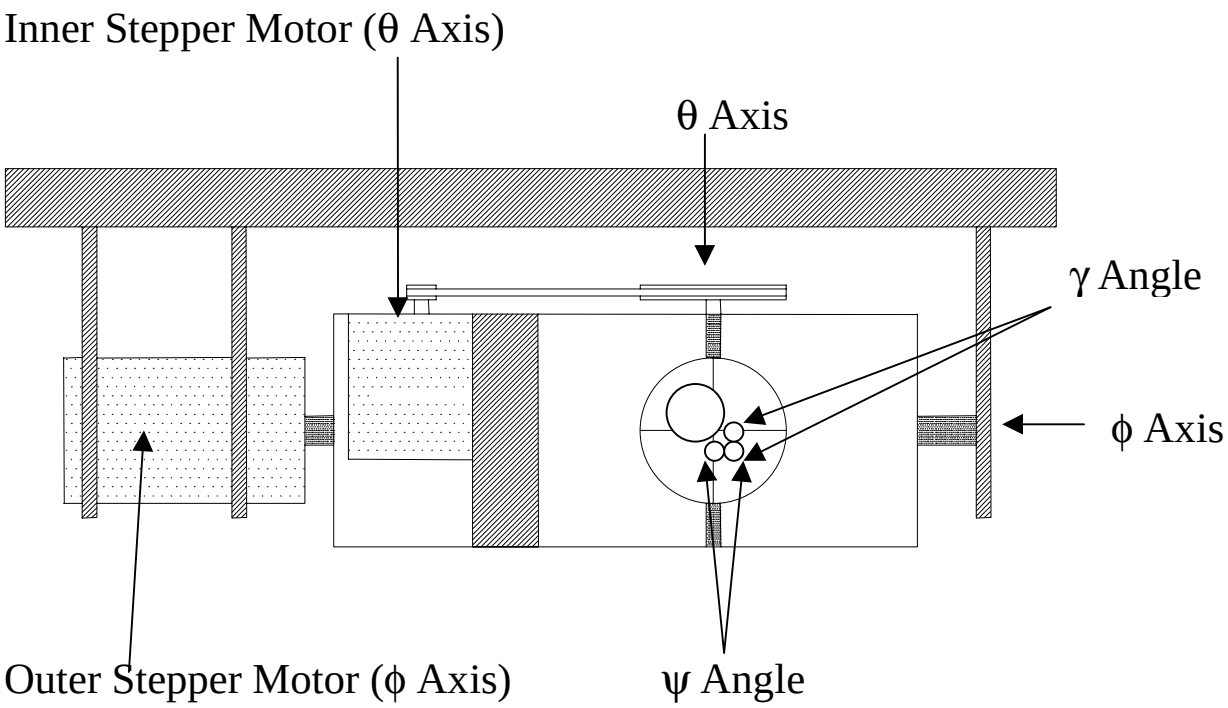

Figure B.2. Diagram of the Acoustic Fish Tracking Sonar (AFTS). The angles to target position from a split beam transducer are measured using two piezo-electric ceramic receivers for comparisons of phase. Once the planar angles (γ, ψ) from the fish reflection are determined, they are used to determine new rotator motor angles (θ, ϕ) towards the target. Motors turn the transducer to follow fish movement.

Sherman (1984) boldly states "All angle-measuring systems, including monopulse, have errors due to various causes." The AFTS system is a monopulse device, i.e. capable of measuring angles in a single-pulse. Error in a single estimation of X, Y, and Z can be introduced in three measurements:

- rotator angles;
- planar angles relative to transducer;
- range to fish target.

Error for ping-to-ping tracking is also important for following an individual fish. The purpose of this appendix is to assess these potential sources of errors, and to document any observations of error.

B.2 Rotator Angles

The sources of error in rotator angles are due to the backlash in the armature housing the split-beam transducer, the resolution of the stepper motor angles, and the fixture of the AFTS housing relative to the sonar, dam or state-plane referenced coordinate system. Backlash in the

outside armature (ϕ, Figure B.2) was measured as +/- 0.10 degrees. Backlash (or belt windup) in the inner armature (θ, Figure B.2) was measured as +/- 0.15 degrees. The outer armature is driven by a stepper motor which half steps (0.9 degrees per half step), but is geared by a factor of ten which means the angle resolution is 0.09 degrees making a total possible error of about +/- 0.2 degrees. The inner armature is geared by a factor of 4.8, making the total possible error of about +/- 0.3 degrees. The mean error is about 0 degrees for both armatures.

B.3 Split-beam Angles

The two split-beam angles are planar angles, that is they are measured in two different planes that include the fish target and the acoustic center between the each pair of piezo-electric ceramics that are used for an angle measurement. The transducer manufacturer aligns the three ceramics to form a right angle so that the planes will be nearly orthogonal to each other. The precision of alignment is a potential error that may affect the estimate of fish position. The design of the BioSonics transducer requires that planar angles be translated by a parallax correction discussed below. This translation is more severe for fish at close range, and is dependent on the range to the fish and on the spacing between the acoustic center of the angle-measuring ceramic pair and the acoustic center of the main transmitter-receiver element. This measurement must also be precise. It is assumed that the acoustic centers are located at the center of the ceramics.

An angle estimate depends on digital quadrature sampling of two signals from a pair of ceramics. Quadrature sampling, angle conversion using phase aperture, parallax correction to large beam, and target detection are all processes which may produce error included in the split-beam angle estimates.

B.3.1 Quadrature Components

The phase differences between a pair of receivers gives us one planar angle to the fish target. Quadrature sampling is one way to estimate phase difference. If the signal *S(t)* from one of the receivers can be expressed as:

$$\begin{aligned} S(t) &= A(t)\cos[\omega_0 t + \varphi(t) + \theta] \\ &= X(t)\cos(\omega_0 t) + Y(t)\sin(\omega_0 t) \end{aligned}$$

The quadrature components *X(t), Y(t)* are the samples one quarter of a wavelength apart:

$$\begin{aligned} X(t) &= A(t)\cos[\varphi(t) + \theta] \\ Y(t) &= -A(t)\sin[\varphi(t) + \theta] \end{aligned}$$

where, θ = arbitrary angle offset

$\varphi(t)$ = phase

$A(t)$ = amplitude

$\omega(t)$ = carrier frequency of signal

The phase of one receiver is estimated by:

$$\varphi(t) = \tan^{-1}\left(\frac{-Y(t)}{X(t)}\right)$$

By repeating this process on two receivers, a phase difference can be calculated. This phase difference $\Delta\varphi(t)$ can only be measured only in the range of plus or minus π radians. It is referenced to the wavelength of the carrier frequency $\omega(t)$ measured in radians s^{-1}.

The next step is to covert the phase difference to an actual angle $\theta(L)$ to the fish target. The phase aperture is the maximum physical angle that can be determined from the electrical phase output, compared between two ceramics separated at distance D between acoustic centers. This angle occurs at phase wrap (Figure B.3), and is equal to plus or minus arcsine(wavelength/distance between receivers). The wavelength λ is equal to the sound speed c times the frequency f in cycles s^{-1}. $\theta(L)$ can be calculated using a small angle approximation:

$$\theta(L) = \sin^{-1}\left(\frac{c\ \Delta\varphi(t)}{2\ f\ D\ \pi}\right)$$
$$\cong \frac{c\ \Delta\varphi(t)}{2\ f\ D\pi}$$

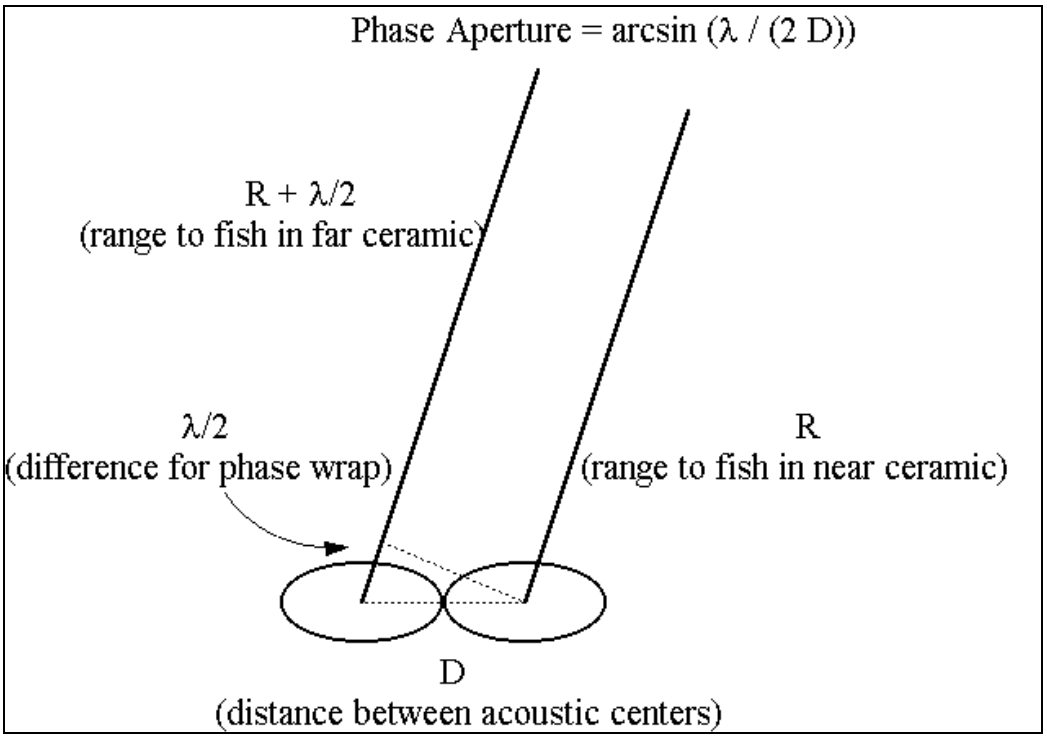

Figure B.3. Phase aperture is defined as the maximum angle from perpendicular before phase wrap occurs. It is a function of 1) the distance D between acoustic centers of the piezo-electric ceramics, which are used to determine a split-beam planar angle and 2), the wavelength λ. The total usable volume is +/- phase aperture.

The phase aperture is the maximum angle before phase wrap occurs, and using the small angle approximation is:

$$\pm \frac{c}{2 f D}.$$

The spacing between the elements for estimating phase difference in the BioSonics 208 kHz split-beam transducer was 0.03018 m. The phase aperture is +/-6.77 degrees letting the speed of sound c be 1480 m/s. For a plus or minus seven degrees phase aperture, the small angle approximation is at most a 0.25% error.

B.3.2 Parallax

Parallax is an error which is encountered because of the difference in location of the main beam ceramic and the pair of ceramics which estimate a planar angle. The parallax correction is performed in the tracking software, and affects the estimated target strength primarily. The parallax to the armature center is not considered, but could represent a slight error in angle for tracking a fish target. The spacing D' between acoustic centers of the main beam ceramic and the pair measuring angle was measured as 0.03735 m for the 208 kHz transducer. The parallax correction is dependent on range R to the tracked fish, and is shown below in reference to the angles in Figure B4:

$$\gamma' = \gamma - \sin^{-1}\left(\frac{\mathrm{D}'\cos\gamma}{R}\right).$$

Ehrenberg (1981) described the error in the split-beam angle estimates. Ehrenberg (1981) presents some standard deviations of split-beam angles as a function of signal to noise ratio after bandpass filtering (Table B.1).

Table B.1. Standard deviation of the angular estimate as a function of signal to noise ratio for single and multiple cross correlation techniques from Ehrenberg (1981).

FILTER OUTPUT SNR (DB)	STANDARD DEVIATION OF ANGULAR ESTIMATE (DEG)		
	ONE CROSS CORRELATION	THREE ADJACENT CROSS CORRELATIONS	FOUR ADJACENT CROSS CORRELATIONS
10	0.7073	0.7103	0.7232
15	0.3937	0.3920	0.3943
20	0.2248	0.2217	0.2211
25	0.1341	0.1293	0.1270
30	0.0879	0.0808	0.0765

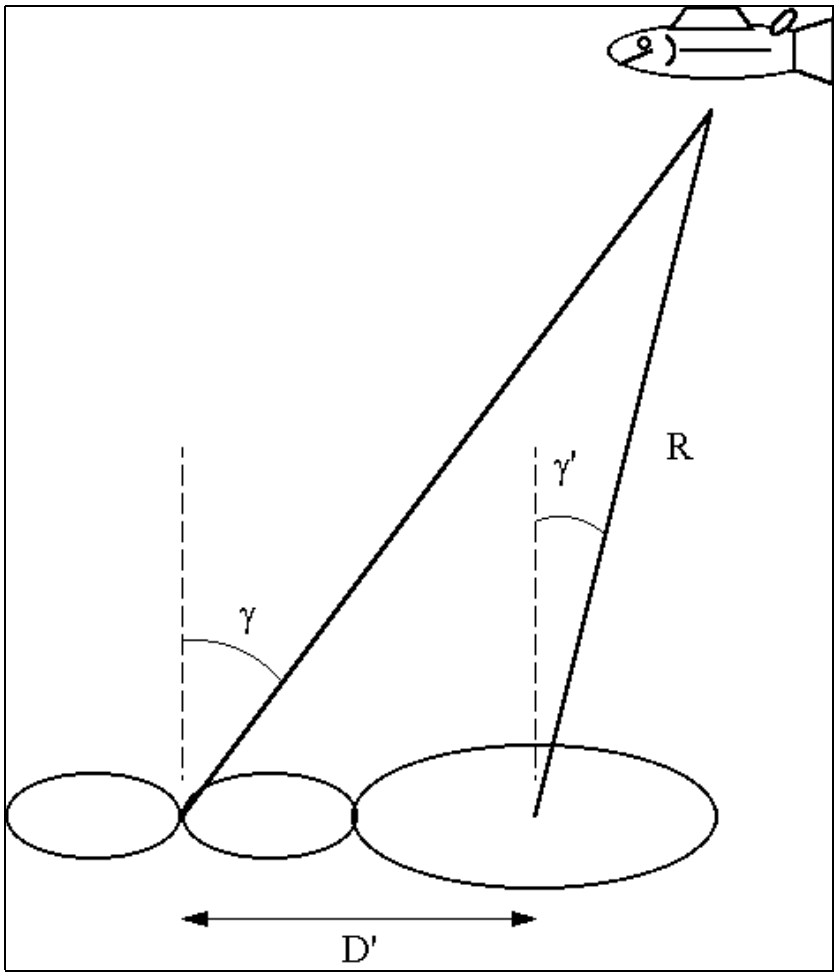

Figure B.4. Schematic showing the parallax (difference between angles γ and γ') from the phase estimate receiver pair and from main beam. Parallax is a function of the distance D' between the acoustic centers and the range R to the fish target.

Table B.1 uses a cross correlation technique for split-beam angle ($\hat{\theta}_L$) measurement. The BioSonics DT6000 split-beam echosounder uses a digital quadrature sampling approach. Roberts (cited in Ehrenberg 1981) estimated electrical angle ($\hat{\theta}_e$) variance from a simulation of quadrature sampling as 1/(2SNR). His results matched Ehrenberg's analytical estimates. For large signal to noise ratios (SNR) (greater than 10 dB) variance in the angles could be estimated as:

$$VAR\left[\Delta\hat{\theta}_e\right] = \frac{1}{SNR}, \text{and}$$

$$VAR\left[\hat{\theta}_L\right] = \left(\frac{c}{\omega_0 d}\right)^2 \frac{1}{SNR},$$

where,

c = speed of sound,

d = distance between acoustic centers of two ceramics used to estimate phase,

ω_0 = angular frequency.

The variance estimate, at a SNR = 10 dB (the signal intensity is 10 times the noise) using speed of sound of 1480 m s^{-1}, 208 kHz, spacing of 0.03735 m is:

$$VAR[\hat{\theta}_L] = \left(\frac{c}{\omega_0 d}\right)^2 \frac{1}{SNR} = \left(\frac{1480}{2\pi\, 208{,}000\, 0.03735}\right)^2 \frac{1}{10} = 0.000141 \text{ radians squared}$$

or 0.462 degrees squared (SD = 0.68 degrees). In the BioSonics implementation of angle data storage, the angles (-6.77 to +6.77) are coded as an integer from 0 to 256, or 0.0529 degrees per coded integer step.

B.4 Target Detection

Target recognition from the reflection in the main (larger) ceramic (see Figure B.4) is a first step before acquiring angles. Ehrenberg (1981) pointed out several estimation procedures for target recognition. BioSonics uses a combination of techniques of cross-correlation, and pulse width relative to finding a threshold of –12 dB.

B.5 Range to Target

The DT digital echosounder samples the voltage output at 41.667 kHz or 41,667 samples per second. This corresponds to 0.01776 m per sample using a two-way reflection (1480 m/s one-way). Therefore at 1 m this resolution in range is about 2% but at 10 m it is about 0.2%. We expect less than one or two resolution steps of possible error when tracking fish.

B.6 Target Tracking

As mentioned above, the operation of AFTS involves two sets of angles: those of the stepper moters and those of the split-beam transducer. To accomplish fish tracking, the split-beam phase angles, γ and ψ needed to be compensated by the stepper motor angles θ and ϕ (Figure B.2).

The following analysis shows the fundamental equations for rotation; it assumes a dam-referenced coordinate system (x, y, z). The x-axis runs along the dam to the right when facing away from the dam, the y-axis points up, and the z-axis points away from the dam. Let the unit vectors in the absolute coordinate system be $\hat{i}$, $\hat{j}$, and $\hat{k}$. Then unit vectors of the rotated coordinate system (ξ,η, and ζ) of the transducer are:

$$e_\xi = \cos\theta\,\hat{i} - \sin\theta\sin\phi\,\hat{j} - \sin\theta\cos\phi\,\hat{k}$$
$$e_\eta = \qquad\qquad \cos\phi\,\hat{j} - \qquad \sin\phi\,\hat{k}$$
$$e_\zeta = \sin\theta\,\hat{i} + \cos\theta\sin\phi\,\hat{j} + \cos\theta\cos\phi\,\hat{k}$$

The unit vector to a fish target is approximately:

$$e_\rho = \sin\psi\, e_\xi - \sin\gamma\, e_\eta - \sqrt{1-\sin^2\gamma-\sin^2\psi}\, e_\zeta$$

In terms of the stepper motor coordinate system the unit vector to the fish is:

$$\begin{aligned} e_\rho \;=\; & \left(\cos\theta\sin\psi \;+\sin\theta\sqrt{1-\sin^2\gamma-\sin^2\psi}\right)\hat{i} \\ & + \left(-\sin\theta\sin\phi\,\sin\psi \;+\cos\phi\,\sin\gamma \;+\cos\theta\sin\phi\sqrt{1-\sin^2\gamma-\sin^2\psi}\right)\hat{j} \\ & + \left(-\sin\theta\cos\phi\,\sin\psi \;-\sin\phi\,\sin\gamma \;+\cos\theta\cos\phi\sqrt{1-\sin^2\gamma-\sin^2\psi}\right)\hat{k} \end{aligned}$$

The new stepper motor angles required to follow the fish are:

$$\theta' = \sin^{-1}\left(\cos\theta\sin\psi \;+\sin\theta\sqrt{1-\sin^2\gamma-\sin^2\psi}\right)$$
$$\phi' = \tan^{-1}\left(\frac{-\sin\theta\sin\phi\,\sin\psi \;+\cos\phi\,\sin\gamma \;+\cos\theta\sin\phi\sqrt{1-\sin^2\gamma-\sin^2\psi}}{-\sin\theta\cos\phi\,\sin\psi \;-\sin\phi\,\sin\gamma \;+\cos\theta\cos\phi\sqrt{1-\sin^2\gamma-\sin^2\psi}}\right)$$

In addition to these two equations for following fish, we have attempted to predict where the fish moves, and rotate the beam axis towards that position. An algorithm predicted incremental movement in Δx, Δy and Δz separately using the following equation (shown for Δx):

$$\Delta x = \frac{\left(x_i - x_{i-1}\right) + 0.5\left(x_{i-1} - x_{i-2}\right) + 0.25\left(x_{i-2} - x_{i-3}\right) + 0.125\left(x_{i-3} - x_{i-4}\right)}{1.875}$$

Our predictive method is an "ad hoc" implementation of a discounted least-squares fit (Brookner 1998) in which the most recent velocity estimate is weighted by unity, the next most by ω=0.5, the next oldest by ω^2, the next by ω^3 and so on. In our "ad hoc" implementation we stop at ω^3 and assume that time between pings is constant. Brookner (1998) describes the prediction line fit which "minimizes the sum of the weighted errors with the weighting decreasing as the data gets older; that is, the older the error, the more it is discounted." In a more rigorous view, the fit should minimize the total error:

$$e_D = \sum_{r=0}^{N} \omega^r\, \varepsilon_{n-r}^2$$

where,

$$0 \le \omega \le 1$$

$$\varepsilon_{n-r} = \hat{x}_{n-r} - x_{n-r}$$

Therefore, the target tracking will occur with these types or errors due to the difference between the predicted location and the actual location measured. We are able to use field collections of tracked fish to estimate what the mean squared error is likely to be.

B.7 Field Estimation

B.7.1 Spatial Closure

Spatial closure is the process of comparing the known position of a target with the position of that target as estimated by a positioning instrument, such as AFTS. Spatial closure occurs when, in our case, AFTS's position for the target closely approximates the known position. We performed spatial closure exercises for AFTS in April and October 2000.

After AFTS was deployed, we positioned a plastic, air-filled sphere 2 m underwater off pier nose MU1-1/FU2-2 (Figure B.5). Ideally, the target was at a known position. Practically, during exercises in April the target moved because the sluice was opened. Thus, although AFTS tracked the target well, we did not know the true position of the target, negating the April spatial closure test.

We returned in October and performed the exercise again with a more rigid frame for the target and the sluice closed. In October, AFTS was deployed on the centerline of the occlusion plate at MU1-1. AFTS was at Elev. 103 ft after the occlusion plate was lowered into position. The target was placed off the MU1-1/FU2-2 pier nose, as in April.

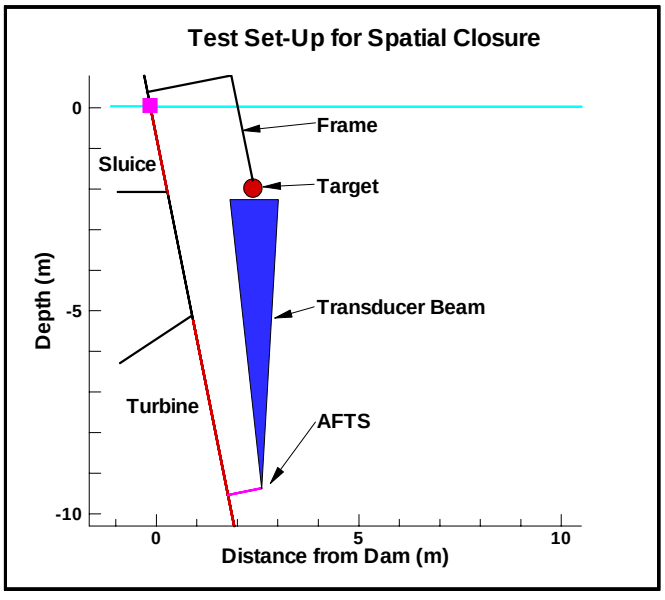

Figure B.5. Side view of set-up used in April 2000 for spatial closure exercise.

AFTS's positions for X and Z were reasonably good, but Y was off by 0.40 m (Table B.2). Standard deviations of the AFTS position estimates were highest for the y-position, less for the x-position and least for the z-position (Table B.2). The z-position is closest to range measurement, which we expect to be closest because it is a time based estimate of the reflection. The y-position corresponds closely to the β axis of AFTS and the x-position to the α axis. It was clear that we were still limited in the knowledge of the reference point because of the mounting and rigidity of the plastic pipe frame. However, the position measured with AFTS was similar to the known position, so we can be reasonably assured of closure.

Table B.2. X, Y, Z positions and standard deviations (S.D.) from October 2000 spatial closure test. Values in meters.

	X	Y	Z	X S.D.	Y S.D.	Z S.D.
Position of target	4.94	-1.20	-14.54	---	---	---
Tracker's estimate	4.87	-1.60	-14.41	0.0352	0.0544	0.0197
Difference	0.07	0.40	0.13	---	---	---

B.7.2 Estimated Errors Due To Split-beam

We used the measurements of the plastic sphere made on 26 October 2000 to illustrate the types of split-beam and rotator angles that AFTS might display. The average echo strength was –39.0 dB (S.D.=4.8) with tracking enabled and –38.8 dB (S.D.=4.6) when manually centered on the acoustic beam axis. The signal to noise ratio was in excess of 20 dB. Table B.3 shows the split-beam angle estimates and rotator positions with their standard deviations.

Table B.3. Angles and standard deviations (s.d.) to a 10 cm plastic hollow sphere, deployed 2 m under the surface at piernose between FU and MU1-1 at The Dalles Dam, 26 October 2000. AFTS was positioned about 15 m below the sphere.

	SPLIT-BEAM ANGLES		ROTATOR ANGLES		STANDARD DEVIATIONS			
	γ	ψ	α	β	S.D.(γ)	S.D.(ψ)	S.D.(α)	S.D.(β)
w/ tracking	-0.0016	-0.0056	-96.3	18.6	0.2302	0.2090	0.2929	0.1562
w/o tracking	-0.1949	0.2048	-96.2	18.4	0.1802	0.1585	0	0

The standard deviations in the split-beam angles nearly match Ehrenberg's (1981) predictions of 0.2 degrees shown in Table B.3. Interestingly, auto tracking adds some variation to these estimates. The standard deviation of the outer armature (β) was less than the inner (α) estimate, and the two estimates follow closely the measurements made for their backlash. One-half of the backlash was about the same as the standard deviation.

B.7.3 Prediction Error

Table B.4 shows that the predicted positional errors are quite similar to the standard deviations of the position shown in Table B.3. The RMS error (0.0162) and the standard

deviation (0.0197) of Z showed the least error because the coordinate is estimated largely from range. This was because AFTS was mounted 15 m below the target and 5 m to the side. Range was estimated quite accurately from the time of the transmission of the pulse to the return of the target echo. The Y coordinate had the largest RMS error (0.0553) and standard deviation (0.0544). The Y coordinate depended largely on the outer stepper motor armature and to a lesser extent on the inner armature and the range. The target presented errors for only a single location. We plan to examine a number of tracked fish at a number of locations to examine the benefits of alternative tracking algorithms.

Table B.4. Root mean square (RMS) error in predicted versus measured coordinate positions estimated by AFTS at The Dalles Dam, 26 October 2000.

	COORDINATE		
	X	Y	Z
RMS Error	0.0387	0.0553	0.0162

B.8 Discussion

The error in AFTS due to the split-beam estimation was predicted based on Ehrenberg (1981) to be due to the signal to noise ratio of the fish reflection. The standard deviation was about 0.7 degrees with a SNR of 10 dB. Errors in the armature movement were only somewhat less, about 0.3 degrees. Therefore, some improvement in tracking can be gained by (a) increasing the signal to noise in the angle measuring receivers, (b) decreasing the backlash of the armatures, and (c) increasing the number of samples in an angle measurement.

The BioSonics system uses about half of the pulse width for angle estimates. If the pulse width is 0.3 msec and samples are taken at about 40 kHz, then there are about six samples of angle measurements, and we expect the variance to be reduced by using all six samples. However, Ehrenberg (1981) showed little improvement by using adjacent samples. It is recommended to investigate if longer pulse durations reduce variance of the estimated planar angle.

Another way of reducing the variance is increasing the signal to noise ratio (SNR). A possible avenue to increase SNR would be to create a vernier split beam which used smaller elements (smaller D between acoustic centers with lower SNR) to locate phase wrap, and larger elements (larger D and larger SNR) to actually make the angle measurement. For example, doubling the area of the receiving ceramic should increase the SNR by a factor of 12.6 or 11 dB. The standard deviation would decrease from 0.7 degrees, for SNR of 10 dB, to 0.1 degrees, for SNR of 21 dB. This would require two additional receivers per planar angle or four additional total. The BioSonics system of using independent circular ceramics will most likely present the lowest sidelobes and hence largest SNR, as long as the ceramic area is as large as a traditional half circle. However, a comparison between designs of various types (and manufacturers) could be made in order to determine gains in SNR.

Improvements to decrease armature backlash may be made by using stepper motors which are micro-stepped and which directly drive the transducer motion. Low backlash gearboxes can be used if gearing is still required.

Appendix C STATISTICAL ANALYSIS OF SFB HYPOTHESES USING MOVEMENT DATA

Movement data from the analysis of states were used to test certain SFB hypotheses (Table C.1). The logic on setup of the hypotheses was as follows. The working hypotheses stated in the report (we called them SFB premises) were the alternative hypotheses in formal testing (H_a). The choice of working hypotheses (SFB premise) was based on anticipated mechanisms important in the passage of smolts at a surface bypass collector.

For each statistical analysis, the null hypothesis was tested with a 1-tailed Z-test for each time block and separately for day and night periods (i.e., total of 6 tests). The dependent variable was an observation of movement in one of two directions in a given hypothesis. Thus, we assumed movement for a particular episode had a binomial distribution. The Z-statistics, p-values and observed proportions estimated along with associated standard error (SE) and asymptotic 95% confidence interval are provided (Tables C.2-C.5). In addition, the separate Z-tests were combined in a meta-analysis that examined the null hypotheses for daytime, nighttime, and all times combined. Also reported are the proportions estimated separately for day and night time periods. A GLIM analysis (McCullagh and Nelder, 1983) was also performed to examine whether the proportions (e.g., up or towards) varied between blocks and day/night periods. An analysis of deviance table (ANODEV) is presented along with F-statistics and p-values for each test.

The assumption of independence in ping-to-ping direction of movement was assessed using 500 tracks from day data and 500 tracks from night data (first 500 tracks each period collected on April 17). A test called “runs up and down” (Sokal and Rohlf 1981, pp. 785-786) was performed. The runs up and down test uses a naturally ordered time series (ping-to-ping for successive tracks) and the sign of the difference from the previous value (direction of movement – X west or east, Y toward or away, and Z up or down). Data for differences in sign between the first ping of a given fish and the last ping of the one before it were discarded because they were invalid. Independence in direction of movement was examined for each dimension (X, Y, Z) separately. The independence assumption was satisfied (Table C.6).

Table C.1. SFB hypotheses tested with Z-statistic.

TEST	NULL HYPOTHESIS	ALTERNATIVE HYPOTHESIS
Attraction	$H_0 : p_{TOWARD} \leq p_{AWAY}$	$H_A : p_{TOWARD} > p_{AWAY}$
	For the area	X: 0 to 9.5
		Y: 1 to 162
		Z: 0 to –3
Shallow Preference	$H_0 : p_{UP} \leq p_{DOWN}$	$H_A : p_{UP} > p_{DOWN}$
	For the area	X: 2 to 8
		Y: 1 to 9.5
		Z: -1.5 to –3.5

Table C.2. Z-test results for Shallow Preference.

$H_0 : \hat{p}_{up} \leq \hat{p}_{down}$ VS. $H_A : \hat{p}_{up} > \hat{p}_{down}$								
Block	Day/ Night	Z Statistic	p-value	$\hat{p}_{UP}$	Sample Size	Stand. Error	Lower 95% Confid. Limit	Upper 95% Confid. Limit
1	0	4.7301	0	0.5276	7331	0.0058	0.5162	0.5391
2	0	11.1833	0	0.5454	15161	0.0041	0.5375	0.5534
3	0	9.6411	0	0.5361	17792	0.0037	0.5288	0.5435
4	0	20.5209	0	0.5632	26317	0.0031	0.5572	0.5693
5	0	7.591	0	0.5532	5098	0.007	0.5394	0.5669
1	1	-1.5597	0.9406	0.4703	691	0.019	0.4331	0.5076
2	1	7.8653	0	0.5799	2421	0.0102	0.56	0.5998
3	1	16.0207	0	0.6368	3428	0.0085	0.6201	0.6536
4	1	19.9983	0	0.7448	1669	0.0122	0.7208	0.7687
5	1	7.65	0	0.6608	566	0.021	0.6196	0.702
Meta-Analysis Statistic	p-value							
$\chi^2_{DAY}(10) = 115.1293$	0	$\hat{p}_{UP,DAY} = 0.5484$						
$\chi^2_{NIGHT}(10) = 92.2259$	0	$\hat{p}_{UP,NIGHT} = 0.6301$						
$\chi^2_{ALL}(20) = 207.3551$	0	$\hat{p}_{UP,ALL} = 0.5573$						

Table C.3. ANODEV for Shallow Preference.

SOURCE	DF	DEV	MDEV	F	P
Total	9	209.07			
Blocks	4	180.0	45.0	$F_{4,4}$=8.2075	.0328
Day/Night	1	7.125	7.125	$F_{1,4}$=1.2995	.3179
Error	4	21.931	5.4828		

Table C.4. Z-test results for Attraction.

$H_0 : \hat{p}_{towards} \le \hat{p}_{away}$ VS. $H_A : \hat{p}_{towards} > \hat{p}_{away}$								
Block	Day/ Night	Z Statistic	p-value	$\hat{p}_{towards}$	Sample Size	Stand. Error	Lower 95% Confid. Limit	Upper 95% Confid. Limit
1	0	23.7993	0	0.5882	18192	0.0037	0.581	0.5955
2	0	36.1685	0	0.5876	42656	0.0024	0.5828	0.5923
3	0	30.0188	0	0.5841	31858	0.0028	0.5786	0.5896
4	0	48.7589	0	0.6049	54052	0.0022	0.6006	0.6091
5	0	19.3647	0	0.5749	16707	0.0039	0.5673	0.5825
1	1	6.6982	0	0.52	27909	0.003	0.5142	0.5259
2	1	4.9438	0	0.51	60997	0.002	0.506	0.514
3	1	21.5335	0	0.5648	27640	0.003	0.5589	0.5707
4	1	24.5518	0	0.5863	20241	0.0035	0.5794	0.5932
5	1	19.3408	0	0.6222	6258	0.0063	0.6099	0.6346
Meta-Analysis Statistic	p-value							
$\chi^2_{DAY}(10) = 115.1293$	0	$\hat{p}_{TOWARDS,DAY} = 0.5914$						
$\chi^2_{NIGHT}(10) = 115.1293$	0	$\hat{p}_{TOWARDS,NIGHT} = 0.5383$						
$\chi^2_{ALL}(20) = 230.2585$	0	$\hat{p}_{TOWARDS,ALL} = 0.5666$						

Table C.5. ANODEV for Attraction.

SOURCE	DF	DEV	MDEV	F	P
Total	9	1626.9			
Blocks	4	723.8	180.95	$F_{4,4}$=1.9779	.2626
Day/Night	1	537.1	537.1	$F_{1,4}$=5.8708	.0725
Error	4	365.95	91.487		

Table C.6. Results of runs up and down test for independence in direction of movement, a basic assumption of the Z-tests.

PERIOD	N	DIMENSION	R	T_S
Day	13487	X	6623	0.99
		Y	6964	0.85
		Z	8391	0.25
Night	28580	X	17213	0.36
		Y	16478	0.51
		Z	19047	0.001

(Page intentionally blank.)